Radionuclide generator based production of therapeutic lutetium-177

Bhardwaj, Rupali

DOI
10.4233/uuid:5afcb3ea-813c-4f7b-ae98-df19ed50f5c2

Publication date
2019

Document Version
Final published version

Citation (APA)
Bhardwaj, R. (2019). *Radionuclide generator based production of therapeutic lutetium-177*. [Dissertation (TU Delft), Delft University of Technology]. https://doi.org/10.4233/uuid:5afcb3ea-813c-4f7b-ae98-df19ed50f5c2

Radionuclide generator based production of therapeutic lutetium-177

Rupali Sangal Bhardwaj

Radionuclide generator based production of therapeutic lutetium-177

Dissertation

for the purpose of obtaining the degree of doctor

at Delft University of Technology

by the authority of the Rector Magnificus prof.dr.ir. T.H.J.J. van der Hagen

chair of the Board for Doctorates

to be defended publicly on the 27th November 2019, 15:00

by

Rupali Sangal BHARDWAJ

Master of Science in Chemistry, University of Delhi, New Delhi, India

born in Shamli, India

The dissertation has been approved by the promotor and the copromotor

Composition of the doctoral committee:

Rector Magnificus	Chairman
Prof.dr. H.T. Wolterbeek	Delft University of Technology, promotor
Dr.ir. A.G. Denkova	Delft University of Technology
Dr. P. Serra. Crespo	Delft University of Technology

Independent members

Prof.dr.ir. J.R. van Ommen	Delft University of Technology
Prof.dr. A.D. Windhorst	Amsterdam University Medical Centre
Prof.dr. J.F. Verzijlbergen	Radboud University Medical Centre
Prof.dr. P.H.Elsinga	University Medical Centre Groningen
Prof.dr. A. van de Wiel	Delft University of Technology

The research presented in this thesis was performed at the Applied Radiation and Isotopes section of the department of Radiation Science and Technology, Faculty of Applied Sciences, Delft University of Technology, the Netherlands.

Visiting address: Mekelweg 15, 2629 JB Delft, the Netherlands.

Dedicated to my husband, Rajat Bhardwaj…

Behind every successful woman, there is a family who trusted and supported her.

Table of contents

Summary

Lutetium-177 (^{177}Lu) is a radionuclide with well-established potential in targeted radionuclide therapy (TRNT). ^{177}Lu emits β^- particles with a tissue penetration depth of 2 mm, which makes it effective in treating small tumors and causes lower toxicity to nearby healthy cells. The β^- emission is also accompanied by gamma ray emission that allows simultaneous imaging of the tumor treatment. The last decade has witnessed a three fold increase in the ^{177}Lu related publications and its demand is expected to grow significantly in the coming years. Currently, the ^{177}Lu availability is completely dependent on the availability of nuclear reactors. They are prone to shutdowns for maintenance, social, economic, political and other unexpected reasons. The exclusive dependency of radionuclide production on nuclear reactors is known to lead to major supply shortages. In general, there is a consensus among the nuclear medicine scientists that new production pathways should be developed that can provide some independence from the nuclear reactor availability.

Radionuclide generators represents the most convenient radionuclide production devices that can provide an onsite and an on-demand supply of a radionuclide without the continuous need of any radionuclide production facility. Their potential in radionuclide production has been very well documented in the existing literature. This research has been aimed at the development of a $^{177m}Lu/^{177}Lu$ radionuclide generator based ^{177}Lu production. However, such a generator has been never reported before and unlike the existing radionuclide generators, it involves the separation of physically and chemically alike nuclear isomers ^{177m}Lu and ^{177}Lu. This thesis has been aimed to study the feasibility and potential of a radionuclide generator based ^{177}Lu production. The proof of concept for the ^{177m}Lu-^{177}Lu separation has been established. A liquid-liquid extraction based ^{177m}Lu-^{177}Lu separation method has been designed which can potentially lead to the production of clinically acceptable ^{177}Lu quality. Additionally, the technical requirements needed to lead to a commercial ^{177m}Lu /^{177}Lu radionuclide generator are discussed and its potential in ^{177}Lu production is being evaluated.

The ^{177m}Lu-^{177}Lu separation is based on the chemical effects occurring during the internal conversion decay of ^{177m}Lu. The internal conversion based decay of ^{177m}Lu is often accompanied with an auger electron cascade, and leaves the atom in a highly charged state, which can lead to bond rupture. This provides with an opportunity to separate the two isomers in the form of complexed ^{177m}Lu and free ^{177}Lu ions. The experimental evidence to this concept is provided in Chapter 2, where the ^{177m}Lu-DOTA-(Tyr^3)-octreotate complex has been retained on a tC-18 silica based column and the ^{177}Lu ions released free after bond rupture have been collected in a mobile phase flow. In equilibrium, the $^{177}Lu/^{177m}Lu$ activity ratio is 0.25, while after separation a $^{177}Lu/^{177m}Lu$ activity ratio up to 250 has been achieved, accounting to a 1,000 times ^{177}Lu enrichment. However, for a clinically acceptable $^{177m}Lu/^{177}Lu$ radionuclide generator, a $^{177}Lu/^{177m}Lu$ activity ratio close to 10,000 is preferred. In this study, it has been found that the $^{177}Lu/^{177m}Lu$ activity ratio is affected by the dissociation of the ^{177m}Lu complex. An increase in the temperature during ^{177}Lu accumulation increases the dissociation and decreases the $^{177}Lu/^{177m}Lu$ activity ratio. Therefore, a liquid-liquid extraction (LLE) based ^{177m}Lu-^{177}Lu separation has been designed where the ^{177}Lu accumulation is performed at 77K.

The LLE based ^{177m}Lu-^{177}Lu separation shown in Chapter 3, involves the use of ^{177m}Lu complex in aqueous phase, and the extraction of released ^{177}Lu in the organic phase (dihexyl ether) using a cation extracting agent. The ^{177}Lu accumulation has been performed at 77K to minimize the dissociation of complexed ^{177m}Lu and the re-association of released ^{177}Lu ions. The potential of ^{177m}Lu-DOTA and ^{177m}Lu-DOTATATE complexes in ^{177m}Lu-^{177}Lu separation have been tested and the effect of different Lu:DOTA molar ratios on the ^{177}Lu extraction efficiency and $^{177}Lu/^{177m}Lu$ activity ratio has been studied. Overall, under certain conditions the $^{177}Lu/^{177m}Lu$ activity ratio up to 3500 have been achieved with a ^{177}Lu extraction efficiency close to 60%. The obtained $^{177}Lu/^{177m}Lu$ activity ratio is very well comparable to the activity ratio present in the clinically used ^{177}Lu. However, the presented method has been performed at lab scale with very low activity levels and has not been yet automatized to lead to a clinically acceptable $^{177m}Lu/^{177}Lu$ radionuclide generator. In Chapter 4, the knowledge from LLE has been translated into a solid phase extraction (SPE) based ^{177m}Lu-^{177m}Lu separation. In SPE, DOTA has been grafted on the surface of commercially available silica and used to complex ^{177m}Lu ions. The synthesized ^{177m}Lu containing solid has been loaded inside a column and left for ^{177}Lu accumulation at 77K. The freed ^{177}Lu ions have been collected under different conditions using different mobile phase flow. However, using this method the highest $^{177}Lu/^{177m}Lu$ activity ratio up to 25 have been achieved which is far worse than what was achieved with LLE. It has been hypothesized that after the immobilization of DOTA on a solid, it can no longer form stable cage like coordination with ^{177m}Lu ions which leads to their fast dissociation during the ^{177}Lu ion removal. The coordination behavior of DOTA complex with Lu ions needs further investigation to lead to an automatable and convenient SPE based $^{177m}Lu/^{177}Lu$ radionuclide generator.

Apart from the ^{177m}Lu-^{177}Lu separation method, the $^{177m}Lu/^{177}Lu$ radionuclide generator will also require ^{177m}Lu as the starting material. The large scale ^{177m}Lu production has been experimentally and theoretically investigated in Chapter 5. The ^{177m}Lu is being produced by the neutron irradiation of a natural Lu_2O_3 sample at the BR2 reactor, Mol, Belgium. The produced ^{177m}Lu activity has been found to be in good agreement with the theoretically estimated ^{177m}Lu activity based on the ^{177m}Lu production cross section of 2.8 b and burn up cross section of 620 b. Further for the large scale ^{177m}Lu production, the effect of ^{176}Lu enrichment, irradiation time and neutron flux on ^{177m}Lu production has been theoretically investigated. It has been found that the ^{177m}Lu can be produced using a short irradiation time of 6-10 days at the high flux reactors. The question about what quantity of ^{177m}Lu (or starting ^{176}Lu enriched target) would be needed to produce sufficient amounts of ^{177}Lu is answered in Chapter 6. It has been found in order to produce clinically relevant ^{177}Lu quantity, the ^{177m}Lu production should start with the irradiation of 1-4 g of ^{176}Lu enriched Lu_2O_3. For instance, the use of 3 g ^{176}Lu enriched Lu_2O_3 target can lead to about 7.4 GBq ^{177}Lu per week for up to 7 months. Additionally, a $^{177m}Lu/^{177}Lu$ radionuclide generator has been modelled and the conditions needed to achieve a high quality ^{177}Lu production has been defined. The $^{177m}Lu/^{177}Lu$ radionuclide generator has the potential to lead to on-site production of high specific activity ^{177}Lu close to the theoretical maximum of 4.1 TBq/mg Lu and with <0.01% ^{177m}Lu. The important requirement would be the use of conditions that can keep the

dissociation rate constants to the order of 10^{-11} s^{-1}. Lastly, the general conclusion from this thesis and the future outlook are presented in Chapter 7.

Overall, this thesis presents a big step in giving an overview on various aspects of a ^{177m}Lu/^{177}Lu radionuclide generator development. It provides with the proof of concept for ^{177m}Lu-^{177}Lu separation and also defines the requirements of a clinically relevant ^{177m}Lu/^{177m}Lu radionuclide generator. The LLE based ^{177m}Lu-^{177}Lu separation method can potentially lead to a ^{177m}Lu/^{177m}Lu radionuclide generator. However, it needs further investigation in several aspects. The current work has been performed on lab scale with low ^{177m}Lu activity levels and the experimental set up is not yet automatized for commercial use. The future investigations should involve the high ^{177m}Lu activity levels in combination with automated LLE based separation modules such as on-column solvent extraction, a continuous flow extraction, membrane-based phase separation, microfluidics based separation and others. Further, the work done in this thesis do not take into account the effect of radiolysis on the ^{177m}Lu-^{177}Lu separation process, and should be carefully accounted in the future research. Lastly, it should be mentioned that the ^{177m}Lu activity used in this thesis is the waste produced during the direct route ^{177}Lu production, and has been provided as in-kind contribution from IDB Holland. The most important question for future research on ^{177m}Lu/^{177}Lu radionuclide generator development would be the large scale ^{177m}Lu production, and the availability of large amounts of ^{176}Lu enriched targets.

Samenvatting

Lutetium-177 (^{177}Lu) is een radionuclide met aangetoonde mogelijkheden binnen de gerichte radionuclide therapie (GRNT). Het zendt β^- deeltjes uit die ongeveer 2 mm diep in weefsel kunnen doordringen, wat het een effectif nuclide maakt voor het behandelen van kleine tumoren waarbij minder schade aan omliggend weefsel toe wordt aangericht. De β^- emissie gaat gepaard met het uitzenden van gamma's wat er voor zorgt dat de tumorbehandeling in beeld gebracht kan worden. Het aantal ^{177}Lu-gerelateerde publicaties is het afgelopen decennium verdrievoudigd, en de verwachting is dat de vraag naar ^{177}Lu ook de komende jaren flink zal toenemen. Op het moment is de productie van ^{177}Lu volledig afhankelijk van de beschikbaarheid van kernreactoren. Deze worden echter regelmatig stil gelegd voor onderhoud, sociaaleconomische, politieke en andere onverwachte redenen. Het is bekend dat de exclusieve afhankelijkheid op kernreactoren voor de radionuclidenproductie kan leiden tot grote beschikbaarheidstekorten. Er bestaat een consensus tussen wetenschappers in de nucleaire geneeskunde dat nieuwe productiemethode ontwikkeld moeten worden die een zekere maat van onafhankelijkheid van de beschikbaarheid van kernreactoren kunnen verschaffen.

Radionuclide generatoren worden gezien als een ideale vorm van radionuclide-productie waarbij gezorgd kan worden voor plaatselijke, on-demand levering van een radionuclide zonder afhankelijk te zijn van een productie faciliteit. De mogelijkheden die zulk een generator biedt zijn zeer goed gedocumenteerd binnen de bestaande literatuur. Dit onderzoek is gericht op de ontwikkeling van een $^{177m}Lu/^{177}Lu$ radionuclide generator voor de productie van ^{177}Lu. Een dergelijke generator is nog niet eerder beschreven, en in tegenstelling tot huidige radionuclide generatoren gaat het hier om de scheiding van de fysisch en chemisch gelijkwaardige isomeren ^{177m}Lu en ^{177}Lu. Dit proefschrift is gericht op het onderzoeken van de haalbaarheid en het potentieel van een ^{177}Lu-productie op basis van een radionuclide generator. Het hoofddoel van deze studie is een proof of concept van de scheiding van ^{177m}Lu en ^{177}Lu tot stand te brengen, en de factoren die hier invloed op hebben in kaart te brengen. Een op de vloeistof-vloeistofextractie van ^{177m}Lu-^{177}Lu gebaseerde scheidingsmethode is ontworpen, welke mogelijk kan leiden tot de productie van een klinisch acceptabele hoeveelheid ^{177}Lu. Hiernaast worden de technische vereisten voor een commerciële $^{177m}Lu/^{177}Lu$ generator besproken en de mogelijkheden voor de productie voor ^{177}Lu worden geëvalueerd.

De scheiding van ^{177m}Lu-^{177}Lu is gebaseerd op de chemische effecten die optreden tijdens het interne conversieverval van ^{177m}Lu. Het op interne conversie gebaseerde verval van ^{177m}Lu gaat vaak samen met een auger elektronen cascade, welke het atoom in een sterk geladen toestand achterlaat en op deze manier zorgt voor het breken van de chemische binding. Dit biedt de mogelijkheid om de twee isomeren, het gecomplexeerde ^{177m}Lu en de vrije ^{177}Lu atomen, te scheiden. Het experimentele bewijs van dit concept wordt geleverd in Hoofdstuk 2, waar de ^{177m}Lu-DOTATAAT verbinding op een tC-18 silica kolom wordt vastgehouden terwijl de ^{177}Lu ionen die zijn vrijgekomen na het breken van de chemische binding worden verzameld in een mobiele fasestroom. In evenwicht is de activiteitsverhouding van $^{177m}Lu/^{177}Lu$ 0.25, terwijl na de scheiding een $^{177m}Lu/^{177}Lu$ activiteitsverhouding van 250 is bereikt. Dit komt overeen met een ^{177}Lu verreikingsgraad van 1000. Voor een klinisch aanvaardbare $^{177m}Lu/^{177}Lu$

generator is echter een activiteitsverhouding van $^{177m}Lu/^{177}Lu$ rond de 10.000 gewenst. In dit onderzoek kwam naar voren dat de activiteitsverhouding van $^{177m}Lu/^{177}Lu$ wordt beïnvloed door de dissociatie van het ^{177m}Lu complex. Een temperatuursverhoging tijdens de accumulatie van ^{177}Lu verhoogt de ontkoppeling en vermindert de $^{177m}Lu/^{177}Lu$ activiteitsverhouding. Er is zodoende een vloeistof-vloeistofextractie (VVE) methode ontwikkeld gebaseerd op de scheiding van ^{177m}Lu-^{177}Lu waarbij het ^{177}Lu wordt geaccumuleerd bij een temperatuur van 77K.

De op VVE gebaseerde scheiding van ^{177m}Lu-^{177}Lu zoals gepresenteerd in Hoofdstuk 3 heeft het ^{177m}Lu complex in de waterige fase, terwijl de na de bondbreuk vrijgekomen ^{177}Lu wordt geëxtraheerd in de organische fase (dihexylether) met behulp van een kation extractiemiddel. De accumulatie van ^{177}Lu is uitgevoerd bij een temperatuur van 77K om de dissociatie van ^{177m}Lu en de herassociatie van vrijgekomen ^{177}Lu ionen te minimaliseren. Twee verschillende verbindingen, ^{177m}Lu-DOTA en ^{177m}Lu-DOTATAAT, zijn getest voor de scheiding van ^{177m}Lu-^{177}Lu, en er is gekeken naar het effect van verschillende Lu:DOTA molverhoudingen op de extractie efficiëntie van ^{177}Lu en de $^{177m}Lu/^{177}Lu$ activiteitsverhouding. Over het algemeen wordt een extractie efficiëntie tot 3500 bereikt onder bepaalde omstandigheden met een ^{177}Lu extractie efficiëntie van bijna 60%. De verkregen $^{177m}Lu/^{177}Lu$ activiteitsverhouding is zeer goed vergelijkbaar met de activiteitsverhouding van ^{177}Lu als gebruikt in de kliniek. De huidige methode is echter enkel getest in het laboratorium met zeer lage hoeveelheiden radioactiviteit, en is nog niet geautomatiseerd tot een klinisch acceptabele ^{177m}Lu-^{177}Lu radionuclidegenerator. De kennis opgedaan bij de ontwikkeling van de VVE methode is in Hoofdstuk 4 omgezet in een scheidingsmethode voor ^{177m}Lu-^{177}Lu gebruikmakend van vastefase extractie (VFE). Bij de VFE methode is DOTA geënt op een commercieel verkrijgbaar silica welke gebruikt wordt om ^{177m}Lu ionen te binden. De ^{177m}Lu bevattende vaste stof is in een kolom geladen en vervolgens bij 77K bewaard voor de accumulatie van ^{177}Lu. De vrijgekomen ^{177}Lu ionen zijn verzameld gebruikmakend van verschillende mobiele fasestromen onder verschillende omstandigheden. Met deze methode is een maximale $^{177m}Lu/^{177}Lu$ activiteitsverhouding van slechts 25 behaald, wat veel minder goed is dan wat gezien werd met de VVE gebaseerde scheidingsmethode. Er is verondersteld dat na de immobilisatie van DOTA op een vaste stof het niet langer een stabiele kooi gecoördineerd met ^{177m}Lu-ionen kan vormen, wat leidt tot snelle dissociatie tijdens de verwijdering van het ^{177}Lu-ion. Het coördinatiegedrag van het DOTA-complex met Lu-ionen moet verder worden onderzocht om te kunnen leiden tot een automatische en handige op VFE gebaseerde ^{177m}Lu-^{177}Lu radionuclidengenerator.

Naast de geoptimaliseerde ^{177m}Lu-^{177}Lu scheidingsmethode vereist de $^{177m}Lu/^{177}Lu$ radionuclidegenerator ^{177m}Lu als uitgangsmateriaal. De grootschalige productie van ^{177m}Lu is zowel theoretisch als experimenteel onderzocht in Hoofdstuk 5. Het ^{177m}Lu is geproduceerd door de neutronenbestraling van een natuurlijk Lu_2O_3 monster in de BR2-reactor, Mol, België. De geproduceerde ^{177m}Lu-activiteit bleek in goede overeenstemming te zijn met de theoretisch geschatte ^{177m}Lu-activiteit op basis van de ^{177m}Lu-productie doorsnede van 2.8 b en werkzame doorsnede van 620 b. Er is verder gekeken naar de theoretische effecten van ^{176}Lu verrijking, bestralingstijd en neutronenflux op de grootschalige productie van ^{177m}Lu. Uit deze studie bleek dat hoge flux reactoren de benodigde hoeveelheid ^{177m}Lu binnen een korte bestralingstijd van 6-10 dagen kunnen produceren. In Hoofdstuk 6 is verder ingegaan op de vraag hoeveel ^{177m}Lu (of hoeveel verrijkt ^{176}Lu startmateriaal) nodig zou zijn om voldoende ^{177}Lu te kunnen produceren. Om klinisch relevante hoeveelheden ^{177}Lu te produceren is 1-4 g verrijkt ^{176}Lu bevattend Lu_2O_3 nodig. De bestraling van 3 g ^{176}Lu verrijkt Lu_2O_3 is bijvoorbeeld genoeg voor de productie van ongeveer 7.4 GBq ^{177}Lu per week voor een totale looptijd tot 7 maanden. Hiernaast is een $^{177m}Lu/^{177}Lu$ generator gemodelleerd waarbij de omstandigheden die nodig zijn voor het produceren van een hoge kwaliteit ^{177}Lu zijn gedefinieerd. De $^{177m}Lu/^{177}Lu$ radionuclide generator biedt de mogelijkheid om op locatie een hoge specifieke activiteit van ^{177}Lu te leveren in de buurt van het theoretische maximum van 4.1 TBq/mg Lu met <0.01% ^{177m}Lu. Hierbij is de belangrijkste vereiste dat de generator gebruikt wordt bij condities die de dissociatiesnelheidsconstante rond de 10^{-11} s^{-1} kunnen houden. Ten slotte worden de algemene conclusie en de vooruitzichten voor de toekomst gepresenteerd in Hoofdstuk 7 van dit proefschrift.

In dit proefschrift wordt een uitgebreid overzicht gegeven van verschillende aspecten in de ontwikkeling van een $^{177m}Lu/^{177}Lu$ radionuclide generator. Het geeft een proof of concept voor de scheiding van ^{177m}Lu-^{177}Lu en definieert de vereisten voor een $^{177m}Lu/^{177}Lu$ radionuclide generator die toegepast kan worden in de kliniek. De ^{177m}Lu-^{177}Lu scheidingsmethode die gebaseerd is op VVE zou kunnen leiden tot de ontwikkeling van een $^{177m}Lu/^{177}Lu$ generator. Er zijn echter nog een aantal gebieden die verder ontwikkeld moeten worden. Het huidige werk is op laboratoriumschaal uitgevoerd met lage ^{177m}Lu activiteit, en de experimentele opstelling is nog niet geautomatiseerd voor commercieel gebruik. Toekomstig onderzoek moet zich richten op het gebruik van hoge ^{177m}Lu activiteitsniveaus tezamen met geautomatiseerde VVE gebaseerde scheidingsmethoden zoals op-kolom oplosmiddel extractie, een continue stroom extractie, membraan-gebaseerde fase extractie, op microfluidics gebaseerde scheidingen en andere scheidingsmethoden. Verder houdt het werk in dit proefschrift geen rekening met het effect van radiolyse op de scheiding van ^{177m}Lu-^{177}Lu, dit zou nader bestudeerd moeten worden. Tot slot moet er worden vermeld dat het ^{177m}Lu dat gebruikt werd in dit proefschrift het afvalproduct is van de directe ^{177}Lu productieroute, en als bijdrage in natura werd verstrekt door IDB Holland. De belangrijkste vraag voor toekomstig onderzoek naar de $^{177m}Lu/^{177}Lu$ radionuclidegenerator is de grootschalige productie van ^{177m}Lu en de beschikbaarheid van grote hoeveelheden verrijkt ^{176}Lu.

Chapter 1

Introduction

1.1. Introduction

Cancer is one of the leading causes of mortalities worldwide and is responsible for an estimated 9.6 million deaths in 2018 [1]. Globally, the total number of cancer cases are expected to increase from 18 million in 2018 to about 29 million by the end of 2040 [2]. The possible cancer treatments include a wide array of options such as surgery, chemotherapy, radiation therapy, targeted radionuclide therapy, photodynamic therapy, immune therapy, hyperthermia and others [3]. The last 50 years have witnessed an increased attention on cancer treatments which can specifically treat the cancerous cell while reducing the damage to the healthy cells [4,5]. An additional emphasis is being made on the treatments which are effective in the treatment of metastasized tumour cells [3,6]. Targeted radionuclide therapy (TRNT) is one such option that effectively target the cancer cells inside the body [7,8], shown schematically in Figure 1.

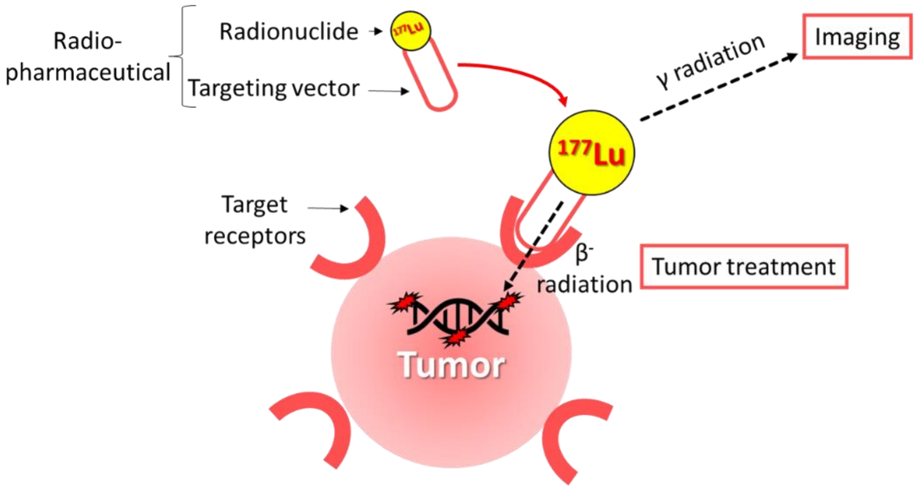

Figure 1: Schematic representation of Targeted Radionuclide Therapy (TRNT) using radiopharmaceutical comprising a targeting vector and lutetium-177

TRNT basically consists of radionuclide that is bonded to a targeting molecule which ensures their interaction with the tumour cells [9,10,11]. It has been reported to be successful in tumour treatment with less severe and infrequent side effects [12]. There has been a considerable increase in the interest and growth of TRNT in the last few years [13], as is evident from several reviews focused on compiling the advances and developments in the field of TRNT [5,10,14-17]. The biological effect of TRNT in tumour treatment is caused by the energy absorbed from the radiation emitted by the radionuclide.

The application of any radionuclide in TRNT is based on the combination of several factors such as 1) the decay characteristics such as physical half-life, decay energy, decay products, tissue penetration depth, 2) availability of radionuclides having high specific activity and radionuclidic purity, 3) a rapid and stable attachment of the radionuclide to the targeting vector while 4) the simultaneous emission of low energy gamma rays is an additional advantage, as it will gives the diagnostic properties along with the required therapeutic properties [18-21]. The current clinical and pre-clinical research on radionuclides for TRNT purposes revolves around several beta-emitting (^{177}Lu, ^{166}Ho, ^{186}Re, ^{188}Re, ^{67}Cu, ^{149}Pm, ^{199}Au, ^{77}Br, ^{153}Sm, ^{105}Rh, ^{89}Sr, ^{90}Y, ^{131}I) and alpha-emitting radionuclides (^{211}At, ^{212}Pb, ^{213}Bi, ^{223}Ra, ^{149}Tb) [22 5,9,23,24]. This thesis is focused on the beta and gamma emitting radionuclide Lutetium-177. Its properties and potential in TRNT are discussed in detail in the following section.

1.2. Lutetium-177 (^{177}Lu): Properties and Potential

The decay characteristics of lutetium-177 makes it a very suitable candidate for its application in targeted radionuclide therapy. They are compiled in Table 1 below:

Table 1: Decay characteristics of lutetium-177

Half-life	Decay mode	β^- emissions (abundance)	γ ray emissions (abundance)	Tissue penetration depth	Daughter isotope
6.7 days	β^-, γ	498 keV (79.3%) 380 keV (9.1%) 176 keV (12.2%)	249.7 (0.2120%) 208.37 (11.00%) 112.95 (6.40%) 71.65 (0.15%)	2 mm	^{177}Hf

The 6.7 days half-life of ^{177}Lu provides logistics advantages of facilitating its worldwide supply [22]. The 0.5 MeV β^- particles have a tissue penetration depth of 2 mm which allows selective deposition of energy inside the tissue cells while sparing the surrounding healthy tissues [25]. Additionally, the accompanying gamma ray emissions of 113 KeV (6.4%), and 208 KeV (11%) allow simultaneous imaging of the tumour treatment and imparts ^{177}Lu with theranostic (both therapeutic and diagnostic) potential (see Figure 1) [21,25].

The above mentioned unique decay characteristics of ^{177}Lu make it advantageous over other widely applied therapeutic β^- emitters, such as ^{131}I and ^{90}Y. ^{90}Y has a tissue penetration depth of 11 mm and often leads to damage of the surrounding healthy cells [26-28]. ^{131}I has a tissue penetration depth of 2 mm, but it emits high energy gamma photons in high abundance (636 keV (7.2%), 364 keV (81.7%), and 284 keV (6.14%)) resulting in extra radiation burden to non-target organs and it also causes a radiological risk to medical staff. [29]. In comparison, the ^{177}Lu has gamma rays of sufficiently low energy to allow imaging while keeping the unwanted radiation dose to the nearby organs adequately low. It is therefore considered as a better alternative to ^{90}Y and ^{131}I in some radio-therapeutic applications [30-33].

Lastly, lutetium is a lanthanide with an oxidation state of +3 and is well known to form complexes with coordination numbers of 6, 7, 8, and 9. The hard Lewis acid chemistry of lutetium provides it with a strong tendency to form complexes with hard donor ligands such as O, F and N [34]. Lutetium is reported to form thermodynamically stable complexes with a wide variety of bifunctional chelating agents such as 1,4,7,10-tetraazacyclododecane-1,4,7,10-tetraacetic acid (DOTA), 1,4,7,10-tetraazacyclododecane-1,4,7-triacetic acid (DO3A), diethylenetriaminepentaacetic acid (DTPA), ethylenediaminetetraacetic acid (EDTA) and others [34-36]. This allows facile labelling of ^{177}Lu with a various biomolecules, antibodies, and other organic ligands, thereby enabling the synthesis of ^{177}Lu based radiopharmaceuticals [37,38]. Finally, it decays to stable hafnium-177 which does not interfere with labelling of most lutetium chelates (and does not induce toxic effects) [39].

1.3. Existing clinical applications of ^{177}Lu based radiopharmaceuticals

The clinical applications of ^{177}Lu based radiopharmaceuticals has been extensively reviewed in the last five years [30,40-42]. In 2015, Banerjee et al. quoted "^{177}Lu is a gold mine for radiopharmaceutical development, and exploring its immense potential for therapeutic applications is still in the early stages" [22]. The development of ^{177}Lu based pharmaceuticals is expected to grow dramatically in the coming few years [18-21,43-45]. A list of ^{177}Lu related radiopharmaceuticals along with their application and current stage of study is shown in Table 2 below:

Table 2: A list of ^{177}Lu based radiopharmaceuticals along with their application and the current stage of study.

Radiopharmaceutical	**Application**	**Stage of Study**	**New incidences in 2018***
^{177}Lu-DOTATATE (Lutathera)	Gastroenteropancratic Neuroendocrine Tumors	FDA approved [46]	< 0.1%#
^{177}Lu-PSMA-DKFZ-617 ^{177}Lu-PSMA-I&T ^{177}Lu-J591	Prostate cancer	Phase II and phase III clinical trials [41,42,47-54]	1.3 million (7.1%)
^{177}Lu-trastuzumab ^{177}Lu-T-AuNP	Breast Cancer	Preclinical [55-58]	2.0 million (11.6%)
^{177}Lu-CC49	Colon Cancer	Preclinical [59-62]	1.8 million (combined colorectum) (10.2%)
^{177}Lu-anti-CD55	Lung cancer	Preclinical [63]	2 million (11.6%)
^{177}Lu-Rituximab ^{177}Lu-teuloimab	Non-Hodgkin's lymphoma	Preclinical and Phase I clinical trials [64-68]	500,000 (2.8%)
^{177}Lu-EDTMP	Bone pain palliation**	Phase I and Phase II clinical trials [69-72]	-**

* total number of cancer incidences in 2018 are 18,078,957. Data taken from http://gco.iarc.fr/ in October, 2018.

neuroendocrine tumours are rare with an estimated annual incidence of ~6.9/ 100,000 [73]

** treatment of cancer induced bone pain, needed in about 80% of the patients having solid tumours [74].

Currently, [^{177}Lu]Lu-DOTATATE is the most widely applied ^{177}Lu based radiopharmaceutical. The ^{177}Lu-DOTATATE is FDA approved for the treatment of gastroenteropancreatic neuroendocrine tumours (GEP-NET) and is used clinically worldwide [46]. A phase 3 study on the use of ^{177}Lu-DOTATATE in the treatment of 229 patients suffering from GEP-NET shows a 79% reduction in risk of tumour progression with an estimated progression free survival of 40 months [75,76]. Another study on the treatment of GEP-NET's using ^{177}Lu-DOTATATE reported a complete or partial tumour shrinkage in 16 percent of a subset of 360 patients [77].

Recently published studies have revealed the possibility of treatment of metastatic prostate cancer using ^{177}Lu-PSMA based radiopharmaceuticals [41,42,47-54]. According to the present literature, greater than 50% patient response was consistently observed in 30%- 70% of the treated cases [42,78]. The response of a 65 year old patient with metastatic prostate cancer towards ^{177}Lu-PSMA-DKFZ-617 is shown in Figure 2. A remarkable decrease in the standardized uptake value of the tumour lesions from 32.67 to 0.38 has been observed after 3 cycles of treatment with ^{177}Lu-PSMA-DKFZ-617 [43].

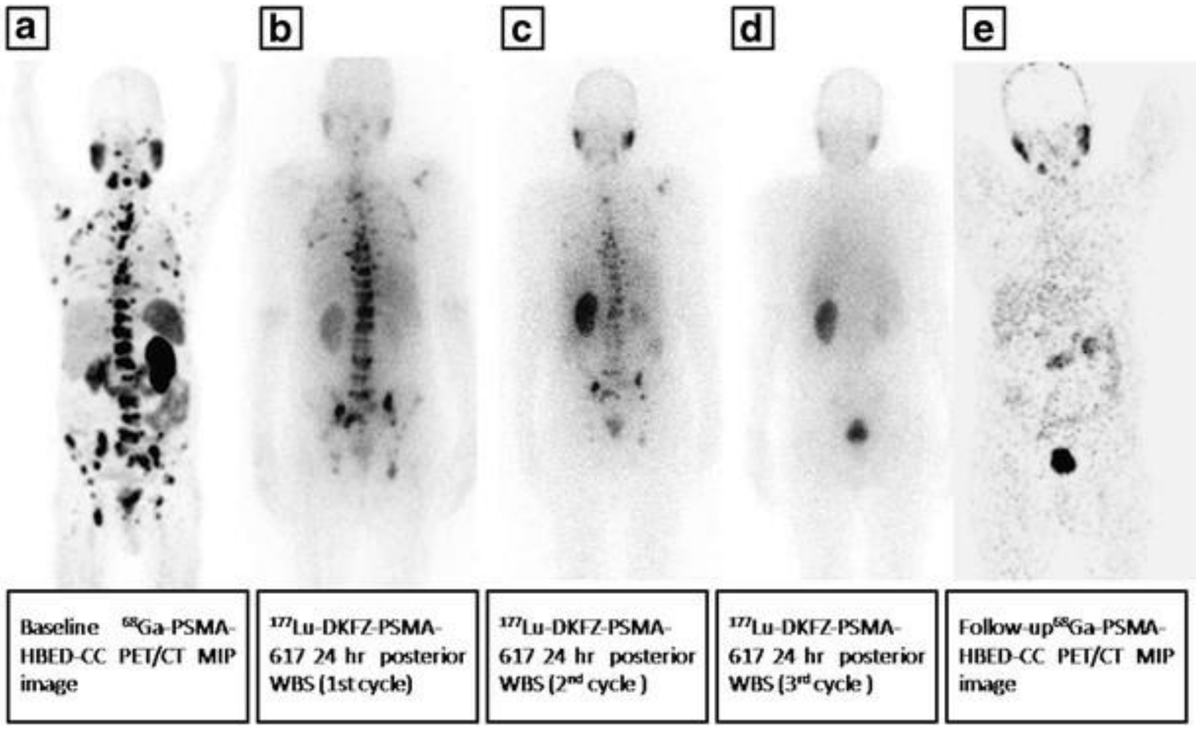

Figure 2: The full body scan of a patient suffering with metastatic castration resistant prostate cancer: The pre-therapy diagnostic scan showed extensive skeletal metastases (a), the three cycles of the treatment using ^{177}Lu-PSMA-DKFZ-617 (b), (c), (d), and post therapy follow up diagnostic scan (e) (taken from reference, Yadav *et al* [43]).

In a recent study among 30 patients, [^{177}Lu]-PSMA-617, has been shown to achieve greater than 50% prostate specific antigen decline in 57% of the treated patients with a low toxicity profile [47]. A phase 2 clinical trial of [^{177}Lu]-PSMA-617 including 200 participants is under progress to prove further its efficacy and potential in metastatic castration resistant prostate cancer (ClinicalTrials.gov Identifier: NCT03392428)[79].

Furthermore, as can be seen from Table 1, the ^{177}Lu based radiopharmaceuticals have also shown potential application in breast, colon, and lung cancer treatment [55-63]. The treatment of Non- Hodgkin lymphoma, and bone pain palliation using ^{177}Lu based radiopharmaceuticals is also in advanced clinical stages [64-72]. Additionally, apart from the ^{177}Lu based radiopharmaceuticals mentioned in Table 1, there are also several other extensively studied ^{177}Lu based radiopharmaceuticals which are currently in the design and development stage for application in radio-synovectomy, radio immunotherapy and others [30,80-89]. Overall, it is evident that the ^{177}Lu radiopharmaceuticals can be potentially applied in a wide range of clinical applications and ^{177}Lu can be expected to play a crucial role in fulfilling the global demand of radionuclides for many targeted radionuclide therapy applications [16,21].

Lastly, the total worldwide incidences of the cancer types corresponding to the potential ^{177}Lu applications are also listed in Table 2. Prostate cancer alone accounted to about 7.1% of the total cancer cases registered in 2018 [90]. The breast, colon, and lung cancer accounted to 11.6%, 10.2% & 11.6% of the total cancer cases registered in 2018, respectively. On combining all the potential applications of ^{177}Lu mentioned in Table 1, it can be foreseen that the ^{177}Lu based radiopharmaceuticals have the potential to be applied in the treatment of at least 40% of the worldwide cancer incidences. However, the research is highly dependent on the access, availability of ^{177}Lu and the associated costs. The current ^{177}Lu production scenario's and the associated limitations are described in section 1.4.

1.4. Current Lutetium-177 production routes and limitations

Currently, the ^{177}Lu production is performed at medium/ high flux nuclear reactors by two different processes known as "direct" or "indirect" production route. The "direct route" involves the irradiation of ^{176}Lu enriched Lu_2O_3 targets while the "indirect route" involves the ^{177}Lu production by the β^- decay of short-lived ^{177}Yb. They are schematically shown in the Figure 3 below:

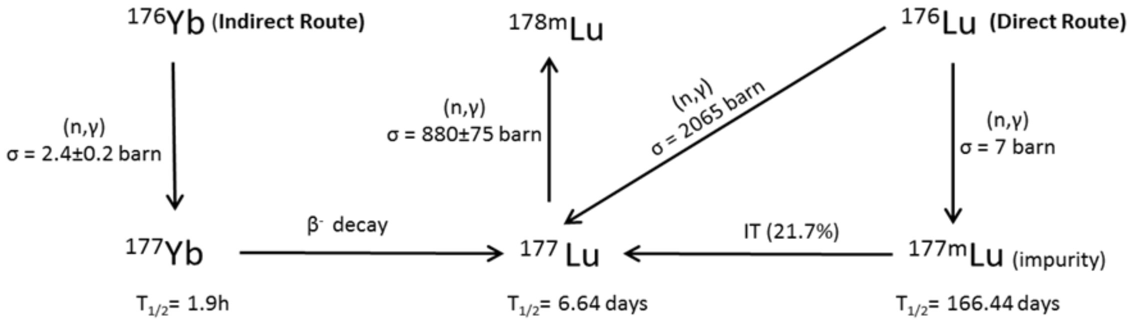

Figure 3: A description of the current ^{177}Lu production routes, "the direct" and "the indirect" production route along with the involved neutron capture cross sections [91]

Production of Lutetium-177 via the direct route

The "direct route" uses ^{176}Lu enriched Lu_2O_3 targets to produce ^{177}Lu via neutron capture, i.e. ^{76}Lu(n, γ)^{177}Lu which has as an advantage of high cross section of 2065 barn **[91]**. However, it results in the production of carrier added ^{177}Lu production since other lutetium isotopes are also present after irradiation. The specific activity of the produced ^{177}Lu depends on the ^{176}Lu enrichment, neutron flux, irradiation and cooling time. In high-flux reactors, ^{177}Lu can be produced with a specific activity of about 2.7 TBq/mg using 75% ^{176}Lu enrichment. This is 65% of the no-carrier added maximum specific activity of 4.1 TBq/mg. In medium flux reactors, ^{177}Lu can be produced with a specific activity of about 740 GBq/mg using targets with about 82% ^{176}Lu enrichment. Additionally, this route has an extra disadvantage of co-production of long-lived ^{177m}Lu as a radionuclidic impurity.

Production of Lutetium-177 via the indirect route

The "indirect route" starts with ^{177}Yb production using ^{176}Yb enriched Yb_2O_3, which then leads to ^{177}Lu production via its β^- decay. It offers the advantage of no-carrier added ^{177}Lu production with specific activity in the ranging in the order of 2.3- 4.0 GBq/ mg Lu, very close to the theoretical maximum specific activity of 4.1 TBq/ mg. However, this route has some shortcomings. First, it needs very expensive, highly enriched ^{176}Yb target because of the low $^{176}Yb(n,\gamma)^{177}Yb$ neutron capture cross section of 2.4 barn. The starting Yb target should be free from any traces of the most natural abundant isotope of Yb, namely ^{174}Yb. The $^{174}Yb(n,\gamma)^{175}Yb$ has a neutron capture cross-section of 65±5 barn. ^{175}Yb has a half-life of 4 days and it decays to ^{175}Lu via beta decay, thereby reducing the specific activity of produced ^{177}Lu [92]. Secondly, the ^{177}Lu production requires separation of chemically very similar Lu^{3+} and Yb^{3+} elements. The presence of any traces of Yb, can adversely affect the ^{177}Lu radiolabelling process because of the similar chemical behaviour of Lu and Yb.

Regardless of all the above-mentioned disadvantages, the ^{177}Lu production via neutron irradiation in nuclear reactors is the only commercially employed ^{177}Lu production route. Most of the research groups worldwide are working on increasing the efficiency of these two routes. At the moment, the global production of this isotope is dependent on the weekly irradiations in 9 nuclear reactors. These nuclear reactors are shown in the Figure 4 below:

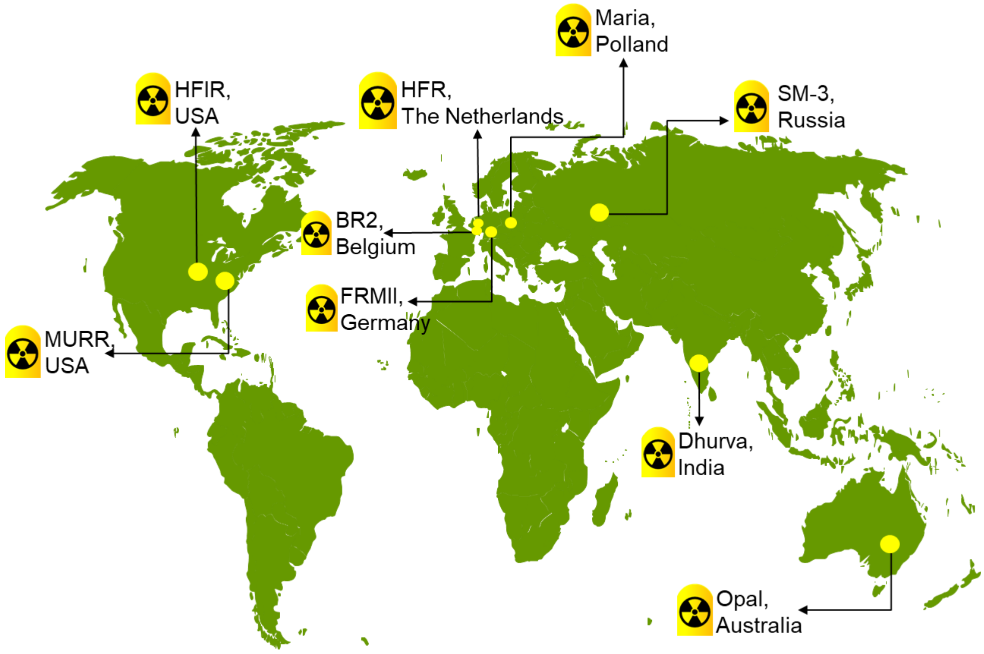

Figure 4: The world map showing the nuclear reactors responsible for global ^{177}Lu production.

Most of the nuclear reactors mentioned in Figure 4 are more than 50 years old, except FRMII and OPAL which are about 20 years old [93]. They are prone to shutdowns for maintenance, social, economic, political and other unexpected reasons. The exclusive dependency of radionuclide production on nuclear reactors is known to lead to major supply shortages. For ^{99m}Tc, (the workhorse of SPECT nuclear diagnostics) the 95% of its global supply is dependent on seven research nuclear reactors and supplied by five target processing facilities. In the period 2008 – 2010, 3 major reactors involved in the production of ^{99}Mo were shut down because of (unforeseen) maintenance reasons. This led to a crisis situation and thousands of patients were denied diagnostic procedures and some were treated with inferior or more expensive radiopharmaceuticals [94,95]. This was followed by about 11 serious disruptions due to temporary reactor shutdowns [96-99]. Learning from the past, there is a uniform consensus among the nuclear medicine scientists that development of production pathways that are more independent on short-term nuclear reactor availability are essential to ensure supply of diagnostic and therapeutic radionuclides[100-102]. For ^{177}Lu production, research has been conducted on the use of charged particle reactions and neutron generators to provide some independence from the nuclear reactor production [22,43,103-106]. However, none of the proposed routes could be envisaged for the large-scale production of ^{177}Lu due to technological and economical challenges.

The radionuclide production via a "radionuclide generator" represents the ideal production system as it can establish on-site, on-demand radionuclide production without a necessary continuous access to an accelerator or research reactor [107]. This thesis is aimed at studying the ^{177}Lu production via a ^{177m}Lu/ ^{177}Lu radionuclide generator. A ^{177m}Lu/ ^{177}Lu radionuclide generator can complement the current production routes and provides some independence from nuclear reactors. The working principle behind the development of a ^{177m}Lu/ ^{177}Lu radionuclide generator is discussed in detail in section 1.5.

1.5. Development of a ^{177m}Lu/ ^{177}Lu radionuclide generator

1.5.1. Radionuclide Generator- a brief introduction

Radionuclide generators are devices that produce a short-lived radionuclide (known as daughter) from the radioactive decay of a long-lived radionuclide (called parent) [108]. Radionuclide generators were historically called ''cows" since the daughter radionuclide was ''milked'' (i.e., separated) from its parent, while the parent continued to generate fresh daughter, just by its ongoing decay events. This way, generators offer a unique advantage of providing on-site and on-demand availability of the desired radionuclide without the continuous need of a nearby reactor, accelerator or any radionuclide production facility [107,109-111]. The radionuclide generators rely on equilibrium between the parent and daughter nuclei, depending on the half-lives of the species involved. The growth of the daughter radionuclide with time for such a system can be described using the Equation 1 below:

$$N_2^t = \frac{\lambda_1}{\lambda_2 - \lambda_1} * N_1^0(exp^{-\lambda_1 t} - exp^{-\lambda_2 t}) + N_2^0 exp^{-\lambda_2 t} \qquad \text{Equation 1}$$

where N_1^0 , N_2^0 are the number of atoms of the parent and daughter radionuclide, respectively present at time t = 0.
N_2^t is the number of the daughter atoms produced after a time t.
λ_1 and λ_2 are the decay constants of the parent and daughter radionuclide, respectively.
The first group of terms reflects the growth of a daughter radionuclide from a parent radionuclide and the decay of these radionuclides, while the second term gives the contribution at any time from the ''daughter'' radionuclides present initially.
Probably the most classic example of such systems is the ^{99}Mo/ ^{99m}Tc radionuclide generator. In this generator, ^{99}Mo is adsorbed on an aluminium oxide chromatographic column and later elution with normal saline solution results in a sodium pertechnetate solution [108]. The availability of ^{99m}Tc via a ^{99}Mo/ ^{99m}Tc generator has played a significant role in the development of ^{99m}Tc labelled radiopharmaceuticals [108]. The current state of the art use of other ^{188}Re, ^{68}Ga, ^{44}Ti, ^{90}Y labelled pharmaceuticals also owes its existence largely to the availability of radionuclide generators [112,113]Overviews of the advantages, principles and criteria for selection of parent/daughter pairs for a radionuclide generator system have been reported and discussed in detail in several reviews [110,111,114-117].

Generally, in generators, the parents and daughters are different in chemistry (i.e. Mo and Tc), which makes that relatively easy and straightforward separation of the immobilized parent and the daughter are possible. The idea of a ^{177m}Lu/ ^{177}Lu radionuclide generator is a unique concept when compared to the existing radionuclide generators, as it involves chemically identical parent/ daughter radionuclide pairs, the ^{177m}Lu and ^{177}Lu.

1.5.2. The ^{177m}Lu/^{177}Lu radionuclide generator- working principle

The ^{177m}Lu/ ^{177}Lu radionuclide generator is based on the use of the long-lived metastable isomer ^{177m}Lu as the parent radionuclide to produce the daughter ^{177}Lu. 78.6% of the ^{177m}Lu decays by beta emission to ^{177m}Hf and 21.4% decays to ^{177}Lu via isomeric transition [118-123].

Isomeric transition (IT) is a process where a metastable nucleus in high energy state loses its excess energy either in the form of a gamma ray emission or through a process known as internal conversion. The internal conversion (IC) process involves the transfer of excess of energy to one of the inner electrons resulting in the emission of that electron from the atom (as shown in Figure 5) [124]. The vacancy created by the emitted electron is rapidly filled by an electron from a higher energy level. In the process of filling the lower shell, the excess energy of the electron in the higher energy level is lost either as a characteristic X-ray photon or it is transferred to an outer electron, resulting in the emission of that electron referred to as an Auger electron (see Figure 5). The process of Auger electron emission leads to the creation of a new vacancy in the higher energy level and the two effects (X- ray emission and Auger electron emission) compete again to fill the newly created vacancy. The particular case of multiple Auger electron emission, is often accompanied with the loss of multiple valence electrons, leaving the atom in a highly positively charged state. The charged state can cause molecular repulsions and may lead to bond rupture if the atom is in a bound state [125,126].

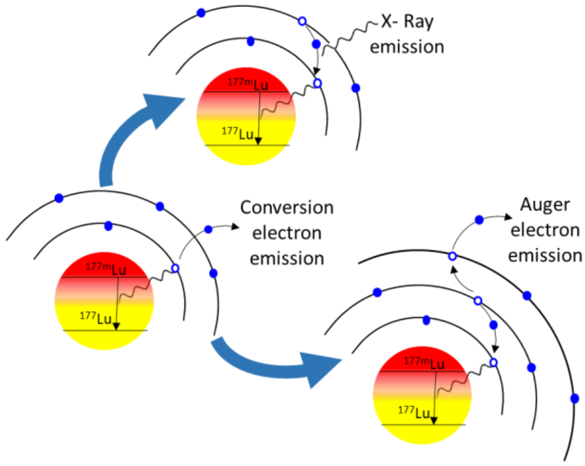

Figure 5: Schematic representation of the process of Internal Conversion

The competition between the conversion electron emission and the γ ray emission during the isomeric transition, is defined by the internal conversion coefficient [26 26]

$$\alpha = \frac{\text{Number of conversion electrons}(\mathrm{I_e})}{\text{Number of gamma rays }(\mathrm{I_\gamma})}$$

The total number of transitions; $\mathrm{I} = \mathrm{I_e} + \mathrm{I_\gamma} = \mathrm{I_\gamma}\,(1 + \alpha)$,
And thus, the probability of internal conversion (P.I.C) is defined as $\frac{\alpha}{1+\alpha}$

The larger the ICC (α) value, the higher is the chance of emission of conversion electrons over the gamma ray emission. The potential of internal conversion in nuclear isomer separation has been experimentally proved in the separation of nuclear isomers such as, ^{80m}Br (α = 298),

^{80m}Te (α ~ 0.26), ^{58m}Co (α ~ 10^3) [127-130]. However, no internal conversion based separation was observed for ^{69}Zn (α = 0.05) and ^{44m}Sc (α = 0.13) isomers (possibly due to their low ICC) [131]. In the particular case of ^{177m}Lu, the 116 keV transition involved in the gamma decay of ^{177m}Lu to ^{177}Lu has an internal conversion coefficient 30.7 [132], implying that about 97% of the transitions are internally converted.

In 2012, the internal conversion of ^{177m}Lu to ^{177}Lu was foreseen as a potential pathway to establish a ^{177m}Lu/ ^{177}Lu radionuclide generator for lutetium-177 production by De Vries and Wolterbeek [43]. It is different from the previously reported cases, as in those cases the bond rupture occurred with chemically separable forms, which do not readily undergo exchange with each other allowing an easy separation [127-130]. However, ^{177}Lu and ^{177m}Lu are chemically indistinguishable nuclear isomers and their separation has never been reported in the literature. The idea behind the internal conversion based ^{177m}Lu- ^{177}Lu separation involves the use of ^{177m}Lu in a bonded state with a complexing agent, followed by the internal conversion based radionuclide decay which will break the bonds and release the newly formed ^{177}Lu as free ion. Thus providing with an opportunity for nuclear isomer separation, where ^{177m}Lu and ^{177}Lu can be distinguished as complexed and free ion respectively. This idea will be elaborated in more details in Chapter 2.

1.5.3. Potential and Challenges

A ^{177m}Lu/ ^{177}Lu radionuclide generator can bring revolutionary advances in the development of ^{177}Lu-based radiopharmaceuticals, by offering the following advantages:

- The long half-life parent (^{177m}Lu, $t_{1/2}$ = 160.44 days) can lead to long-term ^{177}Lu supply without the short-term need of a reactor.
- It would lead to on-site, on-demand production of ^{177}Lu.
- The possible production of no-carrier added, high specific activity ^{177}Lu.

The realization of such a generator has not been demonstrated yet and offers several challenges such as;

- Separation of the chemically alike nuclear isomers ^{177}Lu and ^{177m}Lu.
- The separation process should allow the periodical extraction of the produced ^{177}Lu without any significant manipulation and with many repetitions during the lifetime of the generator.
- Large-scale production of high specific activity ^{177m}Lu as the starting material.
- Very stable ^{177m}Lu bonding to its support throughout the life-time of the generator
- The generator should provide high specific activity ^{177}Lu with high radionuclide purity.

However, overcoming the above mentioned challenges may potentially lead to round-the-clock availability of ^{177}Lu without the continuous dependency on the availability of a nuclear reactor. It can substantially increase the global access to ^{177}Lu and bring significant advances in the research on ^{177}Lu-based pharmaceuticals.

1.6. Scope and Outline of thesis

This thesis focuses on the development of different chemical separation processes to achieve the ^{177m}Lu-^{177}Lu chemical separation and provides an understanding on the factors affecting the separation. A theoretical and experimental assessment on the large scale ^{177m}Lu production is also performed. Lastly, a theoretical evaluation of the potential of ^{177m}Lu/ ^{177}Lu radionuclide generator in lutetium-177 production is presented.

In Chapter 2, reverse phase column chromatography and ^{177m}Lu-DOTATATE complex is used to achieve the ^{177m}Lu-^{177}Lu separation. The effect of temperature on ^{177m}Lu-^{177}Lu separation is studied. The separation is performed under two different modes, the continuous elution and accumulation elution mode. Here, the first proof-of-principle for the internal conversion based ^{177}Lu-^{177m}Lu separation is provided. Prior to separation, the ^{177m}Lu- ^{177}Lu exist in equilibrium with each other and have a ^{177}Lu/ ^{177m}Lu activity ratio of 0.25. In this work, a ^{177}Lu/ ^{177m}Lu activity ratio up to 250 was achieved after separation accounting to a 10,000 times ^{177}Lu enrichment.

Chapter 3 focuses on Liquid-Liquid Extraction based separation of ^{177}Lu and ^{177m}Lu. It describes the use of Liquid- Liquid Extraction (LLE) in combination with a [^{177m}Lu]Lu-DOTA and [^{177m}Lu]Lu-DOTATATE complex, to achieve the ^{177}Lu-^{177m}Lu separation. Here the effect of different Lu:DOTA molar ratios on the ^{177m}Lu-^{177}Lu separation is studied. The ^{177}Lu separation is performed at a regular interval of 7 days for a total time period of up to 30 days. This separation method resulted in the ^{177}Lu/ ^{177m}Lu activity ratios up to 3500.

Chapter 4 describes a solid phase extraction based ^{177}Lu- ^{177m}Lu separation method. It involves the grafting of DOTA on the surface of commercially available amino propyl silica. The successful grafting of DOTA on silica was confirmed by doing the characterization studies such as, ^{13}C-Nuclear Magnetic Resonance (NMR) spectroscopy, infrared spectroscopy, and thermogravimetric analysis (TGA). Here, the ^{177}Lu- ^{177m}Lu separation ratios up to 25 were achieved.

In Chapter 5 a theoretical and experimental evaluation of large-scale ^{177m}Lu production is presented. The ^{177m}Lu related neutron capture cross sections were experimentally verified by performing an irradiation experiment at the BR2 reactor, Belgium. The large-scale production of lutetium-177m was theoretically evaluated in the present nuclear reactor infrastructure and the influence of different factors such as neutron flux, irradiation time and target requirements on ^{177m}Lu production were defined.

Chapter 6 presents the modelling of a ^{177m}Lu/ ^{177}Lu radionuclide generator. In this chapter, the technical requirements and clinical potential of a ^{177m}Lu/ ^{177}Lu radionuclide generator is theoretically evaluated. Finally, in Chapter 7 the general conclusions are presented along with the future outlook.

1.6. References

1 http://www.who.int/news-room/fact-sheets/detail/cancer. (12 september 2018).

2 http://gco.iarc.fr/tomorrow/home. *Cancer tomorrow- IARC*.

3 Arruebo, M. *et al.* Assessment of the Evolution of Cancer Treatment Therapies. *Cancers* **3**, doi:10.3390/cancers3033279 (2011).

4 Jadvar, H. Targeted Radionuclide Therapy: An Evolution Toward Precision Cancer Treatment. *AJR. American journal of roentgenology* **209**, 277-288, doi:10.2214/ajr.17.18264 (2017).

5 Gudkov, S. V., Shilyagina, N. Y., Vodeneev, V. A. & Zvyagin, A. V. Targeted Radionuclide Therapy of Human Tumors. *International journal of molecular sciences* **17**, 33, doi:10.3390/ijms17010033 (2015).

6 Qian, C.-N., Mei, Y. & Zhang, J. Cancer metastasis: issues and challenges. *Chinese journal of cancer* **36**, 38-38, doi:10.1186/s40880-017-0206-7 (2017).

7 Trtic-Petrovic, T. M., Kumric, K. R., Dordevic, J. S. & Vladisavljevic, G. T. Extraction of lutetium(III) from aqueous solutions by employing a single fibre-supported liquid membrane. *J. Sep. Sci.* **33**, 2002-2009, doi:10.1002/jssc.201000042 (2010).

8 Gill, M. R., Falzone, N., Du, Y. & Vallis, K. A. Targeted radionuclide therapy in combined-modality regimens. *Lancet Oncol* **18**, e414-e423, doi:10.1016/s1470-2045(17)30379-0 (2017).

9 Dash, A., F Russ Knapp, F. & RA Pillai, M. Targeted radionuclide therapy-an overview. *Current radiopharmaceuticals* **6**, 152-180 (2013).

10 Cutler, C. S., Hennkens, H. M., Sisay, N., Huclier-Markai, S. & Jurisson, S. S. Radiometals for combined imaging and therapy. *Chemical reviews* **113**, 858-883 (2012).

11 Knapp, F. F. & Dash, A. in *Radiopharmaceuticals for Therapy* (eds F. F. Knapp & Ashutosh Dash) 3-23 (Springer India, 2016).

12 Council, N. R. *Advancing nuclear medicine through innovation*. (National Academies Press, 2007).

13 Zukotynski, K., Jadvar, H., Capala, J. & Fahey, F. Targeted Radionuclide Therapy: Practical Applications and Future Prospects. *Biomarkers in Cancer* **8**, 35-38, doi:10.4137/BIC.S31804 (2016).

14 Cuaron, J. J. *et al.* A proposed methodology to select radioisotopes for use in radionuclide therapy. *AJNR. American journal of neuroradiology* **30**, 1824-1829, doi:10.3174/ajnr.A1773 (2009).

15 Dash, A., Knapp, F. F. & Pillai, M. R. Targeted radionuclide therapy--an overview. *Curr Radiopharm* **6**, 152-180 (2013).

16 Das, T. & Pillai, M. R. Options to meet the future global demand of radionuclides for radionuclide therapy. *Nucl Med Biol* **40**, 23-32, doi:10.1016/j.nucmedbio.2012.09.007 (2013).

17 Carlsson, J., Forssell Aronsson, E., Hietala, S.-O., Stigbrand, T. & Tennvall, J. Tumour therapy with radionuclides: assessment of progress and problems. *Radiotherapy and Oncology* **66**, 107-117, doi:https://doi.org/10.1016/S0167-8140(02)00374-2 (2003).

18 Nitipir, C. *et al.* Update on radionuclide therapy in oncology. *Oncology Letters* **14**, 7011-7015, doi:10.3892/ol.2017.7141 (2017).

19 Yeong, C.-H., Cheng, M.-h. & Ng, K.-H. Therapeutic radionuclides in nuclear medicine: current and future prospects. *Journal of Zhejiang University. Science. B* **15**, 845-863, doi:10.1631/jzus.B1400131 (2014).

20 Gudkov, S. V., Shilyagina, N. Y., Vodeneev, V. A. & Zvyagin, A. V. Targeted Radionuclide Therapy of Human Tumors. *International Journal of Molecular Sciences* **17**, 33, doi:10.3390/ijms17010033 (2016).

21 Das, T. & Banerjee, S. Theranostic Applications of Lutetium-177 in Radionuclide Therapy. *Current Radiopharmaceuticals* **9**, 94-101 (2016).

22 Banerjee, S., Pillai, M. R. & Knapp, F. F. Lutetium-177 therapeutic radiopharmaceuticals: linking chemistry, radiochemistry, and practical applications. *Chem Rev* **115**, 2934-2974, doi:10.1021/cr500171e (2015).

23 Imam, S. K. Advancements in cancer therapy with alpha-emitters: a review. *International Journal of Radiation Oncology*Biology*Physics* **51**, 271-278, doi:https://doi.org/10.1016/S0360-3016(01)01585-1 (2001).

24 Volkert, W. A., Goeckeler, W. F., Ehrhardt, G. J. & Ketring, A. R. Therapeutic radionuclides: production and decay property considerations. *Journal of nuclear medicine : official publication, Society of Nuclear Medicine* **32**, 174-185 (1991).

25 Lassmann, M. & Eberlein, U. Radiation Dosimetry Aspects of (177)Lu. *Curr Radiopharm* **8**, 139-144 (2015).

26 Cremonesi, M. *et al.* Dosimetry for treatment with radiolabelled somatostatin analogues. A review. *Q J Nucl Med Mol Imaging* **54**, 37-51 (2010).

27 Kwekkeboom, D. J. *et al.* Overview of results of peptide receptor radionuclide therapy with 3 radiolabeled somatostatin analogs. *Journal of nuclear medicine : official publication, Society of Nuclear Medicine* **46 Suppl 1**, 62s-66s (2005).

28 Kraeber-Bodere, F. *et al.* Radioimmunoconjugates for the Treatment of Cancer. *Semin. Oncol.* **41**, 613-622, doi:10.1053/j.seminoncol.2014.07.004 (2014).

29 Van Dyke, M., Punja, M., Hall, M. J. & Kazzi, Z. Evaluation of toxicological hazards from medical radioiodine administration. *Journal of medical toxicology : official journal of the American College of Medical Toxicology* **11**, 96-101, doi:10.1007/s13181-014-0412-5 (2015).

30 Banerjee, S., Pillai, M. R. A. & Knapp, F. F. Lutetium-177 Therapeutic Radiopharmaceuticals: Linking Chemistry, Radiochemistry, and Practical Applications. *Chemical Reviews* **115**, 2934-2974, doi:10.1021/cr500171e (2015).

31 Vallabhajosula, S. *et al.* Lutetium-177 may be a better choice for radionuclide therapy than iodine-131 and yttrium-90. *Eur J Nucl Med* **28**, 967-967 (2001).

32 Yordanov, A. T., Hens, M., Pegram, C., Bigner, D. D. & Zalutsky, M. R. Antitenascin antibody 81C6 armed with Lu-177: in vivo comparison of macrocyclic and acyclic ligands. *Nuclear Medicine and Biology* **34**, 173-183, doi:10.1016/j.nucmedbio.2006.11.003 (2007).

33 Hruby, M. *et al.* Lutetium-177 and iodine-131 loaded chelating polymer microparticles intended for radioembolization of liver malignancies. *React. Funct. Polym.* **71**, 1155-1159, doi:10.1016/j.reactfunctpolym.2011.09.003 (2011).

34 Parus, J. L., Pawlak, D., Mikolajczak, R. & Duatti, A. Chemistry and bifunctional chelating agents for binding (177)Lu. *Curr Radiopharm* **8**, 86-94 (2015).

35 Chang, C. A. *et al.* Synthesis, characterization, and crystal structures of M(DO3A) (M = iron, gadolinium) and Na[M(DOTA)] (M = Fe, yttrium, Gd). *Inorganic Chemistry* **32**, 3501-3508, doi:10.1021/ic00068a020 (1993).

36 Benetollo, F., Bombieri, G., Calabi, L., Aime, S. & Botta, M. Structural Variations Across the Lanthanide Series of Macrocyclic DOTA Complexes: Insights into the Design of Contrast Agents for Magnetic Resonance Imaging. *Inorganic Chemistry* **42**, 148-157, doi:10.1021/ic025790n (2003).

37 Viola-Villegas, N. & Doyle, R. P. The coordination chemistry of 1,4,7,10-tetraazacyclododecane-N,N′,N″,N‴-tetraacetic acid (H4DOTA): Structural overview and analyses on structure–stability relationships. *Coordination Chemistry Reviews* **253**, 1906-1925, doi:http://dx.doi.org/10.1016/j.ccr.2009.03.013 (2009).

38 Arisaka, M., Takuwa, N. & Suganuma, H. The Coordination Number of Lu(III) in a Mixed System of Methanol and Water. *J Radioanal Nucl Chem* **245**, 469-473, doi:10.1023/A:1006780404167 (2000).

39 Breeman, W. A. P., de Jong, M., Visser, T. J., Erion, J. L. & Krenning, E. P. Optimising conditions for radiolabelling of DOTA-peptides with 90Y, 111In and 177Lu at high specific activities. *European Journal of Nuclear Medicine and Molecular Imaging* **30**, 917-920, doi:10.1007/s00259-003-1142-0 (2003).

40 Kim, K. & Kim, S.-J. Lu-177-Based Peptide Receptor Radionuclide Therapy for Advanced Neuroendocrine Tumors. *Nucl Med Mol Imaging* **52**, 208-215, doi:10.1007/s13139-017-0505-6 (2018).

41 Ferdinandus, J., Violet, J., Sandhu, S. & Hofman, M. S. Prostate-specific membrane antigen theranostics: therapy with lutetium-177. *Current opinion in urology* **28**, 197-204, doi:10.1097/mou.0000000000000486 (2018).

42 Emmett, L. *et al.* Lutetium 177 PSMA radionuclide therapy for men with prostate cancer: a review of the current literature and discussion of practical aspects of therapy. *Journal of medical radiation sciences* **64**, 52-60, doi:doi:10.1002/jmrs.227 (2017).

43 Vries*, D. J. D. & Wolterbeek, H. T. Tijdschrift voor nucleaire geneeskunde. 899-904 (2012).

44 Chakraborty, S., Vimalnath, K. V., Lohar, S., Shetty, P. & Dash, A. On the practical aspects of large-scale production of 177Lu for peptide receptor radionuclide therapy

using direct neutron activation of 176Lu in a medium flux research reactor: the Indian experience. *J Radioanal Nucl Chem* **302**, 233-243, doi:10.1007/s10967-014-3169-z (2014).

45 Ferro-Flores, G., Arteaga de Murphy, C. & Meléndez-Alafort, L. Third generation radiopharmaceuticals for imaging and targeted therapy. *Current Pharmaceutical Analysis* **2**, 339-352 (2006).

46 https://www.fda.gov/NewsEvents/Newsroom/PressAnnouncements/ucm594043.htm.

47 Hofman, M. S. *et al.* [(177)Lu]-PSMA-617 radionuclide treatment in patients with metastatic castration-resistant prostate cancer (LuPSMA trial): a single-centre, single-arm, phase 2 study. *Lancet Oncol* **19**, 825-833, doi:10.1016/s1470-2045(18)30198-0 (2018).

48 Yadav, M. P. *et al.* (177)Lu-DKFZ-PSMA-617 therapy in metastatic castration resistant prostate cancer: safety, efficacy, and quality of life assessment. *Eur J Nucl Med Mol Imaging* **44**, 81-91, doi:10.1007/s00259-016-3481-7 (2017).

49 Hofman, M. S. *et al.* 785OLutetium-177 PSMA (LuPSMA) theranostics phase II trial: Efficacy, safety and QoL in patients with castrate-resistant prostate cancer treated with LuPSMA. *Annals of Oncology* **28**, mdx370.002-mdx370.002, doi:10.1093/annonc/mdx370.002 (2017).

50 Heck, M. M. *et al.* Clinical experience with 100 consecutive patients treated with Lu-177-labeled PSMA-I&T radioligand therapy for metastatic castration-resistant prostate cancer. *Journal of Clinical Oncology* **36**, 206-206, doi:10.1200/JCO.2018.36.6_suppl.206 (2018).

51 Tagawa, S. T. *et al.* Phase II study of Lutetium-177-labeled anti-prostate-specific membrane antigen monoclonal antibody J591 for metastatic castration-resistant prostate cancer. *Clin Cancer Res* **19**, 5182-5191, doi:10.1158/1078-0432.ccr-13-0231 (2013).

52 Rahbar, K. *et al.* Response and Tolerability of a Single Dose of 177Lu-PSMA-617 in Patients with Metastatic Castration-Resistant Prostate Cancer: A Multicenter Retrospective Analysis. *Journal of nuclear medicine : official publication, Society of Nuclear Medicine* **57**, 1334-1338, doi:10.2967/jnumed.116.173757 (2016).

53 Heck, M. M. *et al.* Systemic Radioligand Therapy with (177)Lu Labeled Prostate Specific Membrane Antigen Ligand for Imaging and Therapy in Patients with Metastatic Castration Resistant Prostate Cancer. *The Journal of urology* **196**, 382-391, doi:10.1016/j.juro.2016.02.2969 (2016).

54 von Eyben, F. E. *et al.* Third-line treatment and (177)Lu-PSMA radioligand therapy of metastatic castration-resistant prostate cancer: a systematic review. *Eur J Nucl Med Mol Imaging* **45**, 496-508, doi:10.1007/s00259-017-3895-x (2018).

55 Rasaneh, S., Rajabi, H., Babaei, M. H. & Daha, F. J. 177Lu labeling of Herceptin and preclinical validation as a new radiopharmaceutical for radioimmunotherapy of breast cancer. *Nuclear medicine and biology* **37**, 949-955 (2010).

56 Yook, S. *et al.* Intratumorally Injected 177Lu-Labeled Gold Nanoparticles: Gold Nanoseed Brachytherapy with Application for Neoadjuvant Treatment of Locally Advanced Breast Cancer. *Journal of nuclear medicine : official publication, Society of Nuclear Medicine* **57**, 936-942, doi:10.2967/jnumed.115.168906 (2016).

57 Cai, Z. *et al.* Local radiation treatment of HER2-positive breast cancer using trastuzumab-modified gold nanoparticles labeled with 177 Lu. *Pharmaceutical research* **34**, 579-590 (2017).

58 Rasaneh, S., Rajabi, H., Babaei, M. H., Daha, F. J. & Salouti, M. Radiolabeling of trastuzumab with 177Lu via DOTA, a new radiopharmaceutical for radioimmunotherapy of breast cancer. *Nucl Med Biol* **36**, 363-369, doi:10.1016/j.nucmedbio.2009.01.015 (2009).

59 Lewis, M. R. *et al.* Biological comparison of 149Pm-, 166Ho-, and 177Lu-DOTA-biotin pretargeted by CC49 scFv-streptavidin fusion protein in xenograft-bearing nude mice. *Nucl Med Biol* **31**, 213-223, doi:10.1016/j.nucmedbio.2003.08.004 (2004).

60 Rogers, B. E. *et al.* Intraperitoneal radioimmunotherapy with a humanized anti-TAG-72 (CC49) antibody with a deleted CH2 region. *Cancer biotherapy & radiopharmaceuticals* **20**, 502-513, doi:10.1089/cbr.2005.20.502 (2005).

61 Chauhan, S. C. *et al.* Pharmacokinetics and biodistribution of 177Lu-labeled multivalent single-chain Fv construct of the pancarcinoma monoclonal antibody CC49. *Eur J Nucl Med Mol Imaging* **32**, 264-273, doi:10.1007/s00259-004-1664-0 (2005).

62 Eriksson, S. E., Ohlsson, T., Nilsson, R. & Tennvall, J. Treatment with unlabeled mAb BR96 after radioimmunotherapy with 177Lu-DOTA-BR96 in a syngeneic rat colon carcinoma model. *Cancer biotherapy & radiopharmaceuticals* **27**, 175-182, doi:10.1089/cbr.2011.1132 (2012).

63 Dho, S. H. *et al.* Development of a radionuclide-labeled monoclonal anti-CD55 antibody with theranostic potential in pleural metastatic lung cancer. *Scientific Reports* **8**, 8960, doi:10.1038/s41598-018-27355-8 (2018).

64 Repetto-Llamazares, A. H., Larsen, R. H., Mollatt, C., Lassmann, M. & Dahle, J. Biodistribution and dosimetry of (177)Lu-tetulomab, a new radioimmunoconjugate for treatment of non-Hodgkin lymphoma. *Curr Radiopharm* **6**, 20-27 (2013).

65 Repetto-Llamazares, A. H. V. *et al.* Combination of (177) Lu-lilotomab with rituximab significantly improves the therapeutic outcome in preclinical models of non-Hodgkin's lymphoma. *European journal of haematology*, doi:10.1111/ejh.13139 (2018).

66 Kolstad, A. *et al.* Efficacy and Safety Results of a Phase 1 Study of ¹⁷⁷ lu-DOTA-HH1 (Betalutin®) with and without HH1 Pre-Dosing for Patients with Relapsed CD37+ Non-Hodgkin B Cell Lymphoma (NHL). *Blood* **126**, 5118-5118 (2015).

67 Blakkisrud, J. *et al.* Tumor-Absorbed Dose for Non-Hodgkin Lymphoma Patients Treated with the Anti-CD37 Antibody Radionuclide Conjugate 177Lu-Lilotomab

Satetraxetan. *Journal of nuclear medicine : official publication, Society of Nuclear Medicine* **58**, 48-54, doi:10.2967/jnumed.116.173922 (2017).

68 Stokke, C. *et al.* Pre-dosing with lilotomab prior to therapy with 177Lu-lilotomab satetraxetan significantly increases the ratio of tumor to red marrow absorbed dose in non-Hodgkin lymphoma patients. *European Journal of Nuclear Medicine and Molecular Imaging* **45**, 1233-1241, doi:10.1007/s00259-018-3964-9 (2018).

69 Shinto, A. S. *et al.* (1)(7)(7)Lu-EDTMP for treatment of bone pain in patients with disseminated skeletal metastases. *Journal of nuclear medicine technology* **42**, 55-61, doi:10.2967/jnmt.113.132266 (2014).

70 Alavi, M., Omidvari, S., Mehdizadeh, A., Jalilian, A. & Bahrami-Samani, A. Metastatic Bone Pain Palliation using ¹⁷⁷ Lu-Ethylenediaminetetramethylene Phosphonic Acid. *World Journal of Nuclear Medicine* **14**, 109-115, doi:10.4103/1450-1147.157124 (2015).

71 Sharma, S., Singh, B., Koul, A. & Mittal, B. R. Comparative Therapeutic Efficacy of (153)Sm-EDTMP and (177)Lu-EDTMP for Bone Pain Palliation in Patients with Skeletal Metastases: Patients' Pain Score Analysis and Personalized Dosimetry. *Front Med (Lausanne)* **4**, 46, doi:10.3389/fmed.2017.00046 (2017).

72 Yuan, J. *et al.* Efficacy and safety of 177Lu-EDTMP in bone metastatic pain palliation in breast cancer and hormone refractory prostate cancer: a phase II study. *Clin Nucl Med* **38**, 88-92, doi:10.1097/RLU.0b013e318279bf4d (2013).

73 Dasari, A., Shen, C., Halperin, D. & et al. Trends in the incidence, prevalence, and survival outcomes in patients with neuroendocrine tumors in the united states. *JAMA Oncology* **3**, 1335-1342, doi:10.1001/jamaoncol.2017.0589 (2017).

74 Editorial. *Radiotherapy and Oncology* **52**, 95-96, doi:https://doi.org/10.1016/S0167-8140(99)00109-7 (1999).

75 Mittra, E. S. Neuroendocrine Tumor Therapy: (177)Lu-DOTATATE. *AJR. American journal of roentgenology* **211**, 278-285, doi:10.2214/ajr.18.19953 (2018).

76 Strosberg, J. *et al.* Phase 3 trial of 177Lu-Dotatate for midgut neuroendocrine tumors. *New England Journal of Medicine* **376**, 125-135 (2017).

77 Brabander, T. *et al.* Long-Term Efficacy, Survival, and Safety of Lu-177-DOTA(0), Tyr(3) octreotate in Patients with Gastroenteropancreatic and Bronchial Neuroendocrine Tumors. *Clinical Cancer Research* **23**, 4617-4624, doi:10.1158/1078-0432.Ccr-16-2743 (2017).

78 Ferdinandus, J., Violet, J., Sandhu, S. & Hofman, M. S. Prostate-specific membrane antigen theranostics: therapy with lutetium-177. *Current opinion in urology* **28** (2018).

79 A Trial of 177Lu-PSMA617 Theranostic Versus Cabazitaxel in Progressive Metastatic Castration Resistant Prostate Cancer (TheraP).

80 Zhang, H. *et al.* Synthesis and evaluation of bombesin derivatives on the basis of pan-bombesin peptides labeled with indium-111, lutetium-177, and yttrium-90 for

targeting bombesin receptor-expressing tumors. *Cancer research* **64**, 6707-6715 (2004).
81 Chakraborty, S., Das, T., Banerjee, S., Sarma, H. D. & Venkatesh, M. Preparation and preliminary biological evaluation of 177Lu-labelled hydroxyapatite as a promising agent for radiation synovectomy of small joints. *Nuclear medicine communications* **27**, 661-668 (2006).
82 Michel, R. B., Andrews, P. M., Rosario, A. V., Goldenberg, D. M. & Mattes, M. J. 177 Lu-antibody conjugates for single-cell kill of B-lymphoma cells in vitro and for therapy of micrometastases in vivo. *Nuclear medicine and biology* **32**, 269-278 (2005).
83 Bander, N. H. *et al.* Phase I trial of 177lutetium-labeled J591, a monoclonal antibody to prostate-specific membrane antigen, in patients with androgen-independent prostate cancer. *Journal of Clinical Oncology* **23**, 4591-4601 (2005).
84 Miao, Y., Hoffman, T. J. & Quinn, T. P. Tumor-targeting properties of 90 Y-and 177 Lu-labeled α-melanocyte stimulating hormone peptide analogues in a murine melanoma model. *Nuclear medicine and biology* **32**, 485-493 (2005).
85 Claringbold, P. G. & Turner, J. H. Pancreatic Neuroendocrine Tumor Control: Durable Objective Response to Combination Lu-Octreotate-Capecitabine-Temozolomide Radiopeptide Chemotherapy. *Neuroendocrinology*, doi:10.1159/000434723 (2015).
86 Liu, D. *et al.* Targeted antisense radiotherapy and dose fractionation using a 177Lu-labeled anti-bcl-2 peptide nucleic acid-peptide conjugate. *Nuclear Medicine and Biology* **42**, 704-710, doi:http://dx.doi.org/10.1016/j.nucmedbio.2015.05.006 (2015).
87 Ando, A. *et al.* 177Lu-EDTMP: a potential therapeutic bone agent. *Nuclear medicine communications* **19**, 587-592 (1998).
88 Stein, R. *et al.* Radioimmunotherapy of a human lung cancer xenograft with monoclonal antibody RS7: evaluation of 177Lu and comparison of its efficacy with that of 90Y and residualizing 131I. *Journal of Nuclear Medicine* **42**, 967-974 (2001).
89 Meredith, R. F., Partridge, E. E., Alvarez, R. D. & Khazaeli, M. Intraperitoneal radioimmunotherapy of ovarian cancer with lutetium-177-CC49. *The Journal of Nuclear Medicine* **37**, 1491 (1996).
90 Cancer Today. *International Agency for Research on Cancer* (2018).
91 International Atomic Energy Agency. *IAEA Nuclear Data Section*, <https://www-nds.iaea.org/relnsd/NdsEnsdf/neutroncs.html> (2015).
92 Erdtmann, G. *Neutron activation tables / Gerhard Erdtmann*. (Verlag Chemie, 1976).
93
94 Ballinger, J. R. Short- and long-term responses to molybdenum-99 shortages in nuclear medicine. *The British Journal of Radiology* **83**, 899-901, doi:10.1259/bjr/17139152 (2010).
95 Gould, P. <Medical isotope shortage reaches crisis level.pdf>. *Nature* **460**, 312-313 (2009).
96 ABN, M. The Global Impact of the Mo-99 Shortage. *Biomed J Sci &Tech Res* **4** (2018).

97 Anon. The French government agrees to decommission Osiris reactor on 31 december 2015. *Revue Generale Nucleaire*, 11 (2014).

98 Tollefson, J. Reactor shutdown threatens world's medical-isotope supply. *Nature* **12** (2016).

99 Mahesh, M. & Madsen, M. Addressing Technetium-99m Shortage. *Journal of the American College of Radiology* **14**, 681-683, doi:10.1016/j.jacr.2017.02.007 (2017).

100 Powe, J., Worsley, D. & Ruth, T. Radioisotope Shortages in Nuclear Medicine: How We Got There and Developing Solutions. *Canadian Association of Radiologists Journal* **61**, 19-22, doi:10.1016/j.carj.2009.11.004 (2010).

101 Ruth, T. J. The medical isotope crisis: how we got here and where we are going. *Journal of nuclear medicine technology* **42**, 245-248, doi:10.2967/jnmt.114.144642 (2014).

102 Metello, L. F. ^{99m}Tc-Technetium Shortage: Old Problems Asking for New Solutions. *Journal of Medical Imaging and Radiation Sciences* **46**, 256-261, doi:10.1016/j.jmir.2015.07.003 (2015).

103 Dzysiuk, N., Kadenko, I., Koning, A. J. & Yermolenko, R. Cross sections for fast-neutron interaction with Lu, Tb, and Ta isotopes. *Physical Review C* **81**, 014610 (2010).

104 Medvedev, D. G., Mausner, L. F., Greene, G. A. & Hanson, A. L. Activation of natural Hf and Ta in relation to the production of 177Lu. *Applied radiation and isotopes : including data, instrumentation and methods for use in agriculture, industry and medicine* **66**, 1300-1306, doi:10.1016/j.apradiso.2008.02.090 (2008).

105 Manenti, S., Bonardi, M. L., Gini, L. & Groppi, F. Physical optimization of production by deuteron irradiation of high specific activity 177gLu suitable for radioimmunotherapy. *Nuclear Medicine and Biology* **41**, 407-409, doi:http://dx.doi.org/10.1016/j.nucmedbio.2014.02.007 (2014).

106 Hermanne, A. *et al.* Deuteron-induced reactions on Yb: Measured cross sections and rationale for production pathways of carrier-free, medically relevant radionuclides. *Nuclear Instruments and Methods in Physics Research Section B: Beam Interactions with Materials and Atoms* **247**, 223-231, doi:http://dx.doi.org/10.1016/j.nimb.2006.03.008 (2006).

107 Knapp, F. F. & Dash, A. in *Radiopharmaceuticals for Therapy* (eds F. F. Knapp & Ashutosh Dash) Ch. 7, 131-157 (Springer India, 2016).

108 Choppin, G. R., Liljenzin, J.-O. & Rydberg, J. in *Radiochemistry and Nuclear Chemistry (Third Edition)* (ed Gregory R. ChoppinJan-Olov LiljenzinJan Rydberg) 94-122 (Butterworth-Heinemann, 2002).

109 Knapp, F. F. & Mirzadeh, S. The continuing important role of radionuclide generator systems for nuclear medicine. *Eur J Nucl Med* **21**, 1151-1165, doi:10.1007/bf00181073 (1994).

110 Knapp, F. F., Pillai, M. R. A., Osso, J. A. & Dash, A. Re-emergence of the important role of radionuclide generators to provide diagnostic and therapeutic radionuclides to

meet future research and clinical demands. *J Radioanal Nucl Chem* **302**, 1053-1068, doi:10.1007/s10967-014-3642-8 (2014).
111 F. Knapp, F. & P. Baum, R. Radionuclide Generators; A New Renaissance in the Development of Technologies to Provide Diagnostic and Therapeutic Radioisotopes for Clinical Applications). *Current Radiopharmaceuticals* **5**, 175-177 (2012).
112 Roesch, F. & J. Riss, P. The Renaissance of the 68Ge/68Ga Radionuclide Generator Initiates New Developments in 68Ga Radiopharmaceutical Chemistry. *Current Topics in Medicinal Chemistry* **10**, 1633-1668, doi:10.2174/156802610793176738 (2010).
113 Pillai, M. R. A., Ashutosh, D. & Knapp, F. F. Rhenium-188: Availability from the 188W/188Re Generator and Status of Current Applications. *Current Radiopharmaceuticals* **5**, 228-243, doi:http://dx.doi.org/10.2174/1874471011205030228 (2012).
114 Prince, J. R. Comments on Equilibrium, Transient Equilibrium, and Secular Equilibrium in Serial Radioactive Decay. *Journal of Nuclear Medicine* **20**, 162-164 (1979).
115 Stang, L. G., Brookhaven National, L. & Commission, U. S. A. E. *Radionuclide generators: past, present, and future*. (Brookhaven National Laboratory, 1969).
116 Lebowitz, E. & Richards, P. Radionuclide generator systems. *Seminars in Nuclear Medicine* **4**, 257-268, doi:10.1016/S0001-2998(74)80013-9.
117 Knapp, F. F., Jr., Callahan, A. P., Mirzadeh, S., Brihaye, C. & Guillaume, M. in *Progress in Radiopharmacy* Vol. 22 *Developments in Nuclear Medicine* (eds P. August Schubiger & Gerrit Westera) Ch. 8, 67-88 (Springer Netherlands, 1992).
118 Hnatowicz, V. Precise measurement of gamma-ray intensities in the decay of 160·9 day isomeric state in177Lu. *Czech J Phys* **31**, 260-268, doi:10.1007/BF01604508 (1981).
119 Alexander, P., Boehm, F., Kankeleit, E. Spin- 23/2- Isomer of Lu-177. *Phys. Rev.*, B284–B290 (1964).
120 Deepa, S., Vijay Sai, K., Gowrishankar, R. & Venkataramaniah, K. The 160.44 day 177mLu as a new gamma calibration standard. *Radiation Physics and Chemistry* **81**, 226-231, doi:http://dx.doi.org/10.1016/j.radphyschem.2011.11.006 (2012).
121 Nethaway, D. R. & Mendoza, B. The half-life and formation cross-section of 177mLu. *Journal of Inorganic and Nuclear Chemistry* **29**, 865-867, doi:http://dx.doi.org/10.1016/0022-1902(67)80069-1 (1967).
122 Kondev, F. G. Nuclear Data Sheets for A = 177. *Nuclear Data Sheets* **98**, 801-1095, doi:http://dx.doi.org/10.1006/ndsh.2003.0006 (2003).
123 Kondev, F. G. *et al.* Gamma-ray emission probabilities in the decay of 177mLu. *Applied Radiation and Isotopes* **70**, 1867-1870, doi:10.1016/j.apradiso.2012.02.029 (2012).
124 L'Annunziata, M. F. in *Handbook of Radioactivity Analysis (Third Edition)* (ed Michael F. L'Annunziata) 1-162 (Academic Press, 2012).
125 Cooper, E. P. On the Separation of Nuclear Isomers. *Physical Review* **61**, 1-5, doi:10.1103/PhysRev.61.1 (1942).
126 Friedlander, G. *Nuclear and radiochemistry*. 3rd ed. edn, 438 (Wiley, 1981).

127 Kibédi, T., Burrows, T. W., Trzhaskovskaya, M. B., Davidson, P. M. & Nestor, C. W. Evaluation of theoretical conversion coefficients using BrIcc. *Nuclear Instruments and Methods in Physics Research Section A: Accelerators, Spectrometers, Detectors and Associated Equipment* **589**, 202-229, doi:https://doi.org/10.1016/j.nima.2008.02.051 (2008).

128 Seaborg, G. T. & Kennedy, J. W. Nuclear Isomerism and Chemical Separation of Isomers in Tellurium. *Physical Review* **55**, 410-410, doi:10.1103/PhysRev.55.410.2 (1939).

129 Lazzarini, E. & Fantola Lazzarini, A. L. On the survival of Co(III) complexes to deexcitation by internal conversion of the 58mCo coordinating atom. *Journal of Inorganic and Nuclear Chemistry* **39**, 207-211, doi:http://dx.doi.org/10.1016/0022-1902(77)80001-8 (1977).

130 Langsdorf, A. & Segrè, E. Nuclear Isomerism in Selenium and Krypton. *Physical Review* **57**, 105-110 (1940).

131 Huclier-Markai, S. *et al.* Optimization of reaction conditions for the radiolabeling of DOTA and DOTA-peptide with (44m/44)Sc and experimental evidence of the feasibility of an in vivo PET generator. *Nucl Med Biol* **41 Suppl**, e36-43, doi:10.1016/j.nucmedbio.2013.11.004 (2014).

132 BrIcc program package version 2.2b. (2009).

Chapter 2

Column chromatography based separation of nuclear isomers, ^{177m}Lu and ^{177}Lu.

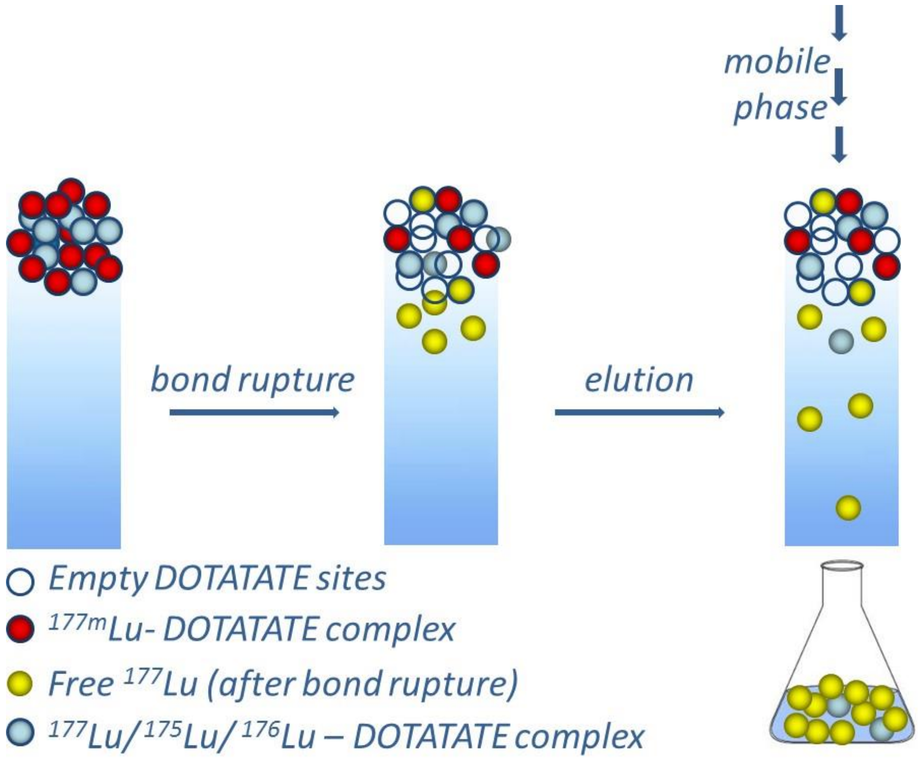

This Chapter has been adapted from:
Bhardwaj, R., van der Meer, A. J. G. M., Das, S. K., De Bruin, M., Gascon, J., Wolterbeek, H. T., & Serra-Crespo, P. (2017). Separation of nuclear isomers for cancer therapeutic radionuclides based on nuclear decay after-effects. Scientific reports, 7, 44242.

Abstract

^{177}Lu has sprung as a promising radionuclide for targeted therapy. The low soft tissue penetration of its β^- emission results in very efficient energy deposition in small-size tumours. Because of this, ^{177}Lu is used in the treatment of neuroendocrine tumours and is also clinically approved for prostate cancer therapy. In this work, we report a separation method that achieves the challenging separation of the chemically identical nuclear isomers, ^{177m}Lu and ^{177}Lu. The separation method combines the after-effects of the nuclear decay, the use of a very stable chemical complex and a chromatographic separation. Based on this separation concept, a new type of radionuclide generator has been devised, in which the parent and the daughter radionuclides are the same elements. The $^{177m}Lu/^{177}Lu$ radionuclide generator provides a new route for the production of therapeutic radionuclide, ^{177}Lu. It can potentially bring significant growth in the research and development of ^{177}Lu based pharmaceuticals.

2.1 Introduction

Lutetium-177 (^{177}Lu) has emerged as a promising radionuclide for targeted radionuclide therapy. The simultaneous emission of low energy β^-, γ-rays and a half-life of 6.64 days have made ^{177}Lu a solid candidate to be the most applied therapeutic radionuclide by 2020 [1]. Its low energy β^- particles with a tissue penetration of less than 3 mm make it suitable for targeting small primary and metastatic tumours, like prostate, breast, melanoma, lung and pancreatic tumours, for bone palliation therapy and other chronic diseases [2-4]. In addition, the emitted γ rays (208.37 and 112.98 keV) allows simultaneous imaging and quantification of the tumour treatment process in vivo [5]. After the success of the pioneering work carried out at Erasmus Medical Centre for treating neuroendocrine tumours with ^{177}Lu-labeled peptides, the treatment is now applied at that hospital to more than 400 patients per year [6-8]. Further, the demand of ^{177}Lu is expected to grow, since it is now clinically approved for use in prostate cancer treatment and many other treatments are in advance advanced clinical trial stages [9-11].

During the production of ^{177}Lu by neutron irradiation of lutetium targets, its nuclear isomer ^{177m}Lu is formed concomitantly [12,13]. A nuclei with the same atomic and mass number but different energy are called nuclear isomers. ^{177m}Lu is a high-energy nuclear isomer with a half-life of 160.44 days. 78.6% of ^{177m}Lu decays by beta emission to ^{177m}Hf and ^{177}Hf and 21.4% decays to ^{177}Lu, the ground state, via isomeric transition [14,15]. Isomeric transition can occur either via internal conversion or γ rays emission (see Figure 1(a)). Internal conversion is a radiationless decay where the excess of nucleus energy is transferred to an electron in the K- L- or M- shell. This energy transfer leads to an auger electron cascade that results in a highly charged state ultimately provoking bond rupture (see Figure 1(b)) [16]. Nuclear isomers of Te, Co and Se have been separated in the past using internal conversion [17-19]. However, in these cases bond rupture resulted in chemically separable forms which do not readily undergo exchange, making the separation feasible. In contrast, in the case of ^{177m}Lu bond rupture leads to chemically alike ^{177}Lu that cannot be separated with the available separation techniques. In the present chapter, we report a separation method that allows the separation of chemically identical nuclear isomers. The method makes use of the nuclear after-effects caused by the internal conversion to separate the newly formed ground state (^{177}Lu) from the metastable state (^{177m}Lu).

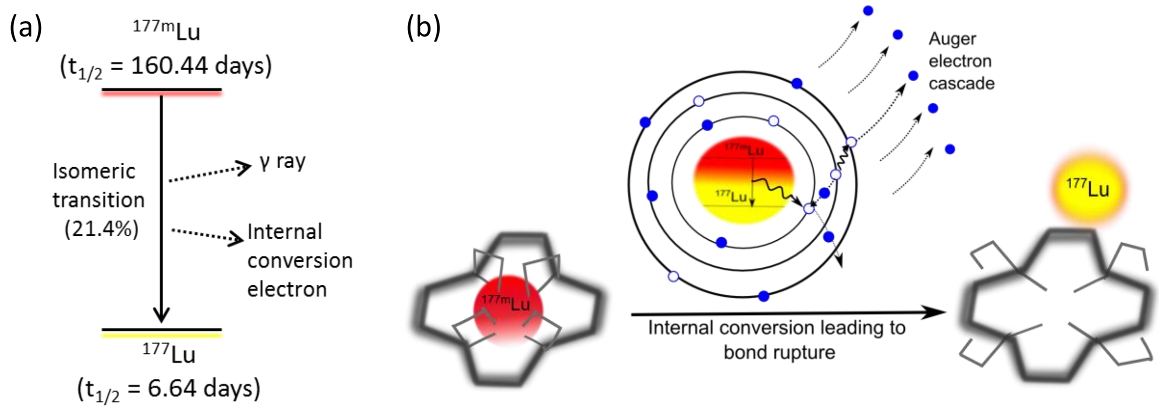

Figure 1. Schematic representation of the decay process. (a) Decay scheme of ^{177m}Lu to ^{177}Lu. (ii) Process of bond rupture. The metastable isomer ^{177m}Lu is coordinated to a very stable complex (left side). During the decay via internal conversion the nucleus excess of energy is transferred to an inner electron causing an auger electron cascade (center). After the cascade the atom is in a highly charge state, the chemical bonds are broken and the freed ^{177}Lu can be separated (right side).

Our nuclear isomer separation process is based on the combination of three elements (see Figure 1(b)): (i) a very inert complex with slow association-dissociation kinetics, (ii) the nuclear after-effects of the internal conversion process that breaks the chemical bonds due to the highly charged state created [20] and (iii) a separation method able to set apart the complexed element and the freed one.

This separation method does not only open up the possibility of separating nuclear isomers, but also a novel radionuclide generator for ^{177}Lu production can be devised on the basis of the much longer half-life of ^{177m}Lu (160.4 days) compared to the 6.7 days half-life of its daughter radionuclide, ^{177}Lu. Radionuclide generators are in-house production devices that provide a specific radionuclide generated through the decay of a parent radionuclide on demand without the need for access to an isotope producing facility [21]. In this way, the inconvenient dependency for irradiations is eliminated and constant, continuous availability of the radionuclide of interest is warranted [22]. However, different from the case at hand, all existing radionuclide generators to date are based on the separation of two different elements that can be chemically separated [23]. While the use of the metastable ^{177m}Lu as the parent radionuclide for ^{177}Lu production was proposed by De Vries and Wolterbeek [24], the realization of a generator has not been demonstrated yet. In order to prove this concept, we have chosen a reversed phase chromatographic system in which ^{177m}Lu-DOTA-(Tyr^3)-octreotate (DOTATATE) complex (with a dissociation constant k_d = 2*10^{-8} s^{-1} at 20°C) is retained in a tC-18 silica column [25]. The tC-18 silica filler has no affinity toward polar metal ions, and thus the bond ruptured ^{177}Lu ions can be eluted off the column using a mobile phase flow, while the ^{177m}Lu-DOTATATE complex exhibits a very long retention time with the chosen mobile phase, and remains immobilized on the column during the experiments (shown schematically in Figure 2(a)). A very similar approach was utilized by Zhernosekov *et al.* to design the

^{140}Nd/^{140}Pr generator. In this case, the parent radionuclide decays via electron capture, a process that leads to an Auger cascade as well. While the parent is retained in a chromatographic column as a complex with DOTATOC, the daughter radionuclide, ^{140}Pr, is separated due to the bond rupture effect caused by the Auger cascade that followed the electron capture nuclear transmutation [26].

2.2 Methods and materials

2.2.1 Materials:

The ^{177m}Lu activity source was provided by IDB Holland. It was approximately 1 mM $LuCl_3$ in 1 M HCl solution with a specific activity of 7.2 MBq. g^{-1} of $LuCl_3$. DOTATATE (Biosynthema) was provided by the Erasmus medical center, Rotterdam. Reversed- phase material, tC-18 silica was purchased in the form of ready to use sep-pak cartridges (Sep-Pak Plus tC18, usable for pH 2–8), from Waters.

2.2.2 Synthesis of ^{177m}Lu-DOTA-(Tyr^3)-octreotate complex:

The ^{177m}Lu solution was adjusted to pH 4 using 1 M NaOH solution, 20 µL of 1 M NaAc-HAc buffer was also added to keep the pH around 4 during the reaction. Lu-DOTA-(Tyr^3)-octreotate, also referred to as Lu-DOTATATE, was synthesized using 0.150 µmoles Lu (150 µL of 1 mM $LuCl_3$ solution, app. 1 MBq ^{177m}Lu) and 0.278 µmoles DOTATATE leading to a total reaction mixture volume about 1 ml. The reaction mixture was then incubated at 80°C for 1 hour. The completion of the reaction was checked using instant thin layer chromatography with 1:1 acetonitrile: water as the mobile phase, and silica as the stationary phase. The reaction conditions resulted in >99% complexation yield.

2.2.3 Experimental setup description:

The experimental set up consists of an HPLC-system consisting of a pump (Shimadzu LC-10Ai), PEEK tubing and a fraction collector for 20 ml vials. The pump was connected to a column made of peek (ID 3 mm x 47 mm). The column was manually filled with tC-18 reversed phase silica (waters). A slurry of tC-18 silica in MeOH was added from one end of the column and the other end was connected with a vacuum pipe. The empty column has a volume of 0.335 mL, after filling the column with silica the void volume is experimentally calculated to be 0.175 mL (details in supplementary info S7). The column was equilibrated with the mobile phase for overnight before injecting the complex. The mobile phase and column were both temperature controlled to the desired temperature by a thermostatic circulation water bath (Colora WK4) and a column water jacket (Alltech). 0, 10, 20, and 30 °C were the studied temperatures.

2.2.4 Mobile phase composition

The mobile phase consists of 5% methanol, 150 mM NaCl solution (ionic strength of 0.148 M) and 10 mM NaAc- HAc buffer (pH-4.3). Mobile phase flux of 0.012 and 0.05 mL/min were used during continuous elution, and 0.1 mL/min is used during accumulation experiments. The whole experimental setup was equilibrated with the mobile phase (for at least two hours) prior to loading of the complex.

2.2.5 Loading of the complex

The complex was loaded on the manually filled tC-18 column using a Rheodyne injector, with a mobile phase flow of 0.1 mL/min. Prior to injection, a 2 µl aliquot was kept aside and measured to know the exact activity loaded on the column. During the first 30 minutes the flow was set to 0.1 mL/min to remove free metal and impurities or side-products. The eluted fraction was then used to measure the amount of activity lost in loading, as impurities/ side products. After the first fraction of 1 hour, the flow rate through the column was adjusted to the desired flow rate at the desired temperature. The same procedure was repeated with three different columns and three different Lu-DOTATATE complexes with the initial activity around 1.45 ± 0.04 MBq, 0.65 ± 0.02MBq, 0.98 ± 0.03 MBq. In all the cases the total initial activity retained on the column is about 98% of the initial activity. Once loaded, a column is used upto three months for doing the measurements. After a maximum period of three months, the column is flushed with pure methanol to remove all the loaded activity.

2.2.6 γ ray spectroscopy analysis

The activity measurements were performed with a well-type HPGe gamma-ray detector. The energy and efficiency calibration of the detector was performed using a certified Eu-152 source, and the efficiency calibration for each lutetium peak was fine-tuned using a known ^{177}Lu, ^{177m}Lu source provided by IDB- Holland to take true-coincidence summing effects into account. The fraction volumes up to 18 mL were collected during the experiments, however all the activity measurements were performed with a fixed 0.4 mL aliquot for a time period of 3 hours. The gamma ray spectra were analyzed using an in-house software to calculate the activity in (Bq. g^{-1}) of each fraction [27]. The activity concentration obtained in Bq. g^{-1} was then multiplied with the total mass of the fraction to know the absolute activity coming out in each fraction. To minimize the errors, all the vials were weighed before and after the fraction collection.

2.2.7 Continuous elution

In the continuous elution mode two flow rates were studied, 0.012, 0.05 mL /min at 10, 20, and 30°C. For each flow rate and temperature six to eight fractions were collected for 6 hour each. Each fraction was measured on the above mentioned well type germanium detector. The individual results and calculations can be found in supplementary information in sections S2 and S3.

2.2.8 Accumulation followed by elution

For accumulation experiments the flow of mobile phase was stopped in the column for 1, 2, 3, 4, 5 days at 10, 20, and 30°C respectively. For flushing the accumulated activity the flow rate of 0.1 mL/min was used and fraction collected in the first 60 minutes was used to measure the efficiency, ^{177}Lu/^{177m}Lu activity ratios. In accumulation experiments, the error bars in activity ratio plots define the instrumental error in the measurement while for efficiency measurements the errors are less than 1%, so they have not been shown in the graphs. Detailed results and explanations have been given in supplementary info S5.

2.3 Results

2.3.1. Continuous elution

Initially, experiments with a continuous flow of mobile phase (or continuous elution) were performed at different temperatures and mobile phase fluxes. The initial ^{177}Lu/^{177m}Lu activity ratio in the ^{177m}Lu-complex was measured to be 0.24 ± 0.03. After loading the complex in the column, it was eluted with a continuous mobile phase with a mobile phase flow of 0.05 mL/min at 20°C. Figure 2(b) displays the obtained ^{177}Lu/^{177m}Lu activity ratio after different elution times. The ^{177}Lu/^{177m}Lu activity ratio changed in the eluted fractions from the value in equilibrium, app 0.24, to an average ratio of 127 ± 14, accounting for an enrichment in ^{177}Lu of more than 500 times. The ratio remains within a small variation up to 60 hours during the continuous elution. The gamma spectra before and after separation of the nuclear isomers are displayed in Figure 2(c) & (d) respectively. The rather complex decay scheme of the mixture injected in the column, that contains ^{177m}Lu, ^{177}Lu and ^{177m}Hf (Figure 2(c)), is in clear contrast with the gamma spectrum of the eluted sample where only the peaks at 113 and 208 keV are observed as the major photo-peaks, from the ^{177}Lu decay. The peaks at 249 KeV and 321 KeV are also present in their expected 0.2% relative gamma yields, however the contribution at 321 KeV is enhanced because of the summation effects in the well type germanium detector.

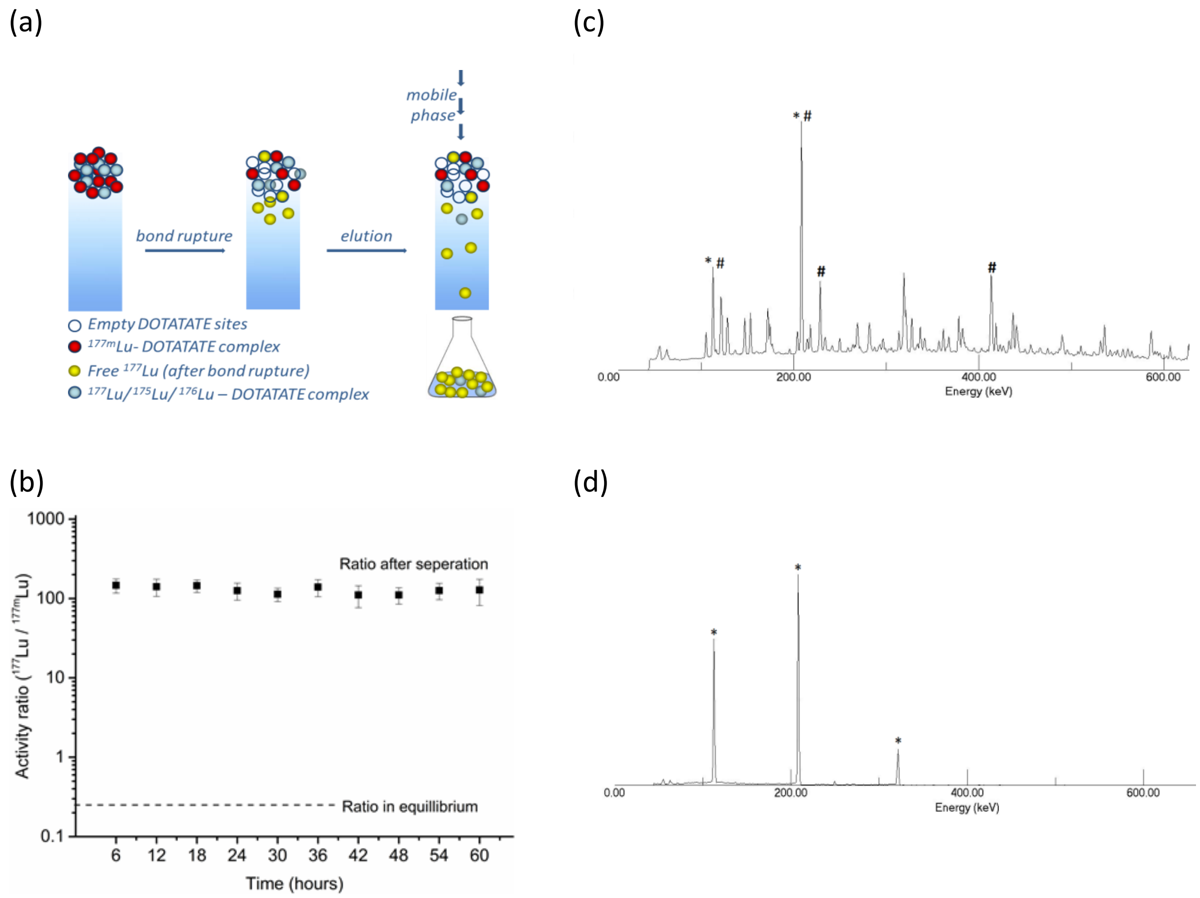

Figure 2: Separation of nuclear isomers ^{177}Lu and ^{177m}Lu (a) Schematic representation of the experimental setup (b) ^{177m}Lu/^{177}Lu activity ratio at continuous elution with a flux of 0.05 mL/min and a temperature of 20°C. (c) γ ray spectra of the mixture injected in the column with photo-peaks having contribution from both ^{177}Lu(*) and ^{177m}Lu(#) (d) γ ray spectra of eluted fraction after separation with major photo-peaks from ^{177}Lu(*), less than 0.5% contribution from ^{177m}Lu. The efficiency of the separation is defined as the ratio of the collected ^{177}Lu activity divided by the theoretical activity of ^{177}Lu produced from the decay of the parent ^{177m}Lu in a specific time (details in supplementary information, Equation S1). Specific time being defined as the time during the collection of the elution fraction, which are 6 hours in the case of continuous elution. During these 6 hours a continuous flow of mobile phase was passed through the column, and the total fraction volume collected after 6 hours was used for the measurement. It is important to note that for the efficiency calculations, the activity that is not collected in a specific period of time is not considered in the efficiency calculation of the following elution fraction. An average of 64 ± 2% efficiency is obtained for the continuous elution experiments at 20°C and 0.05 mL/min as shown in Figure 2(b).

Encouraged by the results of the first ever evidence of ^{177m}Lu and ^{177}Lu isomer separation, we systematically studied the effect of temperature and elution flux on the activity ratios and efficiency. A range of temperatures from 0 to 30°C was applied at two different mobile phase fluxes, 0.012 and 0.05 mL/min (all the data can be found in the supplementary information,

Figure S1 and Table S1). Figure 3 shows the activity ratio and the efficiency at different temperatures for both fluxes. These data and the corresponding standard deviations are the result of averaging six to eight fractions. The activity ratio was remarkably higher at the lower flux for all the temperatures but 0°C, reaching an optimum value of 218 ± 10 at 10°C and 0.012 ml/min. The activity ratio values from 10 to 30°C showed a clear trend for the two fluxes studied, a decrease in their values was observed with the increase in the temperature, reaching a minimum value of 25 ± 3 at 0.05 mL/min and 30°C. The efficiency exhibited a constant trend for both fluxes in the entire temperature range with slightly higher values for 0.05 mL/min, reaching a maximum value of 65 ± 3% at 10°C. Only the elutions at 0°C with a flux of 0.012 mL/min gave a lower efficiency, with a value of 47 ± 4 %.

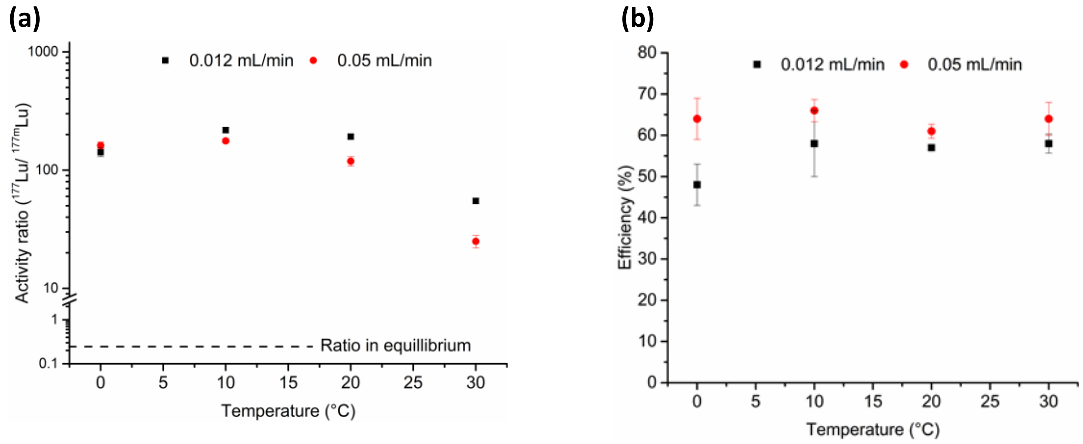

Figure 3: Effect of temperature and flow rate on efficiency(a) Effect of temperature on the ^{177}Lu/^{177m}Lu activity ratio at different flow rates (▪ 0.012 mL/min and • 0.05 mL/min). (b) Effect of temperature on the efficiency of separation at different flow rate (▪ 0.012 mL/min and • 0.05 mL/min).

2.3.2. Accumulation experiments

Accumulation period refers to the total time between elutions during which the flux of mobile phase through the column was stopped. Different accumulation periods of up to 5 days were checked at 10, 20 and 30°C. After a fixed accumulation period, the accumulated activity was eluted with a flux of 0.1 mL/min for 60 minutes. It was optimized after trying different elution fluxes and elution times. The results are summarized in Table S2, Supplementary information.

Figure 4 displays the ^{177}Lu/^{177m}Lu activity ratio and the ^{177}Lu extraction efficiency as a function of accumulation period. For efficiency calculations, the total accumulation period is used as the 'specific time' for the production of ^{177}Lu. The activity ratio followed the same trend as in the previous experiments in terms of temperature dependency. Higher activity ratios were observed at low temperatures for different accumulation periods. Moreover, greater activity ratios were obtained in the accumulation experiments than in continuous elution experiments, reaching a maximum value of 252 ± 12 at 10°C after 5 days of accumulation and a ^{177}Lu enrichment factor of around 1000. In contrast, efficiency values were lower than in the continuous elution experiments, decreasing for all the temperatures studied when the accumulation period was extended. No clear trend with temperature was observed. However, in all the cases there was a decrease in efficiency when extending the accumulation period, reaching a minimum of 40 %.

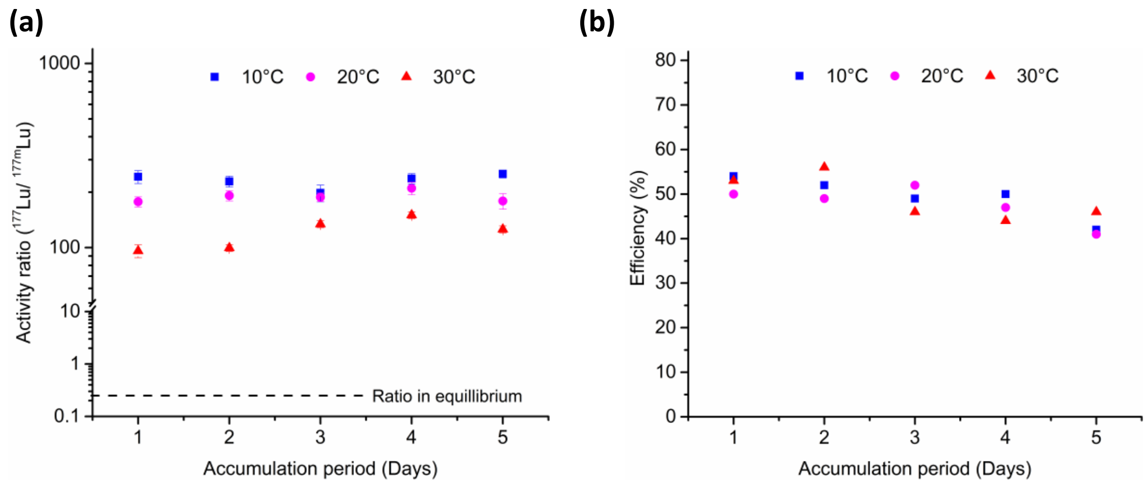

Figure 4: Effect of ^{177}Lu activity accumulation on ratio and efficiency. Accumulation period is the total time between elutions while there is not mobile phase flux. (a)^{177}Lu/^{177m}Lu activity ratio obtained after accumulation period at different temperatures (▪10 °C, •20 °C, ▲30 °C). (b) Efficiency of separation v/s the accumulation time at different temperatures (▪10 °C, •20 °C, ▲30 °C).

2.4 Discussion

The performed method allows for the separation of nuclear isomers. Based on this scheme, we propose a new radionuclide generator for the production of ^{177}Lu in which the parent nuclide is the metastable ^{177m}Lu. The reversed phase chromatographic column can be operated in a variety of conditions, being possible to modify the temperature, mobile phase flux and operation mode. Despite the fact that the experiments were carried out with low levels of activity, the values were high enough to provide reliable information about the generator performance. In all the analysed fractions, the levels of activity were much higher than the detection limit keeping the measurement error very low.

The importance of the internal conversion process on the bond rupture is clear when our system is compared with the work reported by Severin *et al.* In a very similar chromatographic separation setup, the dissociation of a DOTA-^{44m}Sc complex was studied and no bond rupture was observed [28]. ^{44m}Sc decays to a large extend through the emission of gamma rays (ICC=0.1391), while ^{177m}Lu decays mainly via internal conversion (ICC=30.7), therefore having a much greater chance of undergoing bond rupture.

The generator operates in a reliable and constant fashion, as it can be observed in Figure 1(b). After 60 hours of continuous operation the activity ratio values differed only a 1.1 % from the average. This reliability is very important to assure a proper and constant functioning during the long operative life of the generator. The flow rate applied in the elutions was limited by the retention of the Lu-DOTATATE complex. Higher fluxes greater than 0.1 mL/min resulted in displacement of the complex. The elution rates were selected in order to minimize this effect as much as possible.

Temperature showed an important effect on the generator separation performance. It is expected because the association-dissociation kinetics of the Lu-DOTATATE complex are highly influenced by temperature. Dissociation kinetics of Lu-DOTATATE complex were reported by Van der Meer *et al.* using a similar system and an order of magnitude difference was calculated when the temperature was increased from 20 to 37°C [25]. A higher dissociation rate increases the concentration of dissociated ^{177m}Lu in the mobile phase decreasing the value of the activity ratio and the quality of the elution. Conversely, the rate of production of ^{177}Lu by internal conversion is independent of temperature and is only time dependent. The change in the activity ratio at a different temperature was comparable in both modes of operation, continuous elution and accumulation (see Figures 3(b) and 4(b)). The optimal temperature was found to be 10°C, where maximum values of the activity ratio were achieved for both cases. The experiments at 0°C showed results in contradiction with the above explanation of using low temperatures. This can be explained by the fact that at 0°C there might be some other effects that can alter the operation of the generator. Temperature of 0°C is close to the freezing point of the mobile phase and mass transfer of the freed ^{177}Lu may be hindered, limiting the amount of eluted ^{177}Lu and decreasing the values of the activity ratio and the efficiency.

In clear contrast, temperature does not show any effect on the efficiency of the collected ^{177}Lu in any of the operation modes (see Figure 3(a) and 4(a)). The efficiencies were not close to the ideal value of 100%. It can be because of *(i)* some loss of ^{177}Lu ions by adsorption in different parts of the column *(ii)* the uncertainty from the internal conversion process since the efficiency of it, to the best of our knowledge, is unknown. The internal conversion process leads to a complex situation which eventually leads in some cases to bond rupture. Before an accurate value of efficiency of the generator can be given, more needs to be known about the internal conversion process and its effectiveness in the rupture of the chemical bonds.

The effect of the mobile phase flow on the activity ratio and efficiency during the continuous elution experiments can be explained on the basis of observations under different conditions. If the column was eluted with a higher flux than 0.1 mL/min a displacement of the ^{177m}Lu-DOTATATE complex was observed and the activity ratio measured were much worse with greater amounts of ^{177m}Lu . The same may be occurring to some extent when the flux of 0.05 mL/min is compared with 0.012 mL/min, and small amounts of the complex might elute through the column, decreasing the activity ratio (see Figure 3(b)). Moreover, the low flow rate might not be enough to provide a good mass transfer to the freed ^{177}Lu ions and some of them may re-associate back to the ligand, decreasing slightly the efficiency of the elution (see Figure 3(a)).

The effect of the re-association may also explain the results observed in the accumulation experiments. A remarkable decrease in efficiency was observed when the accumulation time was extended (Figure 4(a)). In long periods of time the chances of re-association of freed ^{177}Lu back to the free DOTATATE molecules increases, which decreases the concentration of freed ^{177}Lu in the elutions, and therefore decreases the efficiency. However, in the case of the activity ratio it has a positive effect, as re-association will decrease the amount of ^{177m}Lu ions thereby incrementing the activity ratio values obtained (Figure 4(b)) in comparison with the continuous elution. In continuous elution, the collected ^{177m}Lu is produced by the exclusive contribution of complex dissociation and the eluted ^{177}Lu is due to the combination of complex dissociation and bond rupture. In the case of accumulation, re-association takes place decreasing in the same proportion the concentration of both isomers in the mobile phase. Since the contribution by bond rupture is not altered during the accumulation, the activity ratio value increases due to this phenomenon.

The ^{177m}Lu/^{177}Lu generator could complement the present ^{177}Lu production routes. In the current situation, two different production routes are established: the indirect and direct routes [12,13,29]. In the indirect route, ^{177}Lu is produced as the decay product of the short-lived ^{177}Yb, which is produced by neutron capture of enriched ^{176}Yb [30]. Despite the fact that no-carrier added ^{177}Lu is produced in this process, the high cost of enriched ^{176}Yb and the radiochemical separation of ^{177}Lu from the ^{176}Yb target are limiting its application [31-33]. The direct route produces ^{177}Lu by neutron capture of enriched ^{176}Lu with clinically required specific activity at a lower cost [34,35]. However, as previously mentioned, during the neutron irradiation the long-lived metastable ^{177m}Lu ($t_{1/2}$= 160.44 days) is co-produced, causing a problem in the waste management of medical centres [8,36]. On top of these issues, both routes depend on the constant availability of nuclear reactors since weekly irradiations are needed for the production of ^{177}Lu [37].

The direct route of producing ^{177}Lu provides hospitals with a maximum relative activity of ^{177m}Lu of 0.01-0.02% at the end of bombardment [12]. The maximum activity ratio obtained in our experiments is about 250, when expressed in the same fashion it accounts for a value of about 0.4%. The aim of our system is to prove that both isomers can be separated based on the internal conversion process. A clinical ^{177m}Lu/^{177}Lu generator will need much higher levels of activity and a high resistance to radiation damage that will allow a consistent performance along the life-time of the device. In order to go beyond the proof of concept, the use of more stable chemical complexes will be combined with higher activities. This will allow the creation of a generator with a more flexible and robust performance that may produce non-carrier added ^{177}Lu and will permit a realistic evaluation of a potential generator for clinical use. Such a generator would combine the benefits of the direct and indirect routes, providing a product with higher quality that can eliminate the problems associated with the waste management due to the presence of ^{177m}Lu. Further, the half-life of the parent radionuclide will assure a stable production of ^{177}Lu for months and therefore the generator would terminate the need of weekly irradiation, and the continuous dependency on nuclear reactors to produce ^{177}Lu. With this generator more possibilities will be open for the use of ^{177}Lu in more hospitals and research centres. In contrast, the production of enough ^{177m}Lu to supply the generators with enough activity will need to be thoroughly examined in order to evaluate the feasibility of the clinical application of the ^{177m}Lu/^{177}Lu generator.

Summarizing, the separation of the nuclear isomers ^{177m}Lu/^{177}Lu has been achieved by taking advantage of bond rupture upon decay in a method that may be applied to other mixtures of isomers. In order to achieve the separation, a complex with very high stability needs to be formed with the metastable isomer. The nuclear after-effects of the internal conversion decay process, in which ^{177m}Lu is transmuted to ^{177}Lu, lead to chemical bonds breakage and the ^{177}Lu ions becoming free. By means of retaining the complex ^{177m}Lu-DOTATATE in a polar chromatographic column, the freed ^{177}Lu can be separated by fluxing the column with a mobile phase with the proper polarity. In this way, a new type of radionuclide generator is conceived, in which both the parent and the daughter nuclides are the same element. The generator will open new possibilities for the production and availability of the therapeutic radionuclide ^{177}Lu and can bring significant growth in the research and development of ^{177}Lu based pharmaceuticals.

2.5 Supplementary information

S1: Efficiency of the ^{177m}Lu/ ^{177}Lu generator

The efficiency of ^{177m}Lu/ ^{177}Lu generator is defined as the ratio of the collected ^{177}Lu activity divided by the theoretically produced ^{177}Lu activity.

Theoretical production in time t is estimated by using the Equation;

$$efficiency(\%) = \frac{A_g^t\ (collected)}{A_m^0 \cdot \left(\frac{\lambda_g}{\lambda_g - \lambda_m}\right) \cdot \left[exp^{-\lambda_m.t} - \ exp^{-\lambda_g.t}\right] \cdot B.R \cdot P.I.C.} \cdot 100$$

where A_m^0 = Initial activity of ^{177m}Lu before elution,

λ_g, λ_m = decay constants of ^{177}Lu, ^{177m}Lu respectively,

A_g^t = collected activity of ^{177}Lu at time t,

B.R = branching ratio for ^{177m}Lu to ^{177}Lu decay, 21.4% [38],

P.I.C = probability of internal conversion, $\frac{\alpha}{1+\alpha}$, 96.8%

where α is known as the internal conversion coefficient, and is defined as;

$$\alpha = \frac{number\ of\ de-excitations\ by\ the\ release\ of\ conversion\ electrons}{number\ of\ de-excitations\ via\ gamma\ ray\ emission}$$

Hence, we define the probability of the decay following the internal conversion path as, P.I.C = $\frac{\alpha}{1+\alpha}$. The 116KeV transition involved in the decay of ^{177m}Lu to ^{177}Lu has a theoretical internal conversion coefficient value, α_{th} = 30.7 [39,40]. Thus the P.I.C value is calculated to be 96.8%.

S2: Efficiency plots, while having a continuous flow of mobile phase:

As mentioned before, for each flow rate and temperature six to ten measurements were done and their average along with the standard deviation are plotted in Figure S1

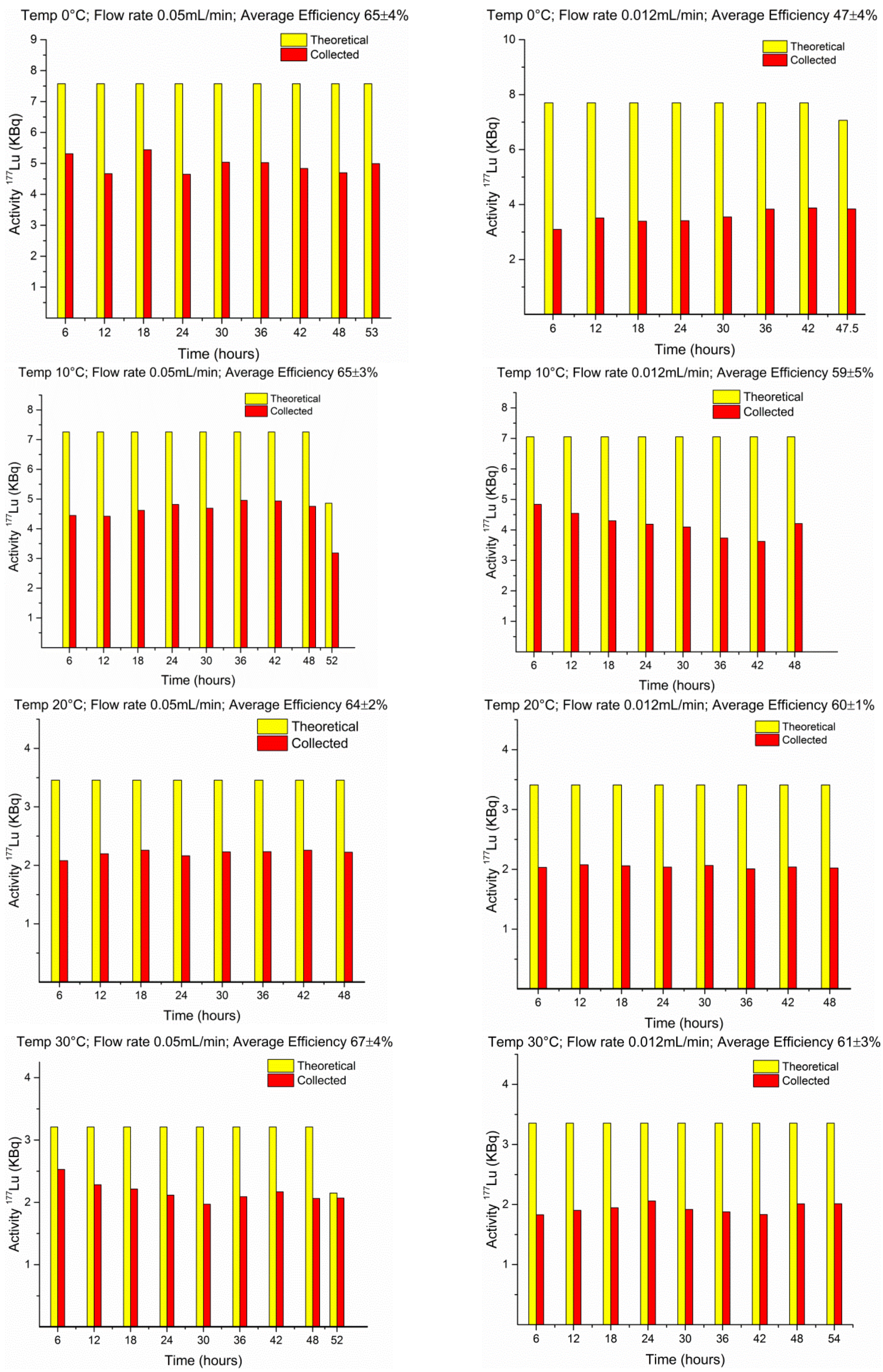

Figure.S1: Efficiency of accumulation at different temperature and flow rates

S3: Ratios obtained in different fractions

Table S1: ^{177}Lu/ ^{177m}Lu activity ratios obtained at different temperatures, and flow rates for different fractions.

Fraction number	Activity Ratio (^{177}Lu/ ^{177m}Lu)							
	at 0°C		at 10°C		at 20°C		at 30°C	
	0.05 mL/min	0.012 mL/min	0.05 mL/min	0.012 mL/min	0.05 mL/min	0.012 mL/min	0.05 mL/min	0.012 mL/min
1	160	134	174	213	147	198	21	56
2	147	131	184	211	141	206	23	51
3	132	135	166	216	145	181	24	55
4	168	136	168	209	126	198	30	52
5	140	146	183	223	139	190	26	58
6	171	158	187	238	106	185	23	59
7	194	161	179		111	190	25	58
8	160				111		26	51
9	178				126			
10	170				128			
Avg±STD	162±12	143±12	177±8	218±11	126±14	192±8	25±3	55±3

S4: Optimisation of elution flux and elution times for accumulation experiments

To optimize the elution flow rate and elution times, we did different accumulations and then different flow rates are used to elute the accumulated activity. The results obtained are summarized below:

Table S2: Optimisation of elution time, elution flux for accumulation experiments

Elution Flux (mL/min)	Elution Time (min)	Elution efficiency	Remark
0.012	120	About 12%	-
0.1	60	> 60%	-
0.5	60	> 100%	More than 100% efficiencies and very poor ^{177}Lu/^{177m}Lu ratios (less than 1), indicates the displacement of complex from the column.

Further, to minimize the volume of eluted activity and to keep the dilution of eluted activity as low as possible. We studied elution profile of Lu-177 after accumulation for an hour while taking the fractions every 5 mins. The result are shown in the plot Figure S4.2. As seen from the plot, a trailing behaviour in the elution of Lu-177 is observed. After elution for about 60 minutes, 60% of the accumulated activity could be removed. Therefore we decided to do the elution of accumulated activity at 0.1 mL/min for 60 minutes.

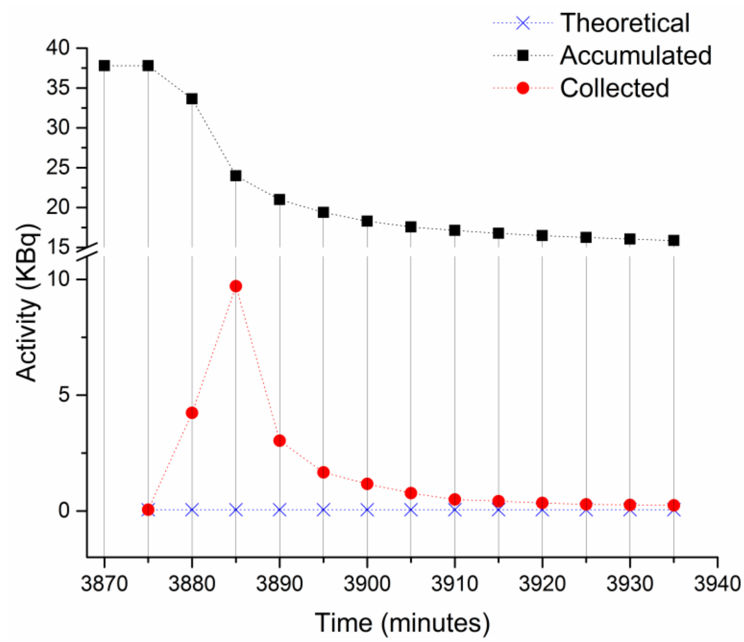

Figure S2. Optimization of elution time while eluting the accumulated activity at 0.1 mL/min.

S5. Detailed results from accumulation experiments.

For accumulation experiments, we were mainly interested in knowing if the separation of the isomers is possible for different accumulation periods. As shown in the Figure 4 of main text, the activity ratios and efficiencies follow almost a constant behaviour, with no substantial change at a particular temp. There was no big deviation from separation, and even under no mobile phase flow for time period upto 5 days the system was capable to separate the two isomers.

Therefore we didn't took many reading for a same experimental point. We did repeat some of these observations twice which gave quite consistent data, the results are shown in the Table below:

Table S3: ^{177}Lu/^{177m}Lu ratio and efficiency obtained for different accumulation periods at 10, 20 and 30°C

Accumulation time	Fraction number	10°C		20°C		30°C	
		Ratio	Efficiency	Ratio	Efficiency	Ratio	Efficiency
1 day	1	242	56	177	11	96	60
	2	200	50	-	-	67	53
	Average	221	53	-	-	82	56
	STDEV	29	4	-	-	21	5
2 day	1	228	52	191	49	99	59
	2	-	-	240	47	83	56

	Average	-	-	216	48	91	57
	STDEV	-	-	35	1	11	2
3 day	1	198	51	126	43	134	49
	2	-	-	188	53	-	-
	Average	-	-	156	48	-	-
	STDEV	-	-	44	7	-	-
4 day	1	237	15	210	50	150	46
		-	-	-	-	190	44
	Average	-	-	-	-	170	45
	STDEV	-	-	-	-	28	2
5 day	1	251	41	179	45	126	46

S6. Summary of the continuous and accumulation experiments;

For a better understanding of the data presented in Figure 3 and Figure 4, the results are summarized in Table 2 and 3 below:

For continuous flow of mobile phase

Table S4: Summary of the ^{177}Lu/^{177m}Lu activity ratios and efficiency obtained under continuous elution mode at 0, 10, 20, and 30°C

Temperature/ °C	^{177}Lu/^{177m}Lu activity ratio		Efficiency (%)	
	0.012 mL/ min	0.05 mL/ min	0.012 mL/ min	0.05 mL/ min
0	142 ± 12	162 ± 11	47 ± 4	65 ± 4
10	218 ± 11	177 ± 8	60 ± 5	65 ± 3
20	192 ± 8	119 ± 11	60 ± 1	64 ± 2
30	55 ± 3	25 ± 3	61 ± 3	67 ± 4

For accumulation and elution experiments

Table S5: Summary of the ^{177}Lu/^{177m}Lu activity ratios and efficiency obtained under accumulation elution mode at 10, 20, and 30°C for an accumulation period of 1, 2, 3, 4, 5 days.

Accumulation time/ day	^{177}Lu/^{177m}Lu activity ratio			Efficiency (%)		
	10°C	20°C	30°C	10°C	20°C	30°C
1	242 ± 20	177 ± 11	96 ± 8	56	50	53
2	229 ± 15	191 ± 12	99 ± 4	52	49	56
3	198 ± 20	125 ± 3	134 ± 6	50	54	47
4	237 ± 15	210 ± 16	150 ± 6	51	47	44
5	251 ± 12	178 ± 17	126 ± 5	43	44	48

S7. Determination of void volume of the column and linear velocities

After filling the column with stationary phase, tC-18 silica, we determined the void volume of the column in order to have an idea about the linear velocities of the mobile phase through the column. The experimental set up involved for determining the void volume of the column is shown in Figure 3. A peek column with dimensions diameter 3 mm and length 47 mm is filled with tC-18 silica. The column is connected with an injector, UV cell and a fraction collector using tubings of known volume (a,b,c).

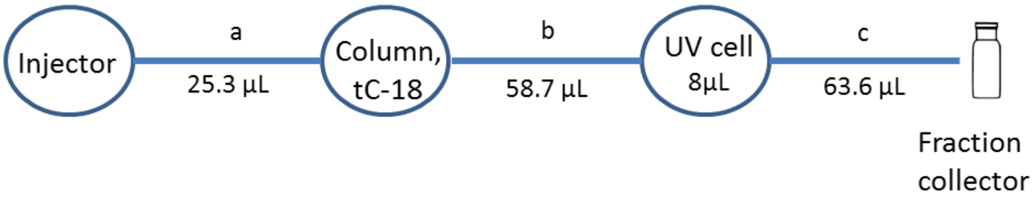

Figure S3. Experimental setup for void volume determination.

1 M $NaNO_3$ is then used as a marker to determine the void volume and it is injected through the injector at two different flow rates 0.3 mL/min and 1.0 mL/min. Once a signal is observed in UV detector, the mobile phase flow through the column is stopped. The results are shown in Table S6;

Table S6: Results for void volume determination

Flow (mL/min)	Marker	Time (sec)	n	SD	Volume (µL) Injector + Column – UV cell (a+b+c)	Volume (µL) Injector + Column (a+b+c) - c	Volume of column (a+b) - a
0.30	$NaNO_3$	51.97	5	0.86	257.84	201.14	175.84

The observed void volume is about 50% of the column volume. Using 0.175 mL as the void volume the linear velocities through the column can be calculated as;
For 0.1 mL/min - 26 mm/min, for 0.05 mL/min – 13.42 mm/min, for 0.012 mL/min – 3.22 mm/min.

2.7 References

1 Pillai, A. M. & Knapp, F. F., Jr. Evolving Important Role of Lutetium-177 for Therapeutic Nuclear Medicine. *Curr Radiopharm* **8**, 78-85 (2015).

2 Banerjee, S., Pillai, M. R. A. & Knapp, F. F. Lutetium-177 Therapeutic Radiopharmaceuticals: Linking Chemistry, Radiochemistry, and Practical Applications. *Chemical Reviews* **115**, 2934-2974, doi:10.1021/cr500171e (2015).

3 Kam, B. L. R. *et al.* Lutetium-labelled peptides for therapy of neuroendocrine tumours. *European Journal of Nuclear Medicine and Molecular Imaging* **39**, 103-112, doi:10.1007/s00259-011-2039-y (2012).

4 Milenic, D. E., Brady, E. D. & Brechbiel, M. W. Antibody-targeted radiation cancer therapy. *Nat Rev Drug Discov* **3**, 488-499 (2004).

5 DeNardo, G. L. & DeNardo, S. J. Concepts, Consequences, and Implications of Theranosis. *Seminars in Nuclear Medicine* **42**, 147-150, doi:10.1053/j.semnuclmed.2011.12.003 (2012).

6 Kam, B. L. R. *et al.* Lutetium-labelled peptides for therapy of neuroendocrine tumours. *European Journal of Nuclear Medicine and Molecular Imaging* **39**, 103-112, doi:10.1007/s00259-011-2039-y (2012).

7 Breeman, W. A. *et al.* Somatostatin receptor-mediated imaging and therapy: basic science, current knowledge, limitations and future perspectives. *European Journal of Nuclear Medicine* **28**, 1421-1429, doi:10.1007/s002590100502 (2001).

8 Bakker, W. H., Breeman, W. A. P., Kwekkeboom, D. J., De Jong, L. C. & Krenning, E. P. Practical aspects of peptide receptor radionuclide therapy with [177Lu][DOTA0, Tyr3]octreotate. *Quarterly Journal of Nuclear Medicine and Molecular Imaging* **50**, 265-271 (2006).

9 Baum, R. P. *et al.* Lutetium-177 PSMA Radioligand Therapy of Metastatic Castration-Resistant Prostate Cancer: Safety and Efficacy. *Journal of Nuclear Medicine*, doi:10.2967/jnumed.115.168443 (2016).

10 Pillai, M. R. A. & Knapp, F. F. Evolving Important Role of Lutetium-177 for Therapeutic Nuclear Medicine. *Current Radiopharmaceuticals* **8**, 78-85, doi:10.2174/1874471008666150312155959 (2015).

11 Bander, N. H. Technology Insight: monoclonal antibody imaging of prostate cancer. *Nat Clin Pract Urol* **3**, 216-225 (2006).

12 Dash, A., Pillai, M. & Knapp, F., Jr. Production of 177Lu for Targeted Radionuclide Therapy: Available Options. *Nucl Med Mol Imaging* **49**, 85-107, doi:10.1007/s13139-014-0315-z (2015).

13 Pillai, M. R. A., Chakraborty, S., Das, T., Venkatesh, M. & Ramamoorthy, N. Production logistics of ^{177}Lu for radionuclide therapy. *Applied Radiation and Isotopes* **59**, 109-118, doi:10.1016/S0969-8043(03)00158-1 (2003).

14 Kondev, F. G. Nuclear Data Sheets for A = 177. *Nuclear Data Sheets* **98**, 801-1095, doi:http://dx.doi.org/10.1006/ndsh.2003.0006 (2003).

15 Kondev, F. G. *et al.* Gamma-ray emission probabilities in the decay of 177mLu. *Applied Radiation and Isotopes* **70**, 1867-1870, doi:10.1016/j.apradiso.2012.02.029 (2012).

16 Cooper, E. P. On the Separation of Nuclear Isomers. *Physical Review* **61**, 1-5, doi:10.1103/PhysRev.61.1 (1942).

17 Seaborg, G. T. & Kennedy, J. W. Nuclear Isomerism and Chemical Separation of Isomers in Tellurium. *Physical Review* **55**, 410-410, doi:10.1103/PhysRev.55.410.2 (1939).

18 Lazzarini, E. & Fantola Lazzarini, A. L. On the survival of Co(III) complexes to deexcitation by internal conversion of the 58mCo coordinating atom. *Journal of Inorganic and Nuclear Chemistry* **39**, 207-211, doi:http://dx.doi.org/10.1016/0022-1902(77)80001-8 (1977).

19 Langsdorf, A. & Segrè, E. Nuclear Isomerism in Selenium and Krypton. *Physical Review* **57**, 105-110 (1940).

20 Piscitelli, F., Ballatore, C. & Smith Iii, A. B. Solid phase synthesis of 2-aminobenzothiazoles. *Bioorg. Med. Chem. Lett.* **20**, 644-648, doi:http://dx.doi.org/10.1016/j.bmcl.2009.11.055 (2010).

21 Knapp, F. F. & Dash, A. in *Radiopharmaceuticals for Therapy* 131-157 (Springer India, 2016).

22 Knapp, F. F., Pillai, M. R. A., Osso, J. A. & Dash, A. Re-emergence of the important role of radionuclide generators to provide diagnostic and therapeutic radionuclides to meet future research and clinical demands. *J Radioanal Nucl Chem* **302**, 1053-1068, doi:10.1007/s10967-014-3642-8 (2014).

23 Choppin, G. R., Liljenzin, J.-O. & Rydberg, J. in *Radiochemistry and Nuclear Chemistry (Third Edition)* (ed Gregory R. ChoppinJan-Olov LiljenzinJan Rydberg) 94-122 (Butterworth-Heinemann, 2002).

24 De Vries, D. J. & Wolterbeek, H. The production of medicinal 177Lu and the story of 177mLu: detrimental by-product or future friend? *Tijdschr. Nucl. Geneeskd.* **34**, 899-904 (2012).

25 van der Meer, A., Breeman, W. A. P. & Wolterbeek, B. Reversed phase free ion selective radiotracer extraction (RP-FISRE): A new tool to assess the dynamic stabilities of metal (-organic) complexes, for complex half-lives spanning six orders of magnitude. *Applied Radiation and Isotopes* **82**, 28-35, doi:http://dx.doi.org/10.1016/j.apradiso.2013.06.021 (2013).

26 Zhernosekov, K. P., Filosofov, D. V., Qaim, S. M. & Rosch, F. A ^{140}Nd/^{140}Pr radionuclide generator based on physico-chemical transitions in ^{140}Pr complexes after electron capture decay of ^{140}Nd-DOTA. *Radiochimica Acta* **95**, 319-327, doi:10.1524/ract.2007.95.6.319 (2007).

27 Blaauw, M. *The holistic analysis of gamma-ray spectra in instrumental neutron activation analysis*, (1993).

28 Severin, G., Munch, M. & Jensen, M. Szilard-Chalmers effect in DOTA-bound ^{44m}Sc. *Journal of Labelled Compounds and Radiopharmaceuticals* **56**, S220, doi:10.1002/jlcr.3058 (2013).

29 Knapp, F. F. & Dash, A. in *Radiopharmaceuticals for Therapy* 71-113 (Springer India, 2016).

30 Hashimoto, K., Matsuoka, H. & Uchida, S. Production of no-carrier-added 177Lu via the 176Yb(n, &;#947;)177Yb &;#8594; 177Lu process. *J Radioanal Nucl Chem* **255**, 575-579, doi:10.1023/a:1022557121351 (2003).

31 Tarasov, V. A. *et al.* Production of no-carrier added lutetium-177 by irradiation of enriched ytterbium-176. *Current Radiopharmaceuticals* **8**, 95-106 (2015).

32 Horwitz, E. P., McAlister, D. R., Bond, A. H., Barrans, R. E. & Williamson, J. M. A process for the separation of 177Lu from neutron irradiated 176Yb targets. *Applied Radiation and Isotopes* **63**, 23-36, doi:https://doi.org/10.1016/j.apradiso.2005.02.005 (2005).

33 Lebedev, N. A., Novgorodov, A. F., Misiak, R., Brockmann, J. & Rösch, F. Radiochemical separation of no-carrier-added 177Lu as produced via the 176Ybn, γ 177Yb→177Lu process. *Applied Radiation and Isotopes* **53**, 421-425, doi:10.1016/S0969-8043(99)00284-5 (2000).

34 Dvorakova, Z., Henkelmann, R., Lin, X., Türler, A. & Gerstenberg, H. Production of 177Lu at the new research reactor FRM-II: Irradiation yield of 176Lu177Lu. *Applied Radiation and Isotopes* **66**, 147-151, doi:http://dx.doi.org/10.1016/j.apradiso.2007.08.013 (2008).

35 Nir-El, Y. Production of ^{177}Lu by neutron activation of ^{176}Lu. *J Radioanal Nucl Chem* **262**, 563-567, doi:10.1007/s10967-004-0476-9 (2004).

36 Maus, S., Buchholz, H.-G. & Schreckenberger, M. ^{177m}Lu impurity: Practical aspects of ^{177m}Lu hospital waste management. *Journal of Nuclear Medicine* **56**, 1248 (2015).

37 Krijger, G. C., Ponsard, B., Harfensteller, M., Wolterbeek, H. T. & Nijsen, J. W. F. The necessity of nuclear reactors for targeted radionuclide therapies. *Trends in Biotechnology* **31**, 390-396, doi:10.1016/j.tibtech.2013.04.007 (2013).

38 Kondev, F. G. Nuclear data sheets for A = 177. *Nuclear Data Sheets* **98**, 801- 1095 (2003).

39 BrIcc program package version 2.2b. (2009).

40 Kibédi, T., Burrows, T. W., Trzhaskovskaya, M. B., Davidson, P. M. & Nestor Jr, C. W. Evaluation of theoretical conversion coefficients using BrIcc. *Nuclear Instruments and Methods in Physics Research Section A: Accelerators, Spectrometers, Detectors and Associated Equipment* **589**, 202-229, doi:http://dx.doi.org/10.1016/j.nima.2008.02.051 (2008).

Chapter 3

Liquid-liquid extraction based ^{177m}Lu-^{177}Lu separation

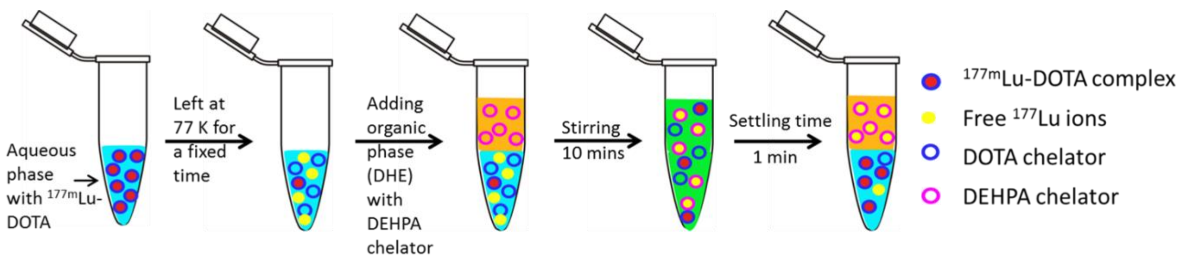

This Chapter has been adapted from:
Bhardwaj, R., Wolterbeek, H. T., Denkova, A. G., & Serra-Crespo, P. (2019). Radionuclide generator-based production of therapeutic ^{177}Lu from its long-lived isomer ^{177m}Lu. EJNMMI Radiopharmacy and Chemistry, 4(1), 13.

Abstract

In this work a Lutetium-177 (^{177}Lu) production method based on the separation of nuclear isomers, ^{177m}Lu & ^{177}Lu, is reported. The ^{177m}Lu-^{177}Lu separation is performed by combining the use of DOTA & DOTA-labelled peptide (DOTATATE) and liquid-liquid extraction. The ^{177m}Lu cations have been complexed with DOTA & DOTATATE and kept at 77K for periods of time to allow ^{177}Lu production. The freed ^{177}Lu ions produced via internal conversion of ^{177m}Lu have been extracted in dihexyl ether using 0.01M di-(2-ethylhexyl)phosphoric acid (DEHPA) at room temperature. The liquid-liquid extractions have been performed periodically for a period up to 35 days. A maximum ^{177}Lu/^{177m}Lu activity ratio of 3500±500 has been achieved with [^{177m}Lu]Lu-DOTA complex, in comparison to ^{177}Lu/^{177m}Lu activity ratios of 1086±40 realized using [^{177m}Lu]Lu-DOTATATE complex. The ^{177}Lu-^{177m}Lu separation has been found to be affected by the molar ratio of lutetium and DOTA. A ^{177}Lu/^{177m}Lu activity ratio up to 3500±500 has been achieved with excess DOTA in comparison to ^{177}Lu/^{177m}Lu activity ratio 1500±600 obtained when lutetium and DOTA were present in molar ratio of 1:1. Further, the ^{177}Lu ion extraction efficiency, decreases from 95±4% to 58±2% in the presence of excess DOTA. The reported method resulted in a ^{177}Lu/ ^{177m}Lu activity ratio up to 3500 after the separation. This ratio is close to the ^{177}Lu/^{177m}Lu activity ratios, attained currently during the direct route ^{177}Lu production for clinical applications (i.e. 4000-10000). However, the reported needs further optimization to lead to a clinically acceptable ^{177m}Lu/^{177}Lu radionuclide generator.

3.1 Background

Radionuclide generators are known to have brought revolutionary opportunities in the development of nuclear medicine [1-4]. The current state of the art of ^{99m}Tc, ^{188}Re, ^{68}Ga pharmaceuticals owe their existence largely to the availability of their corresponding radionuclide generators [5,6]. They offer continuous, on-site and on-demand isolation of a short-lived daughter radionuclide from its longer-lived mother radionuclide. Lutetium-177 (^{177}Lu) is a radionuclide that could also benefit from the advantages of a generator. ^{177}Lu is well-known for its theranostic potential and is expected to play a crucial role in fulfilling the global demand of radionuclides for many targeted radionuclide therapy applications [7,8]. The [^{177}Lu]Lu-DOTATATE has already been FDA approved for the application in neuroendocrine tumour therapy [9]. Currently, other ^{177}Lu radiopharmaceuticals have also entered the clinic in the treatment of prostate cancer, lung cancer, non-Hodgkin lymphoma, bone pain palliation and others [10-14]. Clearly, the demand of ^{177}Lu is only going to increase and radionuclide generator can complement the current production routes. The long half-life of ^{177m}Lu (160.44 days) can potentially lead to on-site and on-demand ^{177}Lu supply for a long period of time without the need of weekly irradiations in nuclear reactor [15,16]. However, the development of ^{177m}Lu/^{177}Lu radionuclide generator needs to tackle the great challenge of separating the physically and chemically alike nuclear isomers ^{177}Lu and ^{177m}Lu.

It has been shown in the past that ^{177}Lu can be separated from ^{177m}Lu due to the chemical effects occurring as a consequence of internal conversion decay of ^{177m}Lu [16]. Internal conversion decay may result in the emission of multiple Auger electrons, often accompanied with the loss of valence electrons and leaving the atom in a highly positively charged state which can result in bond rupture [17]. This principle presents a possibility to separate two isomers, provided that a separation process that can quickly & selectively capture the freed ions is feasible. Additionally, from a radionuclide generator perspective, the separation process should also allow the periodic extraction of the produced daughter radionuclide during the lifetime of the generator.

Previously, a column chromatography based ^{177}Lu-^{177m}Lu separation process has been reported, where the ^{177m}Lu complexed with DOTATATE has been immobilized on a tC-18 silica and the freed ^{177}Lu ions produced after the decay have been separated using a mobile phase flow [16]. The ^{177}Lu/^{177m}Lu activity ratio of 250 has been reached after separation compared to the equilibrium ^{177}Lu/^{177m}Lu activity ratio of 0.25. However, in order to fulfil the clinical demand the separation method should provide ^{177}Lu having minimum breakthrough of ^{177m}Lu. The current direct production route delivers ^{177}Lu with ^{177}Lu/^{177m}Lu activity ratio ranging from 4,000 to 10,000 [18-22], while the indirect production route supplies the no-carrier added ^{177}Lu with almost negligible amount of ^{177m}Lu [23].

In this work, a radionuclide generator for the production of ^{177}Lu based on the pair of nuclear isomer^{177m}Lu-^{177}Lu is presented. The ^{177m}Lu-^{177}Lu separation has been performed using liquid-liquid extraction (LLE). LLE has been explored several times before in the development of other radionuclide generators, such as ^{99}Mo/^{99m}Tc, ^{68}Ge/^{68}Ga, ^{188}Re/^{188}W, and ^{90}Y/^{90}Sr radionuclide generators [24-30]. The present work demonstrates the application of LLE in ^{177}Lu-^{177m}Lu separation which can potentially lead to a ^{177m}Lu/^{177}Lu radionuclide generator.The metastable isomer, ^{177m}Lu, was complexed with the chelating agents (DOTA and DOTATATE) and the freed ^{177}Lu ions was extracted in dihexyl ether using Di-(2-ethylhexyl)phosphoric acid (DEHPA) as the cation extracting agent.

3.2 Materials and Methods

3.2.1 Materials

Lutetium chloride hexahydrate, $LuCl_3.6H_2O$ (≥99.99%), di(2-ethylhexyl)phosphoric acid, DEHPA (97%), di-n-hexyl ether, DHE (97%), sodium acetate (≥99%), chelex resin (chelex-100, 50- 100 mesh) and acentonitrile (99.3%) were purchased from Sigma Aldrich. 1,4,7,10-tetraazacyclododecane N, N′, N′′, N′′′-tetraacetic acid, DOTA (98%) was purchased from ABCR GmBH & Co. KG Germany. DOTATATE was obtained as a kind gift from Erasums Medical Centre (Rotterdam) and was produced by Biosynthema, MO, USA. The lutetium-177 (^{177}Lu) used in the optimization studies was produced by irradiating around 1 mg of natural $LuCl_3.6H_2O$ in the Hoger Onderwijs Reactor Delft (HOR) with a thermal neutron flux of $4.72*10^{12}$ neutrons·s^{-1}·cm^{-2} (less than 1.5% epithermal contribution) and an irradiation time of 10 hours. The solid sample was weighed inside polyethylene capsule and sealed, packed inside polyethylene rabbits. After irradiation, the samples were left for a cooling period of 3 days, resulting in the production of around 17 MBq of ^{177}Lu. The capsules were opened and transferred into a plastic vial containing 2.5 mL, pH-3, HCl solution, resulting in a 1mM [^{177}Lu]$LuCl_3$ solution.

The Lutetium-177m (^{177m}Lu) source was provided by IDB- Holland as a 1mM [^{177m}Lu]$LuCl_3$ solution with about 5 MBq ^{177m}Lu per g of solution.

3.2.2 Methods

3.2.2.1 γ ray spectroscopy analysis

All the activity measurements were performed on a well-type HPGe detector for counting time up to 5 hours to reduce the error from the counting statistics to less than 5%. The measurement of the samples obtained at the end of LLE was repeated after 3-4 half-lives of ^{177}Lu to decrease the background noise and measure the ^{177m}Lu activity with less than 5% uncertainty. The efficiency calibration for different peaks was performed using a known activity of ^{177}Lu source supplied by IDB Holland. The obtained gamma ray spectra were analysed using an in-house software to calculate the activity of each fraction [31]. In order to minimize the error, all the vials were weighed before and after the fraction collection.

3.2.2.2 Preparation of aqueous phase

The ^{177m}Lu containing $LuCl_3$ solution (1mM) was used to prepare [^{177m}Lu]Lu-DOTA complex in three different molar ratios, (1:1, 1:2, 1:4). Typically, 1 mM [^{177m}Lu]$LuCl_3$ solution (0.150 mL, 0.150 µmoles) was mixed with 0.01 M DOTA in different molar ratios 1:1, 1:2, & 1:4 in the presence of 0.150 mL, 1 M sodium acetate- acetic acid buffer at pH 4.3. The reaction mixture was heated at 80°C for 30 minutes. The [^{177m}Lu]Lu-DOTATATE complex was synthesized as reported previously in a Lu:DOTATATE molar ratio of 1:4 [16]. Typically, 1 mM [^{177m}Lu]$LuCl_3$ solution (0.050 mL, 0.050 µmoles) was mixed with 0.200 µmol DOTATATE solution in the presence of 0.150 mL, 1 M sodium acetate- acetic acid buffer (pH- 4.3). The reaction mixture was heated at 80°C for about 1 hour followed by incubation at room temperature for about 1 hour.

The complex formation was confirmed using instant thin layer chromatography. Free ^{177m}Lu ions traces were removed using a cation exchange resin (chelex-100). (Details in S1, supplementary information)

3.2.2.3 Liquid-liquid extraction (LLE) procedure

The schematic representation of LLE to separate the freed ^{177}Lu ions from the complexed ^{177m}Lu ions is shown in Figure 1 below:

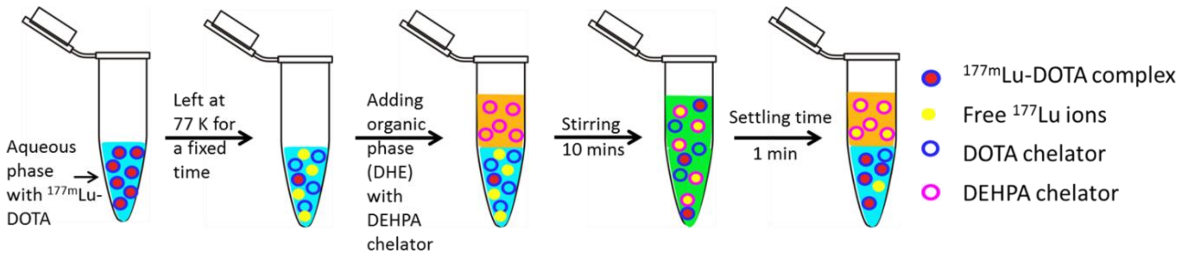

Figure 1: Schematic representation of liquid-liquid extraction to extract the bond-ruptured free ^{177}Lu ions

All the LLE experiments were performed in 2 mL Eppendorf by placing them in a shaking incubator at room temperature. The aqueous and the organic phases were mixed in volumetric ratio (1:1) at 1400 rpm for a stirring time of about 10 minutes. The stirring time of 10 minutes was optimised by studying the ^{177}Lu extraction efficiency as a function of extraction time (see Figure S1(b), S2, supplementary information). At the end of stirring, the layer separation was achieved after a settling time of about one minute. In order to avoid any contamination of the aqueous layer in the organic layer, only the upper 2/3rd organic layer was taken out using a 20- 200uL pipette in all the LLE experiments. The pipetted organic layer was transferred to a pre-weighed vial to know the exact amount of organic phase removed in each extraction.

First, free ^{177}Lu cations were extracted from a 0.3 mL, pH-4, 1 mM [^{177}Lu]$LuCl_3$ solution as the aqueous phase. The organic phase consists of 0.3 mL dihexyl ether containing different DEHPA concentrations, namely 0.01, 0.05, 0.1, 0.15, 0.2, 0.4, 0.6, 1.0, 1.2 and 1.6 M. At the end of LLE, the ^{177}Lu activity in the organic and the aqueous layer was measured using γ ray spectroscopy to obtain the ^{177}Lu extraction efficiency (EE). The EE is defined as the percentage of the ^{177}Lu activity moving from the aqueous phase in to the organic phase after the extraction. All the experiments were performed in triplicate.

Subsequently, the LLE was performed to extract the freed ^{177}Lu ions from the aqueous phase containing [^{177m}Lu]Lu-DOTATATE, [^{177m}Lu]Lu-DOTA complex. For [^{177m}Lu]Lu-DOTATATE complex, the ^{177}Lu extraction was performed successively at varying ^{177}Lu accumulation periods for a total time period of up to 60 days. For, [^{177m}Lu]Lu-DOTA complex, the freed ^{177}Lu ions were extracted successively at every 7 days for a total time period of 35 days. In between the extractions, the [^{177m}Lu]Lu-DOTA and [^{177m}Lu]Lu-DOTATATE complexes were left in a liquid N_2 tank to allow for the accumulation of freed ^{177}Lu ions. The ^{177}Lu separation was performed by bringing the vial out of the liquid N_2 tank and quickly adding the 0.01M DEHPA in DHE in a 1:1 volumetric ratio (0.3 mL: 0.3 mL), at room temperature and 10 minutes of stirring time, as shown schematically in Figure 1. At the end of LLE, the ^{177}Lu and ^{177m}Lu activity in the organic layer was measured using γ ray spectroscopy to calculate the amount of ^{177}Lu and ^{177m}Lu ions extracted in the organic phase and the ^{177}Lu/^{177m}Lu activity ratio.

The ^{177}Lu extraction efficiency is defined as the amount of ^{177}Lu ions that were extracted into the organic phase divided by the theoretically produced ^{177}Lu ions (see section S3, equation S2 in Supplementary Information). The percentage of ^{177m}Lu extracted is defined as the activity of ^{177m}Lu ions measured in organic phase after the LLE divided by the starting activity of the ^{177m}Lu ions in the aqueous phase.

3.3 Results

3.3.1 ^{177}Lu/ ^{177m}Lu separation using [^{177m}Lu]Lu-DOTATATE complex

The ^{177}Lu/ ^{177m}Lu separation was performed using [^{177m}Lu]Lu-DOTATATE complex synthesized in the presence of an excess of DOTATATE (Lu:DOTATATE molar ratio of 1:4). The ^{177}Lu ions production via the decay of ^{177m}Lu is represented by equation S1, Supplementary Information, S3 and the expected growth of ^{177}Lu ions with the increase in the ^{177}Lu accumulation period is shown in Figure S2, Supplementary Information. The amount of ^{177}Lu ions produced increases with an increase in ^{177}Lu accumulation period and reaches a maximum after 32 days of ^{177}Lu accumulation. In the presented results, the freed ^{177}Lu ions were extracted from [^{177m}Lu]Lu-DOTATATE complex by performing LLE successively after different ^{177}Lu accumulation intervals. Figure 2 (a)&(b) show the ^{177}Lu extraction efficiency and percentage of the ^{177m}Lu ions extracted in the organic phase at the end of the LLE at different time intervals, respectively. An average ^{177}Lu extraction efficiency of 60±10% was obtained at the end of LLE. This is 40% less than the 99 ± 2% ^{177}Lu extraction efficiency observed during the LLE of ^{177}Lu ions from a 1mM [^{177}Lu]$LuCl_3$ solution using 0.01M DEHPA in DHE (see Figure S1, supplementary information S2). Additionally, along with the ^{177}Lu ions, 0.0085±0.0015% of the starting ^{177m}Lu activity was also extracted in the organic phase. Figure 2(b), shows the ^{177}Lu/^{177m}Lu activity ratios obtained after different extractions. An increase in the ^{177}Lu/^{177m}Lu activity ratio is observed with an increase in the time interval between the extractions. The maximum ^{177}Lu/^{177m}Lu activity ratio of 1086±40 is obtained on performing the LLE at 43 days after a ^{177}Lu accumulation period of 26 days. A decrease in the ^{177}Lu accumulation period leads to a decrease in the ^{177}Lu/ ^{177m}Lu activity ratios. The ^{177}Lu/^{177m}Lu activity ratios 600±100 was obtained for ^{177}Lu accumulation periods between 6-10 days.

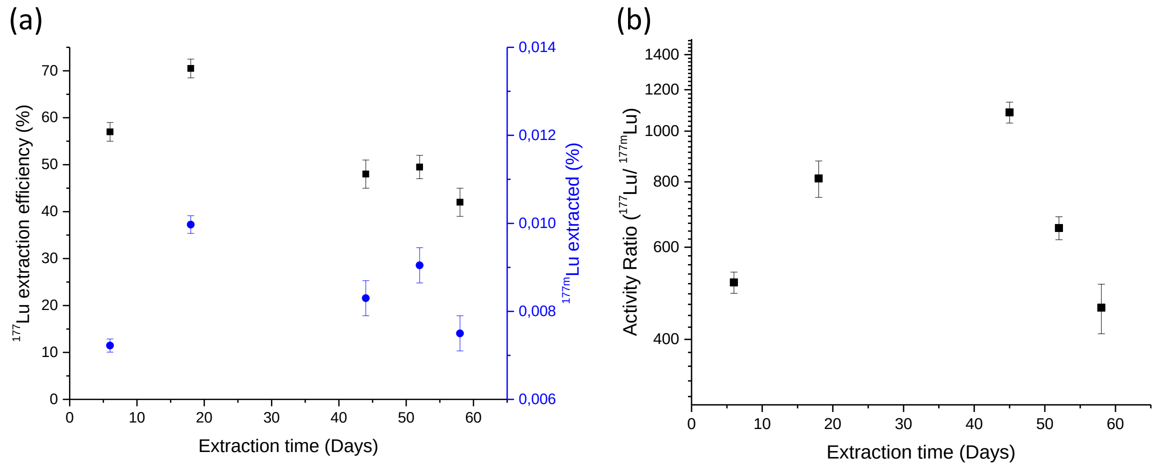

Figure 2: The ^{177}Lu extraction efficiency (y axis, left) and the % ^{177m}Lu extracted (y axis, right) (a), at different extraction time during the successive LLE of free ^{177}Lu ions from [^{177m}Lu]Lu-DOTATATE complex using 0.01M DHEPA in DHE. The ^{177}Lu/^{177m}Lu activity ratio (b) obtained in the organic phase at different extraction time. The error bars represent the error in the individual measurements due to counting statistics.

3.3.2 ^{177}Lu/^{177m}Lu radionuclide separation using [^{177m}Lu]Lu-DOTA complex

The results obtained when the LLE was performed to extract the freed ^{177}Lu ions from the [^{177m}Lu]Lu-DOTA complex are shown in Figure 3&4. The LLE was performed successively at time intervals of 7 days. Figure 3(a) shows the effect of Lu: DOTA molar ratios on ^{177}Lu extraction efficiency. Figure 3(b) displays the percentage of initial ^{177m}Lu activity extracted in the organic phase at the end of LLE for the different Lu: DOTA molar ratios.

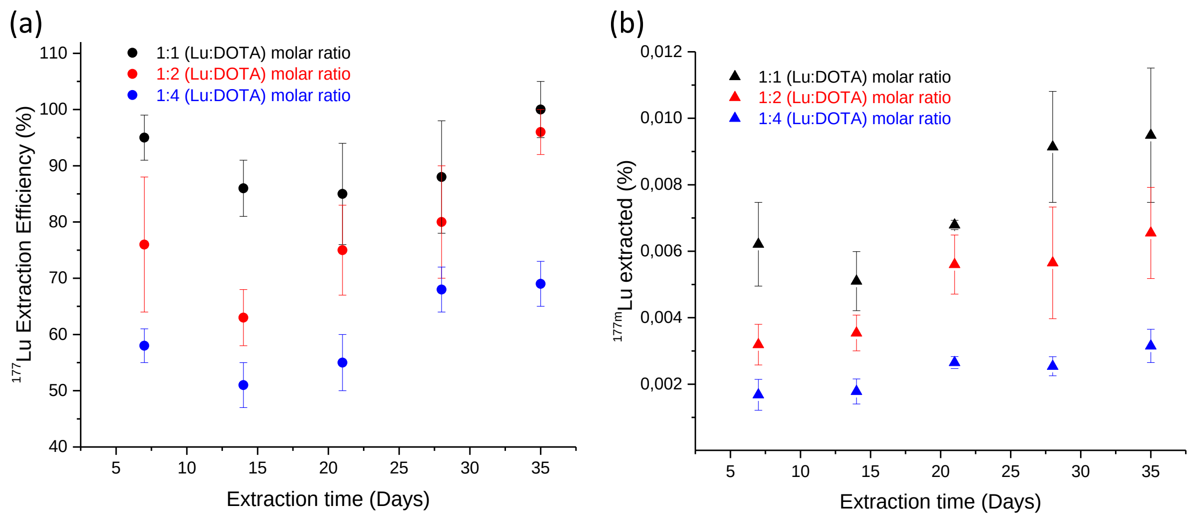

Figure 3: The ^{177}Lu extraction efficiency (a) and the percent ^{177m}Lu extracted (b) at different extraction time during the successive LLE of free ^{177}Lu ions from [^{177m}Lu]Lu-DOTA complex using 0.01M DHEPA in DHE. The experiments were performed for three different Lu: DOTA molar ratios, **(1:1)** in **black**, **(1:2)** in **red** and **(1:4)** in **blue**. The data points represent the average ± STD of three experiments, the individual error in measurements due to counting statistics is less than 5%.

It can be seen from Figure 3(a), that the ^{177}Lu extraction efficiency reaches a maximum value of 95±4% when Lu & DOTA were present in 1:1 molar ratio and decreases to 58±2% for 1:4 Lu:DOTA molar ratio. Further, the ^{177}Lu extraction efficiency remains almost constant for the first three extractions followed by a slight increase during the 4th and 5th extraction, for all the three Lu: DOTA molar ratios. Figure 3(b) shows that 0.0061±0.0015% of ^{177m}Lu activity was extracted in the first extraction when Lu and DOTA were present in 1:1 molar ratio, which got reduced to 0.0020±0.0010% for the Lu:DOTA molar ratio 1:4. The percentage of ^{177m}Lu activity extracted remains almost constant during the successive extractions in the presence of excess DOTA, and increases from 0.0061±0.0015% to 0.0095±0.0015% in the presence of 1:1 Lu:DOTA molar ratio. The error bars in Figure 3 represent the standard deviation in the results of three experiments performed in parallel.

Figure 4, shows the ^{177}Lu/^{177m}Lu activity ratios observed in the organic phase at the end of LLE for the three different Lu:DOTA molar ratios. It reveals that the ^{177}Lu/^{177m}Lu activity ratio increases with an increase in the molar quantities of DOTA. The highest ^{177}Lu/^{177m}Lu activity ratio of 3500±500 was obtained when DOTA was present in excess (1:4) and decreases to around 1500±600 in the presence of 1:1, Lu:DOTA molar ratio. Further, a slight decrease in the ^{177}Lu/^{177m}Lu activity ratios was observed in every successive LLE performed during the 35 days of experiments. The fifth ^{177}Lu extraction performed at the end of the experiments resulted in a 40±5% decrease in the ^{177}Lu/^{177m}Lu activity ratios compared to the ^{177}Lu/^{177m}Lu activity ratio obtained in the first extraction.

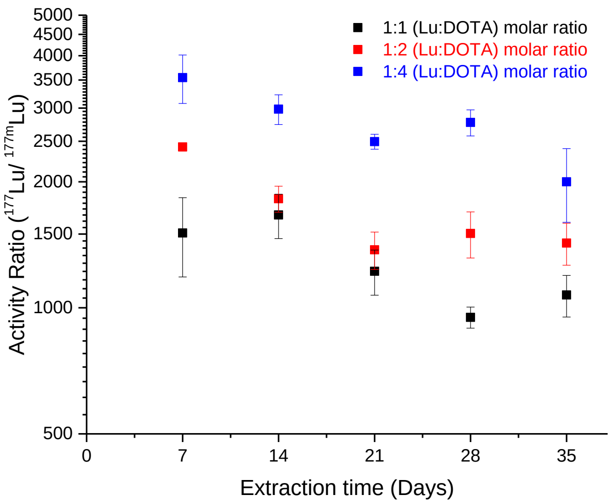

Figure 4: The ^{177}Lu/ ^{177m}Lu activity ratio obtained during the successive LLE of free ^{177}Lu ions from the [^{177m}Lu]Lu-DOTA complex. The experiments were performed with three Lu: DOTA molar ratios, **(1:1)** in **black**, **(1:2)** in **red** and **(1:4)** in **blue**. The data points represent the average ± STD of three experiments, the individual error in measurements due to counting statistics is less than 5%.

Overall, the ^{177}Lu/^{177m}Lu activity ratios obtained using DOTA as chelating agent were about 5 times higher when compared with ^{177}Lu/^{177m}Lu activity ratios obtained using DOTATATE for a ^{177}Lu accumulation period of around 7 days. Also, the percentage of ^{177m}Lu activity extracted in the organic phase was about 5 times higher with DOTATATE than that observed with DOTA as the ^{177m}Lu complexing agent.

3.4 Discussion

The separation of the isomers ^{177}Lu and ^{177m}Lu based on the nuclear decay after effects is achieved using liquid-liquid extraction (LLE) as the separation method and the [^{177m}Lu]Lu-DOTA, [^{177m}Lu]Lu-DOTATATE complexes. The ^{177}Lu production at 77K resulted in negligible dissociation of the starting [^{177m}Lu]Lu-DOTA based complexes, and increases the quality of extracted ^{177}Lu remarkably. The freed ^{177}Lu ions were extracted in the organic phase by performing the LLE at room temperature. The separation was done sufficiently fast resulting in production of limited quantities of free ^{177m}Lu ions.

In the present work, the ^{177}Lu/^{177m}Lu activity ratio of 1086±40 is achieved using [^{177m}Lu]Lu-DOTATATE complex which is about 4 times higher than the previously reported ^{177}Lu/ ^{177m}Lu activity ratio of 250 realized using the same [^{177m}Lu]Lu-DOTATATE complex [16]. In the previously reported method, the ^{177}Lu ion accumulation was performed at 10°C and the temperature could not be decreased further because of experimental limitations. In contrast, the present LLE based separation allows the ^{177}Lu accumulation at 77K. At 77 K, the rate constants for the chemical reactions (i.e. association-dissociation kinetics) are extremely low making the ^{177m}Lu contribution coming from the dissociation of the [^{177m}Lu]Lu-DOTATATE complex negligible during the ^{177}Lu accumulation period. The ^{177m}Lu contribution observed in the present work can be accounted to the dissociation of the [^{177m}Lu]Lu-DOTATATE complex during the LLE at room temperature. After the dissociation, the ^{177m}Lu and ^{177}Lu ions are indistinguishable and they will go into the organic phase with equal rate.

The LLE of ^{177}Lu ions from [^{177m}Lu]Lu-DOTATATE complex resulted in co-extraction of 0.0085±0.0015% of initial ^{177m}Lu activity in the organic phase. This leads to an estimated dissociation rate constant of $1.3*10^{-7}±0.3*10^{-7}$ s^{-1}. For Lu-DOTATATE complex, a dissociation constant rate $2*10^{-8}$ s^{-1} has been reported at pH-4.3 and 20°C [32]. It has also been shown that the Lu-DOTATATE complex is accompanied by the presence of short-lived unstable, mono- and di-protonated (MHL, MH_2L) complex species [32]. These species have a dissociation rate constant of $8*10^{-5}$ s^{-1} (MHL) & $2*10^{-4}$ s^{-1} (MH_2L) at pH-4.3 and 20°C [32]. Therefore, the presently estimated dissociation rate constant does not represent the dissociation of single species, but is rather a combination of the dissociation contribution from three different species i.e. ML, MHL, & MH_2L. Overall, the [^{177m}Lu]Lu-DOTATATE complex behavior clearly highlights the fact that a careful consideration of all the possible species at a certain pH should be given while assessing the role of any complexing agent in ^{177}Lu-^{177m}Lu separation.

The ^{177}Lu/^{177m}Lu activity ratio obtained during the LLE of ^{177}Lu ions from [^{177m}Lu]Lu-DOTATATE complex was found to be influenced by the length of the ^{177}Lu accumulation period. The highest ^{177}Lu/^{177m}Lu activity ratio of 1086±40 was obtained after ^{177}Lu accumulation period of 26 days and decreased to 600±200 for accumulation periods of 5 to 10 days. This was expected as the amount of ^{177}Lu ions produced from the internal conversion of ^{177m}Lu ions grows as the

^{177}Lu accumulation period increases. In contrast, the ^{177m}Lu contribution is only due to dissociation of the complex taking place during the extraction. Additionally, a ^{177}Lu extraction efficiency of 60±10% was observed which can be associated to the loss of free ^{177}Lu ions due to their re-association with the excess complexing agent, as reported before by Bhardwaj et al. [16].

The crucial role of association kinetics on ^{177}Lu- ^{177m}Lu separation is further emphasised by studying the ^{177}Lu-^{177m}Lu separation in the presence of varying amounts of DOTA as the complexing agent. The ^{177}Lu extraction efficiency obtained during the LLE of freed ^{177}Lu ions was affected by the applied ratio of complexing agent. The ^{177}Lu extraction efficiency of 58±2% was achieved in the presence of excess DOTA (Lu:DOTA molar ratio, 1:4), and it increases to 95±4% when Lu:DOTA was present in the molar ratio 1:1, confirming that the association kinetics of freed ^{177}Lu and the excess of DOTA play an important role in the process. Similarly, the extracted ^{177m}Lu activity decreases from 0.0060±0.0015% to 0.0020±0.0010% with the increase in the Lu:DOTA molar ratios from (1:1) to (1:4) respectively, due to the re-association of ^{177m}Lu ions with the excess of DOTA.

The ^{177}Lu/^{177m}Lu activity ratios obtained during the LLE of ^{177}Lu ions from [^{177m}Lu]Lu-DOTA complex were also found to be effected by the starting Lu:DOTA molar ratio. A ^{177}Lu/^{177m}Lu activity ratio up to 3500±500 was achieved when the LLE was performed using aqueous [^{177m}Lu]LuDOTA complex with Lu:DOTA present in the molar ratio 1:4. Remarkably, the ^{177}Lu/^{177m}Lu activity ratios obtained are very close to the ^{177}Lu/ ^{177m}Lu activity ratios of 4000-10000 associated to the “direct-route” production of ^{177}Lu supplied to the clinic [21,22]. These ratios were found to decrease with the decrease in the amount of DOTA, i.e. an activity ratio of 1500±600 was observed when Lu and DOTA were present in the molar ratio 1:1. The presence of excess DOTA leads to a proportional decrease in the amount of both ^{177}Lu and ^{177m}Lu ions due to re-association. However, the ^{177}Lu production from internal conversion of ^{177m}Lu ions adds to a constant positive contribution in the amount of ^{177}Lu ions, which leads to an overall increase in the ^{177}Lu/ ^{177m}Lu activity ratios.

Finally, the observed decrease in the ^{177}Lu/^{177m}Lu activity ratio with the increase in time are well in agreement with the theoretically expected ratios based on the ^{177m}Lu and ^{177}Lu extracted shown in Figure 3 and incorporating the effect of incomplete organic phase removal on every successive extraction (see Figure S3, supplementary information). The reported separation method suffers from the drawback of incomplete organic phase removal during the LLE. The residual 1/3rd of the organic phase left unrecovered after every LLE contains un-extracted ^{177}Lu and ^{177m}Lu ions. The ^{177}Lu ions will reduce to about a half after accumulation time of 7 days, but the ^{177m}Lu ions will remain almost unchanged as they have a half-life of 160.44 days. They will add to the total amount of free ^{177m}Lu ions in the successive extraction and correspondingly to a decrease the ^{177}Lu/ ^{177m}Lu activity ratio. In case of a complete organic phase removal, the separation method could lead to a constant value of ^{177}Lu/^{177m}Lu activity ratio of around 3500 on performing periodic ^{177}Lu extraction every 7 days. Additionally, the use of longer ^{177}Lu accumulation period of 32 days will lead to 1.7 times more ^{177}Lu production compared to 7 days ^{177}Lu accumulation period. This can potentially lead to an activity ratio of 7000 on considering a constant 0.0020±0.0010% ^{177m}Lu contribution due to dissociation and 58±2% ^{177}Lu extraction efficiency. In such a case, the extracted ^{177}Lu would contain a ^{177m}Lu contribution as low as 0.01% and would be comparable to the “indirect route” ^{177}Lu production.

It should be pointed out that the specific activity of the produced ^{177}Lu is not a discussed parameter since the starting ^{177m}Lu source has very low specific activity and therefore also the extracted ^{177}Lu. Consequently the values would not represent a fair comparison with the commercially available ^{177}Lu. Additionally, the extracted ^{177}Lu ions have not been stripped from the organic phase back into the aqueous phase considering that it is a well-reported process in literature [33].

Overall, the presented work is an important milestone towards the development of a ^{177m}Lu/^{177}Lu radionuclide generator. It also opens up the possibility of employing other separation techniques such as micro-fluidic separation [34], membrane based liquid-liquid extraction [35] or an automatized LLE separation devices that can allow the commercialization of LLE based ^{177m}Lu/ ^{177}Lu radionuclide generator. However, there are several aspects that needs to investigated and optimized. Firstly, the back extraction of ^{177}Lu from the organic phase and the complete removal of any traces of organic solvents will be crucial for its potential commercialization. Secondly, this work has been performed at lab-scale with low activity levels and excludes the effect of radiolysis on the proposed ^{177m}Lu-^{177}Lu separation method. This should be carefully evaluated in the future investigations. Lastly, the described method can be further optimized in terms of shorter extraction time, use of lower temperature to perform the ^{177}Lu extraction improve the produced ^{177}Lu quality.

3.5 Conclusion

A novel ^{177m}Lu/^{177}Lu radionuclide generator is developed which combines the ^{177}Lu production via internal conversion of ^{177m}Lu at low temperatures (77 K) and the use of ultra-stable ^{177m}Lu complexes with liquid-liquid extraction. For the best conditions, the use of [^{177m}Lu]Lu-DOTA complex and LLE provides a ^{177}Lu/^{177m}Lu activity ratio of 3500±500, a value that is close to the ^{177}Lu/^{177m}Lu activity ratio 4000-10000 obtained during the ^{177}Lu production via the direct route. Future research will be focused on further optimization of novel ^{177}Lu-^{177m}Lu separation technologies aimed to ultimately lead to a clinically applicable ^{177m}Lu/^{177}Lu radionuclide generator. The round the clock availability of ^{177}Lu via a ^{177m}Lu/ ^{177}Lu radionuclide generator can significantly accelerate the research on ^{177}Lu based radiopharmaceuticals and help in realizing its full potential in nuclear medicine.

A special thanks to Prof. Dr. Marcel De Bruin for his time in discussing the data and designing of experiments.

3.6 Supplementary information

S1. Thin layer chromatography and cleaning of the ^{177m}Lu complexes with chelex resin.

At the end of synthesis, the product formation was confirmed using instant thin layer chromatography using silica plate as the stationary phase and acetonitrile: water (1:4) as the mobile phase. The uncomplexed ^{177m}Lu ions stayed at the bottom (Rf = 0) while the complex moves to the top with the mobile phase ([^{177m}Lu]Lu-DOTA with a Rf = 9 and [^{177m}Lu]Lu-DOTATATE with a Rf = 5). At the end of the labelling, the complexation yields > 99% were obtained.,

The [^{177m}Lu]Lu-DOTA and [^{177m}Lu]Lu-DOTATATE complexes are passed through activated chelex resin to remove any free un-complexed Lutetium ions. The chelex resin was activated by washing with water (2- 3 times) and 0.1M sodium acetate-acetic acid buffer, pH 4.3 (2- 3 times). The activated resin and the synthesized Lu complex were left stirring together at 20°C for about 10 minutes. At the end of 30 minutes, the aqueous complex was pipetted out using a 20-200 µL pipette. The aqueous complex was then transferred in a pre-weighed vial, and a small aliquot was used to measure the initial ^{177m}Lu activity.

S2. ^{177}Lu extraction efficiency as a function of time and DEHPA concentration.

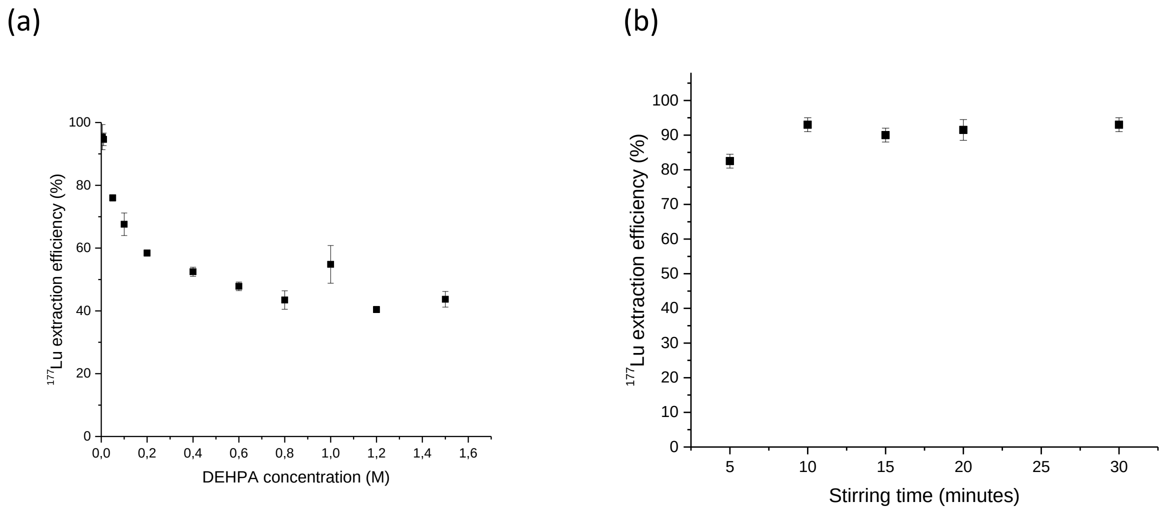

Figure 5: The ^{177}Lu extraction efficiency of 0.3mL, 1mM [^{177}Lu]$LuCl_3$ as a function of varying DEHPA concentration in dihexylether (a) and as a function of phase stirring time (b). Data points represent the average and standard deviation for six experiments.

S3. ^{177}Lu extraction efficiency

The ^{177}Lu ions are produced as a result of the internal conversion of ^{177m}Lu ions to ^{177}Lu ions. The ^{177}Lu production is defined by the equation below;

$$A_g^t = A_m^0 \cdot \left(\frac{\lambda_g}{\lambda_g - \lambda_m}\right) \cdot \left[exp^{-\lambda_{m}.t} - exp^{-\lambda_g.t}\right] \cdot B.R \cdot P.I.C. \qquad \text{Equation 1}$$

where A_m^0 = Initial activity of ^{177m}Lu before elution, λ_g, λ_m = decay constants of ^{177}Lu, ^{177m}Lu respectively, A_g^t = activity of ^{177}Lu at time t, B.R = branching ratio for ^{177m}Lu to ^{177}Lu decay, 21.4% [36], P.I.C = probability of internal conversion, 96.8% [16],

The growth in the amount of ^{177}Lu ions with the increase in the ^{177}Lu accumulation period is shown Figure 2 below;

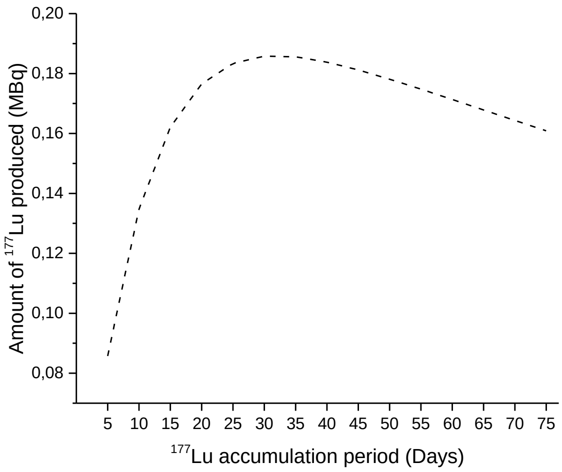

Figure 6: The amount of ^{177}Lu produced from 1 MBq of ^{177m}Lu for different ^{177}Lu accumulation period as calculated by using equation 1.

The efficiency of ^{177}Lu collection after ^{177m}Lu/ ^{177}Lu separation is defined as the ratio of the collected ^{177}Lu activity in the organic phase divided by the theoretically produced ^{177}Lu activity during the accumulation time. It is represented by the equation 2 below;

$$efficiency(\%) = \frac{A_g^t\ (collected) * (\frac{V_{total}}{V_{collected}})}{A_g^t} \cdot 100 \qquad \text{Equation 2}$$

where A_g^t is the total amount of ^{177}Lu produced after an accumulation time t (as defined in equation 1), $A_g^t\ (collected)$ is the ^{177}Lu activity measured in the organic phase after LLE, V_{total} and $V_{collected}$ are the total organic volumes and the organic fraction collected after SE respectively, t = time of ^{177}Lu separation (7 days).

^{177}Lu/ ^{177m} Lu activity ratios with time after Liquid- Liquid Extraction

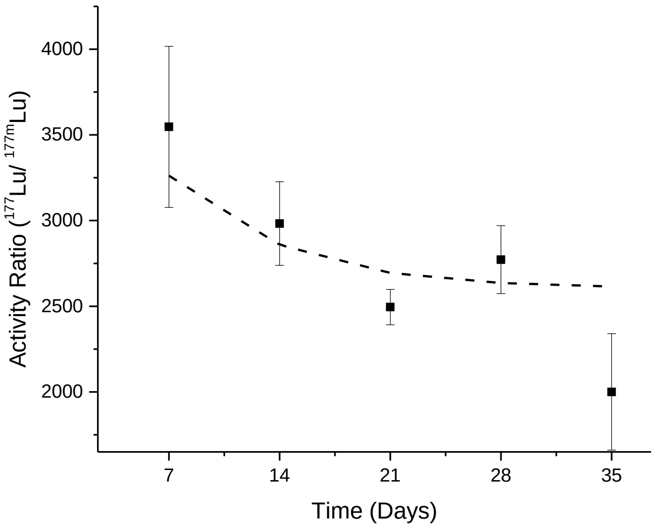

Figure 7: The ^{177}Lu/ ^{177m}Lu activity ratio obtained at different elution time when the LLE is performed with [^{177m}Lu]Lu-DOTA complex synthesized in a molar ratio 1:4. The data points represent the experimentally observed ratios, while the dotted line represents the expected activity ratios with 60% ^{177}Lu extraction efficiency and 0.002% ^{177m}Lu ions leakage.

3.7 References

1 Knapp, F. F. & Dash, A. in *Radiopharmaceuticals for Therapy* 131-157 (Springer India, 2016).

2 Knapp, F. F. & Mirzadeh, S. The continuing important role of radionuclide generator systems for nuclear medicine. *Eur J Nucl Med* 21, 1151-1165, doi:10.1007/bf00181073 (1994).

3 Knapp, F. F., Pillai, M. R. A., Osso, J. A. & Dash, A. Re-emergence of the important role of radionuclide generators to provide diagnostic and therapeutic radionuclides to meet future research and clinical demands. *J Radioanal Nucl Chem* 302, 1053-1068, doi:10.1007/s10967-014-3642-8 (2014).

4 F. Knapp, F. & P. Baum, R. Radionuclide Generators; A New Renaissance in the Development of Technologies to Provide Diagnostic and Therapeutic Radioisotopes for Clinical Applications). *Current Radiopharmaceuticals* 5, 175-177 (2012).

5 Roesch, F. & J. Riss, P. The Renaissance of the 68Ge/68Ga Radionuclide Generator Initiates New Developments in 68Ga Radiopharmaceutical Chemistry. *Current Topics in Medicinal Chemistry* 10, 1633-1668, doi:10.2174/156802610793176738 (2010).

6 Pillai, M. R. A., Ashutosh, D. & Knapp, F. F. Rhenium-188: Availability from the 188W/188Re Generator and Status of Current Applications. *Current Radiopharmaceuticals* 5, 228-243, doi:http://dx.doi.org/10.2174/1874471011205030228 (2012).

7 Das, T. & Banerjee, S. Theranostic Applications of Lutetium-177 in Radionuclide Therapy. *Current Radiopharmaceuticals* 9, 94-101 (2016).

8 Das, T. & Pillai, M. R. Options to meet the future global demand of radionuclides for radionuclide therapy. *Nucl Med Biol* 40, 23-32, doi:10.1016/j.nucmedbio.2012.09.007 (2013).

9 <Radionuclide generators current and future applications in nuclear medicine.pdf>.

10 Banerjee, S., Pillai, M. R. & Knapp, F. F. Lutetium-177 therapeutic radiopharmaceuticals: linking chemistry, radiochemistry, and practical applications. *Chem Rev* 115, 2934-2974, doi:10.1021/cr500171e (2015).

11 Emmett, L. *et al.* Lutetium 177 PSMA radionuclide therapy for men with prostate cancer: a review of the current literature and discussion of practical aspects of therapy. *Journal of Medical Radiation Sciences* 64, 52-60, doi:10.1002/jmrs.227 (2017).

12 Hofman, M. S. *et al.* [(177)Lu]-PSMA-617 radionuclide treatment in patients with metastatic castration-resistant prostate cancer (LuPSMA trial): a single-centre, single-arm, phase 2 study. *Lancet Oncol* 19, 825-833, doi:10.1016/s1470-2045(18)30198-0 (2018).

13 Repetto-Llamazares, A. H. V. *et al.* Combination of (177) Lu-lilotomab with rituximab significantly improves the therapeutic outcome in preclinical models of non-Hodgkin's lymphoma. *European journal of haematology*, doi:10.1111/ejh.13139 (2018).

14 Dho, S. H. *et al.* Development of a radionuclide-labeled monoclonal anti-CD55 antibody with theranostic potential in pleural metastatic lung cancer. *Scientific Reports* 8, 8960, doi:10.1038/s41598-018-27355-8 (2018).

15 De Vries, D. J. & Wolterbeek, H. The production of medicinal 177Lu and the story of 177mLu: detrimental by-product or future friend? *Tijdschr. Nucl. Geneeskd* 34, 899-904 (2012).

16 Bhardwaj, R. *et al.* Separation of nuclear isomers for cancer therapeutic radionuclides based on nuclear decay after-effects. *Scientific Reports* 7, 44242, doi:10.1038/srep44242 (2017).

17 Cooper, E. P. On the Separation of Nuclear Isomers. *Physical Review* 61, 1-5, doi:10.1103/PhysRev.61.1 (1942).

18 Dvorakova, Z., Henkelmann, R., Lin, X., Türler, A. & Gerstenberg, H. Production of 177Lu at the new research reactor FRM-II: Irradiation yield of 176Lu(n,γ)177Lu. *Applied Radiation and Isotopes* 66, 147-151, doi: (2008).

19 Pawlak, D., Parus, J. L., Sasinowska, I. & Mikolajczak, R. Determination of elemental and radionuclidic impurities in 177Lu used for labeling of radiopharmaceuticals. *J Radioanal Nucl Chem* 261, 469-472, doi:10.1023/B:JRNC.0000034887.23530.f6 (2004).

20 Knapp, F. F. J. A., K.R.; Beets, A.L.; Luo, H.; McPherson, D.W. & Mirzadeh, S. Nuclear medicine program progress report for quarter ending September 30, 1995, report,.

21 Das, T., Chakraborty, S., Banerjee, S. & Venkatesh, M. On the preparation of a therapeutic dose of 177Lu-labeled DOTA–TATE using indigenously produced 177Lu in medium flux reactor. *Applied Radiation and Isotopes* 65, 301-308, (2007).

22 Chakraborty, S., Vimalnath, K. V., Lohar, S., Shetty, P. & Dash, A. On the practical aspects of large-scale production of 177Lu for peptide receptor radionuclide therapy using direct neutron activation of 176Lu in a medium flux research reactor: the Indian experience. *Journal of Radioanalytical and Nuclear Chemistry* 302, 233-243, doi:10.1007/s10967-014-3169-z (2014).

23 Watanabe, S. *et al.* Production of highly purified no-carrier-added 177Lu for radioimmunotherapy. *J Radioanal Nucl Chem* 303, 935-940, doi:10.1007/s10967-014-3534-y (2015).

24 Le Minh, T. & Lengyel, T. On the separation of molybdenum and technetium crown ether as extraction agent. *J Radioanal Nucl Chem* 135, 403-407, (1989).

25 Fikrle, M., Kučera, J. & Šebesta, F. Preparation of 95mTc radiotracer. *J Radioanal Nucl Chem* 286, 661-663, doi:10.1007/s10967-010-0737-8 (2010).

26 Bhatia, D. S. & Turel, Z. R. Solvent extraction of99mTc/VII/ with methylene blue into nitrobenzene. *J Radioanal Nucl Chem* 135, 77-83, doi:10.1007/BF02163538 (1989).

27 Boyd, R. E. Technetium-99m generators—The available options. *The International Journal of Applied Radiation and Isotopes* 33, 801-809, (1982).

28 Ehrhardt, G. J. & Welch, M. J. A new germanium-68/gallium-68 generator. *Journal of nuclear medicine: official publication, Society of Nuclear Medicine* 19, 925-929 (1978).

29 Mushtaq, A., Bukhari Tanveer, H. & Khan Islam, U. in *Radiochimica Acta* Vol. 95 535 (2007).

30 Dutta, S. & Mohapatra, P. K. Studies on the separation of 90Y from 90Sr by solvent extraction and supported liquid membrane using TODGA: role of organic diluent. *J Radioanal Nucl Chem* 295, 1683-1688, doi:10.1007/s10967-012-2233-9 (2013).

31 Blaauw, M. *The holistic analysis of gamma-ray spectra in instrumental neutron activation analysis*, (1993).

32 van der Meer, A., Breeman, W. A. P. & Wolterbeek, B. Reversed phase free ion selective radiotracer extraction (RP-FISRE): A new tool to assess the dynamic stabilities of metal (-organic) complexes, for complex half-lives spanning six orders of magnitude. *Applied Radiation and Isotopes* 82, 28-35, (2013).

33 Trtic-Petrovic, T. M., Kumric, K. R., Dordevic, J. S. & Vladisavljevic, G. T. Extraction of lutetium(III) from aqueous solutions by employing a single fibre-supported liquid membrane. *J. Sep. Sci.* 33, 2002-2009, doi:10.1002/jssc.201000042 (2010).

34 Davide, C., M., P. J. & W., S. G. The use of microfluidic devices in solvent extraction. *Journal of Chemical Technology & Biotechnology* 89, 771-786, doi:doi:10.1002/jctb.4318 (2014).

35 Pedersen-Bjergaard, S. & Rasmussen, K. E. Liquid-phase microextraction with porous hollow fibers, a miniaturized and highly flexible format for liquid–liquid extraction. *Journal of Chromatography A* 1184, 132-142, (2008).

36 Kondev, F. G. Nuclear data sheets for A = 177. *Nuclear Data Sheets* 98, 801- 1095 (2003).

Chapter 4

Solid phase extraction based separation of the nuclear isomers ^{177m}Lu and ^{177}Lu

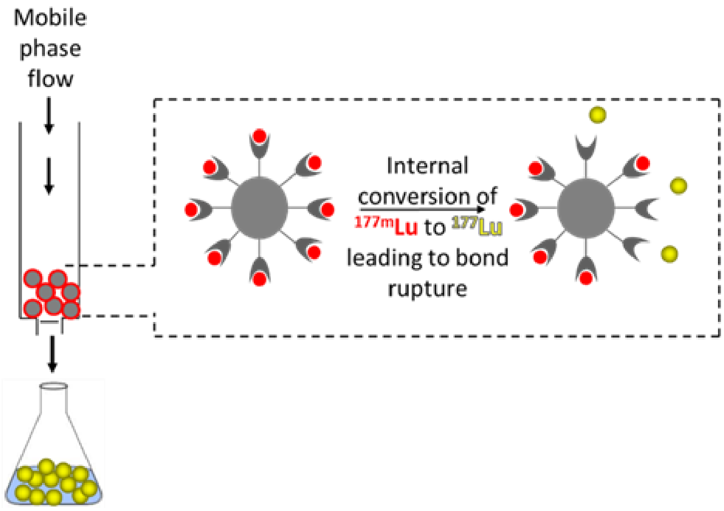

Abstract

In this chapter, a solid phase extraction based ^{177m}Lu-^{177}Lu separation method has been investigated for its feasibility to be used in the radionuclide generator. The use of 2,2',2"-(10-(2,6-dioxotetrahydro-2H-pyran-3-yl)-1,4,7,10-tetraazacyclododecane-1,4,7-triyl)triacetic acid, (DOTAGA-anhydride) allowed grafting of DOTA (1,4,7,10-tetraazacyclododecane N,N',N'',N'''-tetraacetic acid) complex on the surface of commercially available amino propyl silica. The grafting of DOTA has been confirmed by several characterization techniques. The thermogravimetric analysis reveals that the 0.33 mmol DOTA groups have been grafted per gram of silica. However, during the Lu ion complexation, a 10 times low Lu adsorption capacity of 0.03 mmol.g^{-1} could be achieved under the studied reaction conditions. The results indicate that the grafting of DOTA on solid affects the Lu coordination and also influences the kinetics of Lu-DOTA complexation. The weak coordination resulted in high ^{177m}Lu leakage, while the unreacted DOTA groups interferes with the ^{177}Lu release. This is evident from the 0.3% ^{177m}Lu leakage combined with a ^{177}Lu extraction efficiency of 25%. Overall, the results show a ^{177m}Lu-^{177}Lu separation with a maximum ^{177}Lu/^{177m}Lu activity ratio of 25. But this is still far away from clinically acceptable activity ratio of 10,000 for which future work is recommended.

4.1. Introduction:

Lutetium-177 (^{177}Lu) is a radionuclide with tremendous potential in the field of nuclear medicine [1]. [^{177}Lu]Lu-DOTATATE has been approved for neuroendocrine tumor treatment and clinical studies involving the application of other ^{177}Lu based radiopharmaceuticals in the treatment of prostate cancer, bone pain palliation among others are in progress [1]. Recently, a $^{177m}Lu/^{177}Lu$ radionuclide generator for ^{177}Lu production has been proposed [2] and is anticipated to bring significant advances in the development of ^{177}Lu based radiopharmaceuticals [3]. It offers unique advantage of onsite, on-demand ^{177}Lu production without the need of a nearby radionuclide production facility. The development of the $^{177m}Lu/^{177}Lu$ radionuclide generator involves the challenging separation of the physically and chemically identical nuclear isomers, ^{177m}Lu and ^{177}Lu. The ^{177m}Lu-^{177}Lu separation has been based on the internal conversion decay of ^{177m}Lu and the proof of concept has been already established [4]. Further, the reported liquid- liquid extraction (LLE) based ^{177m}Lu-^{177}Lu separation technique has shown promising potential in producing clinically acceptable ^{177}Lu quality [3]. However, the commercial applicability of LLE based radionuclide generators is limited by several shortcomings such as, ease of utilization, automation, reproducibility, undesired use of organic solvents and others [3].

Solid phase extraction (SPE) has been considered as one of the most convenient method that can allow circumventing the above-mentioned limitations [5]. Its operational simplicity, amenability to automation, and ability to obtain daughter radionuclide using low amount of eluting solvents makes it a very attractive separation technique. The SPE has been explored in the past for the development of $^{99m}Mo/^{99}Tc$, $^{68}Ge/^{68}Ga$ and $^{188}W/^{188}Re$ radionuclide generator [6-9]. Typically, in a SPE based radionuclide generator, the parent radionuclide is attached to a solid support and the produced daughter radionuclide is eluted in a liquid phase using an eluting agent [5]. SPE has never been applied for the separation of physically & chemically identical parent-daughter radionuclide pair. The SPE based ^{177m}Lu-^{177}Lu separation requires a solid support that should i) be chemically stable ii) allows ^{177m}Lu complexation and iii) it should permit the elution of free ^{177}Lu ions while retaining the complexed ^{177m}Lu ions.

Amino propyl silica (APS) is one of the extensively studied and often used starting material for the preparation of different solid supports [10-14]. The presence of amine groups provides a facile way to couple it with a wide variety of functional groups such as acids, esters and others [15]. There are several reports involving the grafting of small molecules [16-19] and macrocyclic compounds [20-23] on APS surface. However, the application of majority of these solids lies in metal ion recovery [17,18,21-24] or use as silica supported metal catalysts [16] and has never been used for any radionuclide generator development.

In this work the chelator DOTA, which is well known to complex Lu ions, has been grafted on the commercially available amino propyl silica support. The synthesized solid has been characterized and tested for its Lu adsorption behavior. Lastly, ^{177m}Lu cations have been adsorbed on the solid surface and tested under different elution conditions that can allow the removal of ^{177}Lu ions while keeping the leakage of complexed ^{177m}Lu ions minimal.

4.2. Experimental

4.2.1. Synthesis of DOTA grafted silica (DAGSi)

The grafting of DOTA on APS has been performed using the commercially available precursor, DOTAGA-anhydride, as shown in Figure 1. Aminopropyl silica (WAT023513) was supplied by Waters as Sep-Pak Aminopropyl (NH_2) Plus Light Cartridge. 2,2′,2″-(10-(2,6-dioxotetrahydro-2H-pyran-3-yl)-1,4,7,10-tetraazacyclododecane-1,4,7-triyl)triacetic acid (DOTAGA-anhydride) was purchased from Chematech. N,N′-Diisopropylethylamine (DIPEA) and Dimethylformamide (DMF) were purchased from Sigma Aldrich. All the chemicals were used as purchased without any further purification.

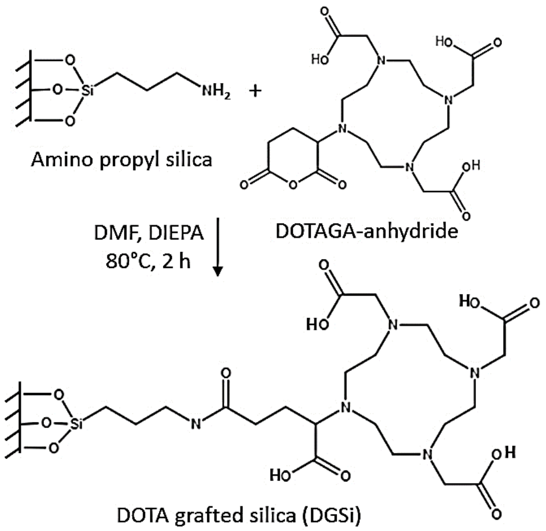

Figure 1: Schematics of grafting of DOTAGA-anhydride on amino propyl silica

DOTAGA-anhydride (80mg, 0.18 mmol, 3 eqv) was weighed and transferred in a glass tube containing 3-4 mL DMF. DIPEA (50uL, 10 times excess) was added to it in 3 equal portions at a time interval of 10 minutes with continuous stirring. Finally, Amino Propyl Silica (APS) (60mg, 0.06mmol, 1 eqv) was added and the reaction mixture was left for stirring at 80°C for 2 hours. After 2 hours, the reaction mixture was brought to room temperature and the suspension was centrifuged. The separated solid was washed with 0.1M HCl deionized water and dried. The reaction conditions were based on the reported protocol involving the reaction between the propyl amine group and DOTAGA-anhydride in liquid phase [25].

4.2.2. Characterization

Scanning electron microscopy (SEM) experiments were conducted in a JEOL JSM-IT100 microscope operated at an accelerating voltage of 20 kV. The experiments were performed to characterize the surface morphology of the silica particles before and after DOTA immobilization. Solid-state ^{13}C- Nuclear Magnetic Resonance Spectroscopy were performed at 17.6 TonaBruker Advance spectrometer equipped with a 4mm triple channel MAS probe (Bruker, Karlsruhe, Germany). Diffuse reflectance infrared Fourier transform spectroscopy (DRIFTS) was carried out in a Nicolet 8700 equipped with a high temperature and pressure cell using a liquid nitrogen cooled MCT/A detector. Spectra were recorded from 4000 to 1000 cm^{-1} wavenumbers with 128 scans and a resolution of 4 cm^{-1}. The DRIFT spectra reported in the present work were obtained at 100 °C in order to remove any interference from the adsorbed water content. Thermo-gravimetric analysis (TGA) was performed on a Mettler Toledo TGA/SDTA1 with a sample robot (TSO 801RO) and gas control (TSO 800GC1). The temperature was linearly increased from 30 to 900°C at a heating rate of 5°C.min^{-1} under an air flow (100 cm^3 min^{-1}). Grafting percentage of different DOTA moieties on the silica surface was calculated by subtracting the weight loss of the untreated aminopropyl silica particles from the loss after the modification with DOTA. The number of DOTA groups immobilized per g silica (mmol per g) was calculated using the equation below:

$$n_0 = \frac{weight\ loss\ of\ the\ modified\ silica\ particles\ (g)}{total\ silica\ particle\ mass\ (g) * M_w\ of\ the\ bonded\ organic\ molecules\ (g\ mol^{-1})} \quad \text{Equation 1}$$

Lastly, the presence of free amino groups was checked using the Kaiser test kit supplied by Sigma Aldrich, 60017.

4.2.3. Lutetium-177 and lutetium-177m sources

The lutetium-177 (^{177}Lu) used in the study was produced by irradiating 1-2 mg of $LuCl_3$ at the Hoger Onderwijs Reactor Delft (HOR) with a thermal neutron flux of 4.72*10^{12} n cm^{-2} s^{-1} (epithermal neutron flux of less than 7.08*10^{11} n cm^{-2} s^{-1}) and an irradiation time of 10 hours, followed by 3 days of cooling period. The ^{177m}Lu source was provided by IDB- Holland as a 1 mM acidic solution with 5 MBq ^{177m}Lu per g of solution. For the ^{177m}Lu/ ^{177}Lu radionuclide generator experiments, about 0.2- 0.3 MBq ^{177m}Lu was used per experiment.

4.2.4. Study of Lu adsorption on the DOTA Grafted Silica

About 5 mg of the solids were used for batch adsorption studies. They were taken in an eppendorf and cold Lu ions spiked with ^{177}Lu (about 10 KBq) were added to it in 4- 5 times excess molar ratio. For amino silica, the adsorption was studied at three different pH values, 4.3, 5.6 and 7.3. The APS showed negligible retention of Lu ions at pH 4.3, therefore the adsorption for DAGSi was studied only at pH 4.3. The pH during the adsorption was maintained using 0.5 M buffer sodium acetate-acetic acid buffer. The buffer and the Lu ions were added to the solid in an eppendorf. It was left stirring at 80°C for about 2 hours, followed by an incubation period of about 1 hour at room temperature. The solid suspension were then transferred to 1mL empty chromatographic column, 40mm * 5.6mm (supplied by Bio Rad) using a pipette. These columns were connected with a luer lock syringe for a simple single step elution. The columns were eluted manually. First, the excess amount of liquid was flushed out of the column by applying pressure using the empty syringe. It was followed by a wash with 10mM sodium acetate-acetic acid buffer at pH 4.6 and 10 mM DTPA pH 5, (about 2 mL each). The initial activity and the decant liquids were collected and measured using a well type gamma counter (Wallac 2480 Automatic Gamma counter from Perkin Elmer Technologies) to measure the amount of active Lu ions retained by silica. The total Lu adsorption capacity *q* in mol.g^{-1} was calculated using the Equation 1,

$$q\ (mol.g^{-1}) = \frac{Counts_{initial} - Counts_{final}}{Counts_{initial}} * \frac{C_o * V}{1000 * m}$$

where, $Counts_{initial}$ are the initial ^{177}Lu counts before the adsorption and $Counts_{final}$ represents the total ^{177}Lu counts in the eluate liquid after the loading and the washing steps. C_o, represents the total concentration of cold Lu ions used in the experiments, V is the volume, and m is the mass of silica used.

Instrumental Neutron Activation Analysis was also used to determine the adsorption capacity of the synthesized DOTA grafted silica. The cold lutetium ions were adsorbed on the surface of APS and DGSi, using the same protocol as mentioned previously in sec 1.4.2. After the cleaning with DTPA, about 2 mg of the material was bombarded at the Hoger Onderwijs Reactor Delft (HOR) with a thermal neutron flux of $4.72*10^{12}$ cm^{-2} s^{-1} (epithermal neutron flux of less than $7.08*10^{11}$ cm^{-2} s^{-1}) and an irradiation time of 10 hours, followed by 3 days of cooling period. The ^{177}Lu activity of the silica particles was measured on a well-type germanium detector to perform a quantitative evaluation on the amount of Lu ions per g solid.

4.2.5. Gamma ray spectroscopy

The activity measurements were performed using a well-type HPGe gamma-ray detector. The energy and efficiency calibration of the detector was performed using a certified Eu-152 source, and the efficiency calibration for each lutetium peak was fine-tuned using a known ^{177}Lu, ^{177m}Lu source provided by IDB- Holland to take true-coincidence summing effects into account.

4.2.6. Study of Lu elution behavior on the DOTA grafted silica

In this work, three different eluents namely 10mM sodium acetate- acetic acid buffer solution (pH 4.3), 10mM DTPA (pH 5), and 1% DEHPA in DHE were applied as eluting agent. Typically, ^{177}Lu ions were complexed with 5- 6 mg of DAGSi using the protocol mentioned in section 2.4.1. After the complexation and washing steps, the columns with a known initial ^{177}Lu activity were obtained. A luer lock syringe was attached to one end of the column, and the eluents (10mM pH-4.3 buffer solution, 10mM DTPA (pH 4.6), 1% DEHPA in DHE) were passed through the column dropwise by manually inserting pressure on the syringe. For each eluent, the elution fraction volumes of 0.2mL, 1 mL and 2 mL were collected and measured using gamma ray spectrometry to determine the percentage ^{177}Lu activity leaked in each fraction.

4.2.7. ^{177m}Lu- ^{177}Lu separation

The ^{177m}Lu ions were adsorbed on the surface of DAGSi using the adsorption and washing protocol as detailed previously in sec 2.4.1. About 5 mg of the DAGSi was taken in an Eppendorf. It was left in contact with about 0.30 mL of 1 mM Lu solution containing about 0.3 MBq ^{177m}Lu and the pH during the absorption was maintained using 0.5 M buffer sodium acetate-acetic acid buffer. The reaction mixture was left stirring at 80°C for about 2 hours, followed by an incubation period of about 1 hour at room temperature. It was then washed with pH- 4.3 NaAc buffer and 10 mM pH-5 DTPA solution. The washes were collected and measured using gamma ray spectroscopy to determine the amount of ^{177m}Lu ions loaded on the silica. The ^{177m}Lu containing solids were then transferred to 1mL empty chromatographic column, 40mm * 5.6 mm (length * diameter) (supplied by Bio Rad) using a pipette. These columns were transferred in a 10 mL centrifuge tube followed by placing them in whirl-pak sampling bag (supplied by sigma aldrich, product number. Z527009) and they were moved inside a liquid nitrogen tank, to allow the ^{177}Lu production during the accumulation period. After a ^{177}Lu accumulation period of 7 days, the columns were eluted using pH- 4.3 sodium acetate- acetic acid buffer solution as eluent and elution fraction volumes of 0.2 mL were collected. Gamma ray spectroscopy was used to determine the ^{177}Lu, ^{177m}Lu activity collected in each eluted fraction.

4.3. Results and Discussion

The synthesized DOTA grafted silica have been characterized and tested for i) stability ii) Lu absorption capacity iii) Lu elution behavior and iv) the ^{177m}Lu- ^{177}Lu separation performance, and the results are discussed below:

4.3.1. Synthesis and characterization

The surface morphology of the starting amino propyl silica and the synthesized DOTA grafted silica particles were examined by SEM analysis (Figure 2).

Starting APS	DOTA grafted silica (DGSi)
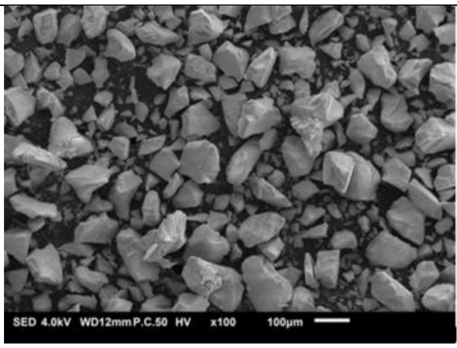	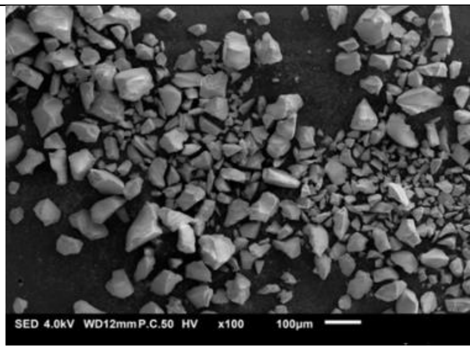

Figure 2: SEM images of a) Amino propyl silica (APS) b) DOTAGA-anhydride grafted silica (DGSi) (c) DOTA grafted silica (DAGSi) (d) DOTA tris-t-butyl ester grafted silica (DEGSi)

Figure 2(a) shows that the original amino propyl silica contained uniformly distributed particles of about 10-20 µm. At the end of modification, a majority of the particles retained their size and remained unaffected (Figure 2(b)). To further analyze the particles, several characterization studies were performed, as shown in Figure 3. Figure 3(a), (b) shows the IR, ^{13}C-NMR spectra of the amino propyl silica before and after the grafting of DOTA, respectively while the Figure 3(c), (d) shows the TGA analysis which allowed the quantification of the amount of DOTA molecules grafted on the surface of silica.

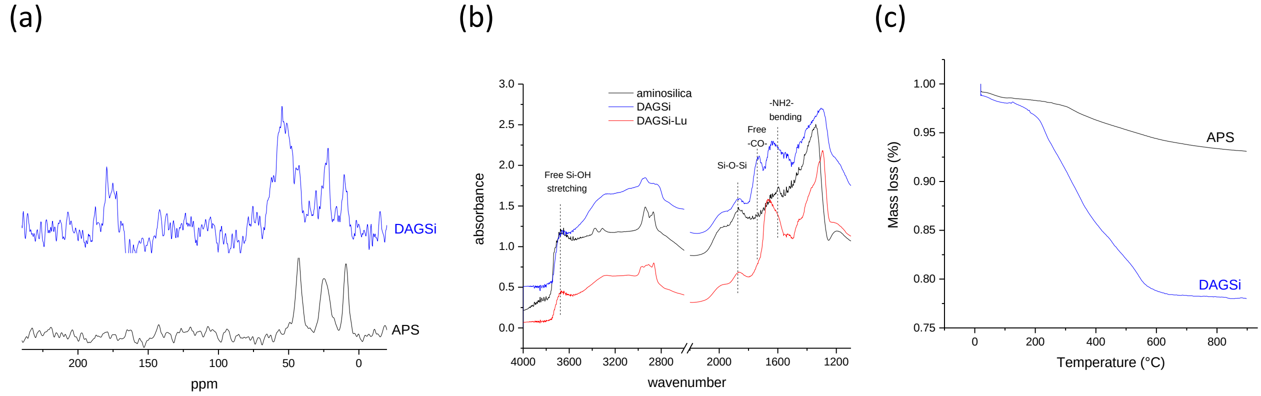

Figure 3: Characterization studies (a) 13C-NMR spectra of aminopropyl silica (APS) (in black) and DOTAGA- Grafted Silica (DAGSi) (in blue) (b) FT-IR spectra of aminopropyl silica (APS) (in black), DOTAGA- Grafted Silica (DAGSi) (in blue) and DAGSi after the coordination with Lu ions (in red) (c) TGA of aminopropyl silica (APS) (in black), DOTAGA- Grafted Silica (DAGSi) (in blue).

Figure 3(a) shows the ^{13}C-NMR spectra of APS (in black) and DAGSi (in blue). The ^{13}C-NMR of APS consists of three peaks at 10(C1), 27(C2) and 43(C3) ppm. They are assigned to the carbon chain of amino propyl group as $SiCH_2(1)CH_2(2)CH_2(3)NH_2$, accordingly [10]. The ^{13}C-NMR spectra of DAGSi showed additional broad peaks around 50 ppm and 170 ppm, which can be ascribed to the aliphatic CH_2 groups and the carbonyl carbons of the DOTA, respectively. Additionally, an upfield shift from 27 ppm to 21 ppm was observed for the peak corresponding to C2 carbon of amino silica, along with a shoulder peak at 27 ppm. The upfield shift from 27 ppm to 21 ppm can be attributed to binding of amino groups with the DOTA groups, while the shoulder peak indicates a small part of unreacted amino groups [10].

Figure 3(b) shows the IR spectrum of APS (in black), DAGSi (in blue), and DAGSi after Lu complexation (in red). The IR spectrum of APS exhibits a sharp peak around 3675cm^{-1}, which is characteristic for the silanol groups present on the surface of silica [26-28]. The three peaks at 3376, 3310 cm^{-1} and 1595 cm^{-1} can be assigned to characteristic N-H stretching vibrations and to the NH_2 deformation mode of free amino groups [14,29]. The bands around 3000-2800 cm^{-1} belongs to the C-H stretching vibrations [26,30]. The peak at 1868 cm^{-1} is characteristic of the Si-O vibration of the silica structure [31] and the broad peak around 1349 cm^{-1} can be attributed to Si-O-Si asymmetric stretching vibration [32]. After the reaction with DOTAGA-anhydride, the peaks corresponding to NH stretching vibrations and to the NH_2 deformation mode of free amino groups disappears with the appearance of new bands around 1720 cm^{-1}, 1652cm^{-1} (see DAGSi spectra, in blue). The peaks at 1720 cm^{-1}, 1652cm^{-1} correspond to the free –COOH groups and –CO-NH- group which confirms the successful coupling of DOTA molecules to the amino propyl groups. Further, after the loading of Lu ions on the surface of DAGSi, the peak at 1720 cm^{-1} disappears indicating the successful coordination of carboxylic acids with Lu ions (see Figure 1(b), DAGSi-Lu spectra, in red). Further, the DAGSi also gave a positive Kaiser test, which confirms the presence of unreacted primary amino groups.

Figure 3(c) shows the TGA spectra of APS (in black) and DAGSi (in blue). It can be seen that both solids exhibits a mass loss in the temperature range 200- 900°C that corresponds to the organic groups. For APS, a mass loss of 5.4% has been observed which matches the manufactures specifications of 1 mmol amino propyl groups per gram silica. For DAGSi, a much higher organic mass loss of 20.6% was observed. The increased organic mass loss is attributed to the DOTA groups grafted on the surface and corresponds to 0.33 mmol DOTA groups per g of silica (in accordance with Equation 1).

To summarize, the characterization studies shown in Figure 3 indicates the successful coupling of DOTA groups on the surface of amino propyl silica and establishes a novel strategy to immobilize DOTA groups on the surface of commercially available silica. Additionally, under the studied reaction conditions, some free amino groups remain present on the surface of DAGSi as indicated by the IR, ^{13}C-NMR, and a positive Kaiser test.

4.3.2. Lutetium adsorption

The adsorption of lutetium on DOTA grafted silica can happen either via the chemical complexation of Lu ions with the DOTA ligands or by undesired physical adsorption on the surface. The pH showing minimal interference with the chemical complexation of Lu ions has been determined and the results are shown in Table 1.

Table 1: The lutetium adsorption capacity of amino propyl silica (APS) and DOTAGA grafted silica (DAGSi).

pH	Lu uptake	
	APS	DAGSi
4.3	0.02±0.002 nmol g^{-1}	0.03±0.005 mmol g^{-1}
5.6	0.3±0.003 nmol g^{-1}	Not tested
8.5	4.4±0.022 nmol g^{-1}	Not tested

Table 1 shows that for APS an increase in Lu adsorption capacity was observed with the increase in the pH. The lowest lutetium ion adsorption of 0.02 nmol.g^{-1} was obtained at pH 4.3 increasing to about 4 nmol.g^{-1} at pH 8.3. This is expected as the APS surface has been reported to have an iso-electric point around pH 6- 7 [14]. An increase in the pH leads to an increased negative charge on the APS surface and thus a higher affinity for positively charged Lutetium ions. Thus, pH-4.3 has been used for the Lu complexation, as it is also considered as an ideal pH for the Lu-DOTA complexation.

For DAGSi, the Lu absorption capacity of 0.03 mmol.g^{-1} has been observed (see Table 1) in comparison to 0.02 nmol.g^{-1} observed for amino propyl silica. The increased Lu uptake confirms the successful immobilization of DOTA groups on the surface of APS. However, the observed Lu uptake was 10 times less than the amount of DOTA grafted on the surface (0.33mmol.g^{-1} shown in Figure 3(d)). This was unexpected, as Lu has been known to form a stable cage like coordination with DOTA in a 1:1 stoichiometry under the studied reaction conditions [33]. This suggests that under the studied reaction conditions, not all the DOTA groups were accessible to Lu ions. It can also be due to the changed coordination behavior or slowed kinetics of complex formation after the grafting of DOTA on a solid surface. The change in the coordination behavior of metal ions after the immobilization of DOTA groups on solid surface was previously observed for Pd-DOTA complex [22]. It was suggested that Pd(II) gets coordinated with neighboring carboxylic groups instead of the coordination with N atoms in the cage structure [22]. Presently, we did not investigate the exact nature of Lu ion complexation with the surface and should be performed in future to have a better understanding of the coordination mechanism.

4.3.3. Lutetium elution behavior

The ^{177m}Lu-^{177}Lu separation requires an eluting agent that minimizes the leakage of the complexed ^{177m}Lu ions while allowing the release of the freed ^{177}Lu ions. ^{177}Lu cations were complexed with the DAGSi and then different eluents were passed through the column to study the Lu leakage. The percent ^{177}Lu leakage was studied as a function of elution fraction volume, as shown in Figure 4 below. The Figure 4(a), 4(b), 4(c) represents the elution fractions of 2 mL, 1 mL and 0.2 mL respectively, collected using three different eluents namely, pH-4.3 sodium acetate-acetic acid buffer, aqueous pH-5 solution with 10 mM DTPA, and 0.5% DEHPA in DHE.

(a) (b) (c)

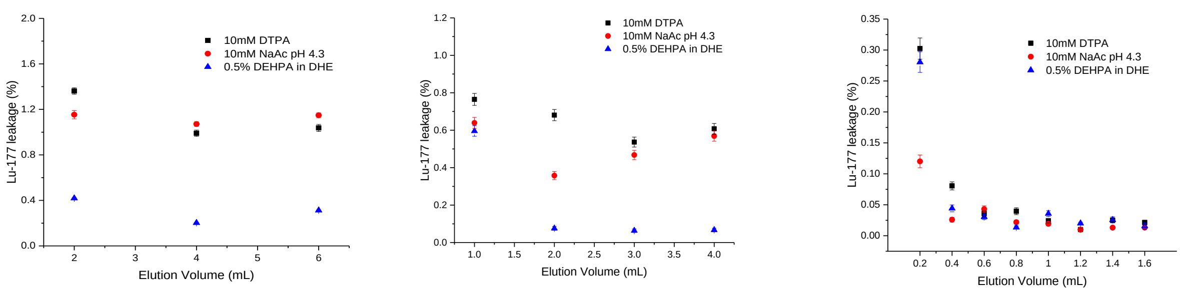

Figure 4: The Lu elution profiles as a function of elution fraction 2 mL (a) 1mL (b) 0.2 mL (c) obtained for the three different eluents namely, 10mM sodium acetate- acetic acid buffer (pH- 4.3), 10 mM DTPA (pH-5) and 0.5% DEHPA in DHE.

Figure 4(a) shows that for the studied eluents, the Lu leakage varies in the order of 0.4%- 1.5%. The percent Lu leaked remain almost constant when three successive fractions of 2 mL were collected. The lowest Lu leakage of 0.4% was observed on using 0.5% DEHPA in DHE as an eluent. The weaker interactions between the hydrophobic organic solvent and hydrophilic silica surface can possible explain the detected low Lu leakage. However, Lu leakage of the order of 0.002% has been observed previously using Lu–DOTA complex in the liquid phase (Chapter 3). The much higher Lu leakage observed in the current study points to the fact the Lu is not coordinated in the expected stable cage like coordination with the DOTA complex.

In order to reduce the Lu leakage smaller fractions of 1mL and 0.2mL were collected, and the results are shown in Figure 4(b) and Figure 4(c). As expected, the decrease in the elution fraction volume leads to a proportional decrease in the percent Lu ions leakage. Further, for elution fraction volumes of 0.2 mL, the first fraction contained the Lu leakage ranging from 0.1%- 0.3%, and decreases to less than 0.05% in the subsequent fractions (see Figure 4(c)). The 0.1% Lu leakage is still far from the previously observed Lu leakage of 0.002%, but for the studied SPE extraction it provides with a possibility to decrease the ^{177m}Lu leakage during the ^{177}Lu-^{177m}Lu separation.

Lastly, it should be mentioned that the use of ether as an eluent solvent damages the column materials, and they could not be reused. Therefore, a dihexyl ether based eluent was not used in ^{177m}Lu-^{177}Lu separation experiments and only the pH-4.3 NaAc buffer was used with the collection of 0.2 mL elution fraction volumes.

4.3.4. ^{177m}Lu-^{177}Lu separation

The ^{177m}Lu-^{177}Lu separation experiments were performed using DOTAGA grafted silica (DAGSi). The ^{177m}Lu ions were complexed with DAGSi, and the solids were left at 77K to allow for ^{177}Lu accumulation for a period of 7 days. At the end of accumulation, the ^{177}Lu ions were eluted 10 mM NaAc buffer (pH-4.3) and elution fraction volume of 0.2 mL were collected. The ^{177}Lu/^{177m}Lu activity ratio obtained in each elution fraction is shown in Figure 5(a) and Figure 5(b) displays the corresponding ^{177}Lu extraction efficiency and the percentage of starting ^{177m}Lu activity leaked.

(a) (b)

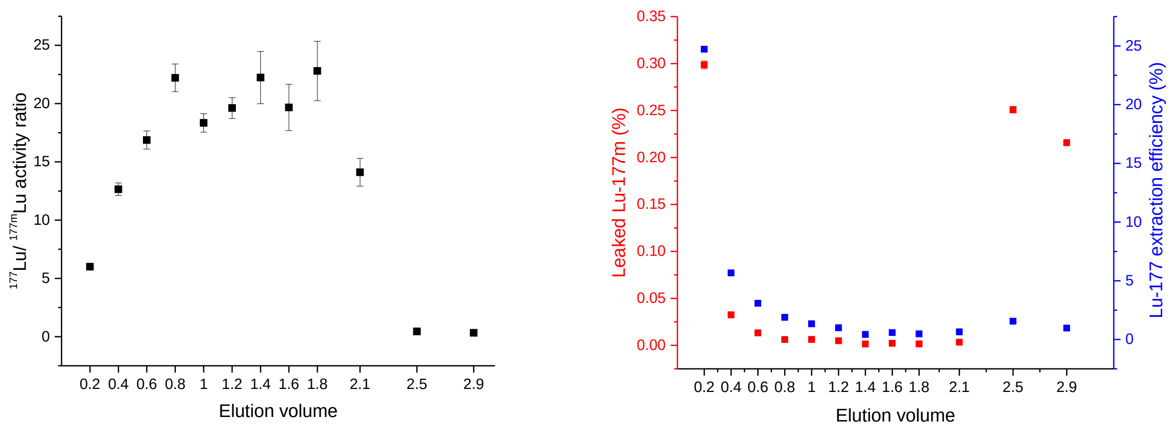

Figure 5: The ^{177}Lu/ ^{177m}Lu activity ratio as a function of elution fraction volume (0.2mL, each) (a) and the corresponding ^{177}Lu extraction efficiency, the leaked ^{177m}Lu (b) obtained using pH-4.3 NaAc buffer as eluent. The presented data has been based on one experiment, and the error bars represents the error during the gamma ray spectroscopy measurements.

Figure 5(a) shows that the ^{177}Lu/^{177m}Lu activity ratio varies in the collected elution fraction. The first fraction exhibited very low ^{177}Lu/^{177m}Lu activity ratio of 5, which increases to 25 for the fourth to eighth fraction and decreases further in the subsequent elution fractions. The observed trend can be explained on the basis of the results shown in Figure 5(b). As can be seen, the highest ^{177m}Lu leakage of 0.3% was observed in the first fraction and decreases to around 0.01- 0.04% in the successive elution fractions. Similarly, the highest ^{177}Lu extraction efficiency of 25% was observed in the first fraction, and decreases to less than 5% in the successive fractions. On combining all the fractions, an overall ^{177}Lu extraction efficiency of about 50% has been achieved. Further, the Lu ion removal does not exhibit a sharp peak but a tailing profile over the period of eluted volume. This suggests that either there are multiple binding sites or that Lu that is released can re-associate which also explains the observed low ^{177}Lu extraction efficiencies. This observation again points out to the weak coordination of ^{177m}Lu ions possibly due to their interaction with more than one DOTA group.

To summarize, the SPE based separation offers the possibility of building an easy to automatize, user friendly ^{177m}Lu- ^{177}Lu separation technique. The presented separation method could lead to ^{177}Lu enrichment of 100 times compared to the ^{177}Lu/^{177m}Lu activity ratio of 0.25 when present in equilibrium with each other. However, currently it is inapplicable in designing a ^{177m}Lu/^{177}Lu radionuclide generator because the obtained ratios are far from the clinically preferred ^{177}Lu/^{177m}Lu activity ratio of 10,000. The main challenge lies in designing the solid supports which forms a stable coordination with ^{177m}Lu and causes minimal interference during ^{177m}Lu-^{177}Lu separation. The currently used DOTA grafted amino propyl silica did not allow the formation of stable cage coordinated Lu:DOTA complex under the studied reaction conditions. Further, the unreacted DOTA groups interfered in ^{177m}Lu complexation and ^{177}Lu release, ultimately leading to poor ^{177m}Lu-^{177}Lu separation. In future, this can be possibly minimized by the use of solid supports having low functional group density. For instance, the use of a support with a functional group density of 10 µmol.g^{-1} (100 times lower than currently used APS) can significantly reduce the interference in ^{177m}Lu complexation, ^{177}Lu release and can potentially allow the loading of up to 2 GBq ^{177m}Lu per mg solid.

4.4. Conclusions

The presented work is the first step in designing a solid phase extraction based ^{177m}Lu-^{177}Lu separation. It establishes a strategy to immobilize DOTA groups on the surface of commercially available silica. The use of commercially available DOTAGA-anhydride allows easy and facile conjugation of DOTA moiety on silica surface. Presently, DOTA immobilized silica was used as a solid support to facilitate the ^{177m}Lu-^{177}Lu separation. The grafting of DOTA on silica surface affected the Lu-DOTA complexation and the stable cage coordination of Lu ions could not be achieved under the studied reaction conditions. This resulted in high ^{177m}Lu leakage during the ^{177}Lu-^{177m}Lu separation and the highest ^{177}Lu/^{177m}Lu activity ratio of 25 could be achieved when the ^{177m}Lu contribution is reduced to 0.01%. Overall, the solid phase extraction presents an easy to automatize, user friendly and reproducible ^{177m}Lu-^{177}Lu technique. However, it needs further optimization and a careful evaluation of the kinetics of association and dissociation of Lu ions in order to reach high ^{177}Lu/^{177m}Lu activity ratio.

4.5. References

1 Banerjee, S., Pillai, M. R. & Knapp, F. F. Lutetium-177 therapeutic radiopharmaceuticals: linking chemistry, radiochemistry, and practical applications. *Chem Rev* 115, 2934-2974, doi:10.1021/cr500171e (2015).

2 De Vries, D. J. & Wolterbeek, H. The production of medicinal 177Lu and the story of 177mLu: detrimental by-product or future friend? *Tijdschr. Nucl. Geneeskd* 34, 899-904 (2012).

3 Bhardwaj, R., Wolterbeek, H. T., Denkova, A. G. & Serra-Crespo, P. Radionuclide generator based production of therapeutic 177Lu from its long-lived isomer 177mLu. *EJNMMI Radiopharmacy and Chemistry* submitted (2019).

4 Knapp, F. F. & Dash, A. in *Radiopharmaceuticals for Therapy* 131-157 (Springer India, 2016).

5 Dash, A. & Chakravarty, R. Pivotal role of separation chemistry in the development of radionuclide generators to meet clinical demands. *RSC Advances* 4, 42779-42803, doi:10.1039/C4RA07218A (2014).

6 Roesch, F. Maturation of a key resource - the germanium-68/gallium-68 generator: development and new insights. *Curr Radiopharm* 5, 202-211 (2012).

7 Muddukrishna, S. N., Narasimhan, D. V. S. & Desai, C. N. Extraction of99mTc into MEK from large quantity of molybdate retained on alumina column. *J Radioanal Nucl Chem* 145, 311-320, doi:10.1007/BF02163421 (1990).

8 Braun, T., Imura, H. & Suzuki, N. Separation of99mTc from parent99Mo by solid-phase column extraction as a simple option for a new99mTc generator concept. *J Radioanal Nucl Chem* 119, 315-325, doi:10.1007/BF02162611 (1987).

9 Sakr, T. M., Nawar, M. F., Fasih, T. W., El-Bayoumy, S. & Abd El-Rehim, H. A. Nano-technology contributions towards the development of high performance radioisotope generators: The future promise to meet the continuing clinical demand. *Applied Radiation and Isotopes* 129, 67-75, (2017).

10 Caravajal, G. S., Leyden, D. E., Quinting, G. R. & Maciel, G. E. Structural characterization of (3-aminopropyl)triethoxysilane-modified silicas by silicon-29 and carbon-13 nuclear magnetic resonance. *Analytical Chemistry* 60, 1776-1786, doi:10.1021/ac00168a027 (1988).

11 Rostamzadeh, P., Mirabedini, S. M. & Esfandeh, M. APS-silane modification of silica nanoparticles: effect of treatment's variables on the grafting content and colloidal stability of the nanoparticles. *Journal of Coatings Technology and Research* 11, 651-660, doi:10.1007/s11998-014-9577-8 (2014).

12 Yang, J. J., El-Nahhal, I. M., Chuang, I. S. & Maciel, G. E. Synthesis and solid-state NMR structural characterization of polysiloxane-immobilized amine ligands and their metal complexes. *Journal of Non-Crystalline Solids* 209, 19-39, d (1997).

13 Sudhölter, E. J. R., Huis, R., Hays, G. R. & Alma, N. C. M. Solid-state silicon-29 and carbon-13 NMR spectroscopy using cross-polarization and magic-angle-spinning

techniques to characterize 3-chloropropyl and 3-aminopropyl-modified silica gels. *Journal of Colloid and Interface Science* 103, 554-560, (1985).

14 Palmai, M. *et al.* Preparation, purification, and characterization of aminopropyl-functionalized silica sol. *J Colloid Interface Sci* 390, 34-40, doi:10.1016/j.jcis.2012.09.025 (2013).

15 Montalbetti, C. A. & Falque, V. Amide bond formation and peptide coupling. *Tetrahedron* 61, 10827-10852 (2005).

16 Tamami, B., Farjadian, F., Ghasemi, S. & Allahyari, H. Synthesis and applications of polymeric N-heterocyclic carbene palladium complex-grafted silica as a novel recyclable nano-catalyst for Heck and Sonogashira coupling reactions. *New Journal of Chemistry* 37, 2011-2018, doi:10.1039/C3NJ41137K (2013).

17 Kocyigit, O., Erdemir, S. & Yilmaz, M. Sorption of Cu(II) onto silica gel immobilized calix[4]arene derivative with tripodal structure. *Journal of Inclusion Phenomena and Macrocyclic Chemistry* 72, 137-147, doi:10.1007/s10847-011-9951-4 (2012).

18 Gangoda, M. E., Wijekoon, A., Gregory, R. B. & Khitrin, A. K. Multinuclear nuclear magnetic resonance spectroscopic and high-performance liquid chromatographic characterization of silica, grafted with specifically deuterated 4-((propylamino)methyl)benzoic acid. *Journal of Chromatography A* 1458, 90-98, (2016).

19 Jal, P. K., Patel, S. & Mishra, B. K. Chemical modification of silica surface by immobilization of functional groups for extractive concentration of metal ions. *Talanta* 62, 1005-1028, (2004).

20 Sander, L. C. & Wise, S. A. Synthesis and characterization of polymeric C18 stationary phases for liquid chromatography. *Analytical Chemistry* 56, 504-510, doi:10.1021/ac00267a047 (1984).

21 Hirose, K., Nakamura, T., Nishioka, R., Ueshige, T. & Tobe, Y. Preparation and evaluation of novel chiral stationary phases covalently bound with chiral pseudo-18-crown-6 ethers. *Tetrahedron Letters* 44, 1549-1551, (2003).

22 Wu, F. *et al.* Novel polyazamacrocyclic receptor decorated core-shell superparamagnetic microspheres for selective binding and magnetic enrichment of palladium: synthesis, adsorptive behavior and coordination mechanism. *Dalton transactions* 45, 9553-9564, doi:10.1039/C6DT01024E (2016).

23 Zhai, R. *et al.* Metal ion-immobilized magnetic nanoparticles for global enrichment and identification of phosphopeptides by mass spectrometry. *RSC Advances* 6, 1670-1677, doi:10.1039/C5RA22006H (2016).

24 Erdem, A., Shahwan, T., Çağır, A. & Eroğlu, A. E. Synthesis of aminopropyl triethoxysilane-functionalized silica and its application in speciation studies of vanadium(IV) and vanadium(V). *Chemical Engineering Journal* 174, 76-85, (2011).

25 Bernhard, C. *et al.* DOTAGA-anhydride: a valuable building block for the preparation of DOTA-like chelating agents. *Chemistry (Weinheim an der Bergstrasse, Germany)* 18, 7834-7841, doi:10.1002/chem.201200132 (2012).

26 Capel-Sanchez, M. C., Barrio, L., Campos-Martin, J. M. & Fierro, J. L. G. Silylation and surface properties of chemically grafted hydrophobic silica. *Journal of Colloid and Interface Science* 277, 146-153, (2004).

27 Dugas, V. & Chevalier, Y. Surface hydroxylation and silane grafting on fumed and thermal silica. *Journal of Colloid and Interface Science* 264, 354-361, (2003).

28 Newby, J. J., Legg, M. A., Rogers, B. & Wirth, M. J. Annealing of silica to reduce the concentration of isolated silanols and peak tailing in reverse phase liquid chromatography. *Journal of Chromatography A* 1218, 5131-5135, (2011).

29 Socrates, G. *Infrared characteristic group frequencies : tables and charts*. 2nd ed. edn, viii, 249 pages : illustrations ; 24 x 27 cm (Wiley, 1994).

30 Kulkarni, S. A., Ogale, S. B. & Vijayamohanan, K. P. Tuning the hydrophobic properties of silica particles by surface silanization using mixed self-assembled monolayers. *Journal of Colloid and Interface Science* 318, 372-379, (2008).

31 Blitz, J. P., Murthy, R. S. S. & Leyden, D. E. Studies of silylation of Cab-O-Sil with methoxymethylsilanes by diffuse reflectance FTIR spectroscopy. *Journal of Colloid and Interface Science* 121, 63-69, (1988).

32 Vansant, E. F. M., Voort, P. v. d. & Vrancken, K. C. *Characterization and chemical modification of the silica surface*. 550 p. : ill. (Elsevier, 1995).

33 Desreux, J. F. Nuclear magnetic resonance spectroscopy of lanthanide complexes with a tetraacetic tetraaza macrocycle. Unusual conformation properties. *Inorganic Chemistry* 19, 1319-1324, doi:10.1021/ic50207a042 (1980).

Chapter 5

A theoretical and experimental investigation of ^{177m}Lu production

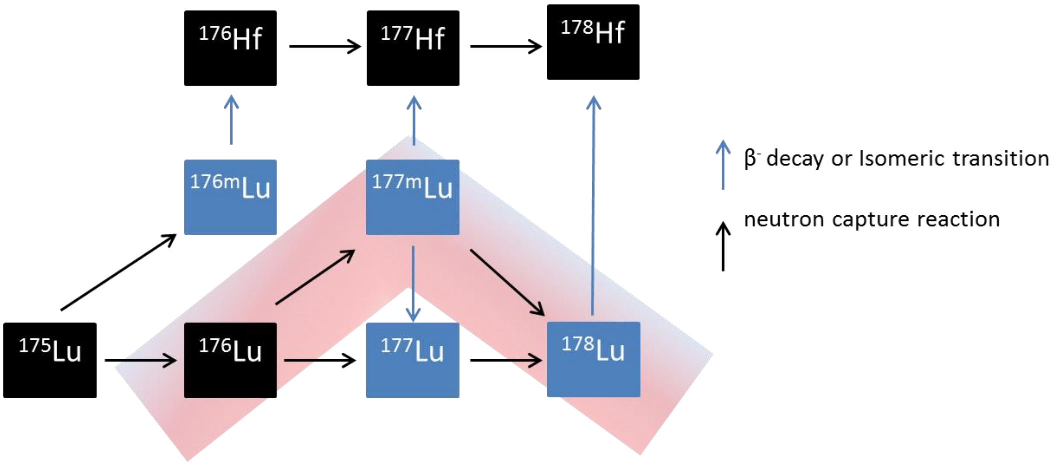

This Chapter has been adapted from:

Bhardwaj, R., Bernard, P., Sarilar, M., Wolterbeek, H. T., Denkova, A.G., & Serra-Crespo, P. (2019). Large scale production of Lutetium-177m for use in $^{177m}Lu/^{177}Lu$ radionuclide generator. Applied Radiation and Isotopes, submitted

Abstract

An estimation of the ^{177m}Lu production is crucial in the development of a $^{177m}Lu/^{177}Lu$ radionuclide generator, however some inconsistencies exist in the relevant cross sections. Therefore in this work, ^{177m}Lu has been produced by irradiation of natural Lu_2O_3 targets at the BR2 reactor (Mol, Belgium) and the data obtained together with literature values have been used to theoretically investigate the production of ^{177m}Lu at different neutron fluxes, irradiation times and enrichment of ^{176}Lu. The irradiation time (t_{max}) needed to reach the maximum ^{177m}Lu production has been found to change from 42, 12, 4 days with the increase in the thermal neutron flux from $2*10^{14}$, $8*10^{14}$, $2.5*10^{15}$ n cm^{-2} s^{-1}, respectively while keeping the maximum ^{177m}Lu activity unaffected. The results of our calculations suggest that 0.11 TBq ^{177m}Lu with a specific activity of 0.3 TBq. g^{-1} Lu can be produced in a short irradiation time of 4 days using 1g of 84.44% ^{176}Lu enriched Lu_2O_3 and a thermal neutron flux of $2.5*10^{15}$ n cm^{-2} s^{-1}.

5.1. Introduction

The interest in lutetium-177 in nuclear medicine has grown tremendously in the past few years [1]. Its attractive decay characteristics (i.e. a 6.64 day half-life) as well as the emission of both low energy β^- rays (penetration depth of 2 mm) and γ rays (208.37 and 112.98 keV) upon decay, allow for simultaneous imaging and radionuclide therapy [2]. Currently, ^{177}Lu is commercially produced through either the indirect or direct production routes [3]. A new production route has been suggested by De Vries *et al.* based on the supply of ^{177}Lu via a ^{177m}Lu/^{177}Lu radionuclide generator [4]. This generator has been based on the challenging separation of chemically and physically alike isomers, ^{177m}Lu & ^{177}Lu. Recently, Bhardwaj *et al* have provided the experimental evidence on ^{177m}Lu and ^{177}Lu separation thereby confirming the possibility of ^{177m}Lu/^{177m}Lu radionuclide generator based ^{177}Lu production [5,6].

Radionuclide generators have played an important role in the development and applications of radiopharmaceuticals [7]. Similarly, a ^{177m}Lu/ ^{177}Lu radionuclide generator can be expected to boost the ^{177}Lu radiopharmaceutical development by providing cost effective, carrier-free, on demand and onsite availability of ^{177}Lu. This generator can be especially very attractive for hospitals, which are not currently using ^{177}Lu on a weekly basis. However, there are several challenges before this concept can be implemented into a commercial ^{177}Lu production route. One of the main challenge is the large-scale production of ^{177m}Lu, the parent radionuclide needed for the ^{177m}Lu/^{177}Lu radionuclide generator. It is crucial to ascertain if the available nuclear research reactor infrastructure is capable of producing sufficient ^{177m}Lu activity to support the ^{177}Lu generator production. This paper aims at investigating the ^{177m}Lu production in high- and medium-flux nuclear reactors by the neutron irradiation of ^{176}Lu enriched Lu_2O_3 targets.

^{177m}Lu is usually co-produced in small quantities during the direct route production of ^{177}Lu. Most of the ^{177m}Lu related studies uses these small amounts to define its decay characteristics or cross sections and they are not focused on the ^{177m}Lu production optimisation [8-10]. In general, the radionuclide production in nuclear reactors has a directly proportional relationship with three factors namely: the neutron flux, the neutron capture cross section and the number of target atoms [11]. For ^{177m}Lu production, there are some discrepancies in literature regarding its production neutron capture cross sections. The International Atomic Energy Agency (IAEA) reports the thermal neutron capture cross section (σ) as 2.8 b and a resonance integral (I_o) of 4.7 b for ^{177m}Lu production ($^{176}\mathrm{Lu}(n,\gamma)^{177m}\mathrm{Lu}$) [12], this value is also supported by Roig, Bélier et al and Dash, Pillai et al [13,14]. In NGATLAS, the atlas of neutron capture cross section, 3 different thermal neutron capture cross sections (7 ± 2, 2.1 ± 0.7, 3.18 ± 0.3 b) are reported for ^{177m}Lu production [15]. There are several reports that supports the ^{177m}Lu production neutron capture cross section as 7 b [1,8,16,17]. Further, the ^{177m}Lu production will also have a negative contribution from its burn-up reaction that can co-occur during the ^{177m}Lu production. The neutron capture cross section for the burn-up of ^{177m}Lu (σ ($^{177m}\mathrm{Lu}(n,\gamma)^{178}\mathrm{Lu}$)) is not reported in IAEA database and has different values quoted in other literature. In the nuclear data sheets, ^{177m}Lu burn-up neutron capture cross sections of 4.8 b, and 3.2±0.3 b [18] are reported. However, in contrast to these numbers, a ^{177m}Lu burn-up cross section of up to 626 ± 45 b is reported by Roig et al [14,19-21]. The large discrepancies present in the existing literature regarding the ^{177m}Lu production and burn-up neutron capture cross section makes the estimation of large-scale ^{177m}Lu production unreliable.

In the present work, the ^{177m}Lu production has been experimentally performed at the BR2 reactor (Mol, Belgium) using natural Lu_2O_3 targets. The experimentally produced ^{177m}Lu activity is used to validate the ^{177m}Lu-related cross sections reported in literature. Using the experimentally validated cross sections, a theoretical study on large-scale ^{177m}Lu production is performed for medium/high-flux reactors. The effect of irradiation time and neutron flux on ^{177m}Lu production is presented. Further, the effect of ^{176}Lu enrichment on ^{177m}Lu production is evaluated for a neutron flux of $8*10^{14}$ n cm^{-2} s^{-1} available at the BR2 reactor (Mol, Belgium).

5.2. Experimental

5.2.1 Sample preparation

The irradiation target materials were purchased from the National Institute of Standards and Technology (NIST). The NIST standard $Lu(NO_3)_3$ solution (reference material number 3130a) was provided as 9.979 ± 0.030 mg Lu g^{-1} solution. The NIST standard $Zn(NO_3)_3$ solution (reference material number 3168a) was provided as 10.007 mg g^{-1} ± 0.020 mg g^{-1} and was used as the thermal neutron flux monitor.

The solutions were weighed in quartz tubes of about 6mm internal diameter and 60 mm length. The solutions were then evaporated to dryness, and the samples were calcined at 800°C for 10 hours to convert the $Lu(NO_3)_3$ and $Zn(NO_3)_3$ into Lu_2O_3 and Zn_2O_3 respectively. The quartz tubes were sealed and loaded inside the aluminium insert of an aluminium cold-welded irradiation capsule with quartz wool on top and bottom [22]. The sample preparation protocol has been pre-verified by irradiating a known amount of lutetium target at the Hoger Onderwijs Reactor Delft (HOR) with a thermal neutron flux of $4.72*10^{12}$ n cm^{-2} s^{-1} (epithermal neutron flux of less than $7.08*10^{11}$ cm^{-2} s^{-1}) and an irradiation time of 10 hours. At the end of irradiation, the ^{177}Lu activity produced was measured using gamma-ray spectrometry. The experimentally measured ^{177}Lu activity was found to be in good correlation with the theoretically predicted ^{177}Lu activity. Thus, it was concluded that the steps involving evaporation, calcination of the starting sample and sealing of the quartz tube did not lead to any loss in the starting lutetium content.

For ^{177m}Lu production, the quartz tubes containing Lu and Zn were placed at 1 cm distance from each other along the axial profile of the neutron flux. The difference in the positions of Lu and Zn monitor can lead to up to 10% difference in the thermal neutron flux experienced by the Zn monitor and the Lu target.

5.2.2 Neutron irradiation

The neutron irradiation was performed at the BR2 reactor (Mol, Belgium) in two different irradiation positions, with two different neutron fluxes of $2.1*10^{14} \pm 0.05*10^{14}$ n cm^{-2} s^{-1} and $8.4*10^{14} \pm 0.25*10^{14}$ n cm^{-2} s^{-1} as shown in Table 1. An additional 5% epithermal neutron flux was used at the irradiation positions during the ^{177m}Lu activity production calculations.

Table 1: Details of the irradiated samples and the involved irradiation parameters.

	Irradiation 1	**Irradiation 2**
Target mass (natural Lu_2O_3)	0.1126 mg	0.1157 mg
Thermal neutron flux	$2. 1*10^{14} \pm 0.05*10^{14}$ n cm^{-2} s^{-1}	$8.4*10^{14} \pm 0.25*10^{14}$ n cm^{-2} s^{-1}
Effective irradiation time	28 days	26 days

The high-flux position with a thermal neutron flux of $8.4*10^{14}$ n cm^{-2} s^{-1} is not accessible during the operation of the reactor. Therefore, an irradiation period of 26 days covering a whole irradiation cycle (28 days interrupted by a 2-day intermediate shutdown, 4 days after start-up) was carried out. After the irradiation, the samples were allowed to decay for a cooling period of about 3 months. The irradiated vials could not be measured as such because of the co-production of long-living ^{60}Co as a radionuclidic impurity, which resulted in a significant increase in the background of the gamma ray spectrum. Therefore, at the end of cooling (EOC), the sealed quartz tubes containing Lu and Zn were opened and transferred into separate vials containing pre-weighed amounts (about 2 ml) of 0.1 N HCl. The vials were heated at 80°C for 60 minutes to ensure complete dissolution of the Lu and Zn in 0.1 N HCl. An aliquot of about 100 µL was weighed and transferred to polyethylene vials. The vials were measured using gamma ray spectrometry to do a quantitative evaluation of the ^{177}Lu, ^{177m}Lu and ^{65}Zn activities.

5.2.3 Activity measurements

The activity measurements were performed with a well-type HPGe gamma-ray detector. The energy and efficiency calibration of the detector was performed using a certified Eu-152 source, and the efficiency calibration for each lutetium peak was fine-tuned using a known ^{177}Lu, ^{177m}Lu source provided by IDB- Holland to take true-coincidence summing effects into account.

5.3. Theoretical calculation of ^{177m}Lu production yield

This section describes the neutron capture reactions, neutron capture cross section and neutron flux parameters used in calculating the theoretical ^{177m}Lu production yield.

5.3.1. Neutron capture reactions

The possible neutron capture reactions co-occurring during the irradiation of a Lu_2O_3 target are summarised in Figure 1 (black arrows) below.

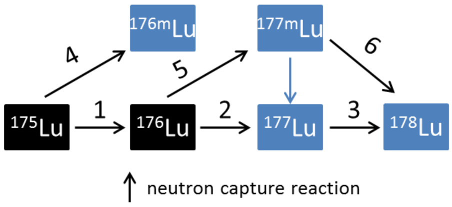

Figure 1: Neutron capture reaction affecting the ^{177m}Lu production. The blue and black boxes indicate unstable and stable nuclides, respectively. Blue arrows indicate radioactive decay and black arrows indicate neutron capture reaction.

Figure 1 shows that the ^{177m}Lu production (reaction 5) is accompanied by five other neutron capture reactions involving different Lu isotopes. These neutron capture reactions will contribute to the ^{176}Lu target burn-up and will also effect the total activity and the specific activity of the produced ^{177m}Lu. Therefore, they are accounted simultaneously while optimising the ^{177m}Lu production. In general, the radionuclide production is defined using the following equation [11],

$$\frac{dN_{product}}{dt} = \left(\frac{dN_{target}}{dt}\right)_{growth} - \left(\frac{dN_{target}}{dt}\right)_{decay} - \left(\frac{dN_{product}}{dt}\right)_{burn-up} \qquad \text{(Equation 1)}$$

For the case of ^{177m}Lu production, the Equation 1 was re-defined as:

$$\frac{dN_{^{177m}\mathrm{Lu}}}{dt} = N_t * \sigma_1 * \varphi_{thermal} - N_{^{177m}\mathrm{Lu}} * \lambda - N_{^{177m}\mathrm{Lu}} * \sigma_2 * \varphi_{thermal} \qquad \text{(Equation 2)}$$

where N_t are the initial number of ^{176}Lu target atoms,
$N_{^{177m}\mathrm{Lu}}$, are the number of formed ^{177m}Lu nuclei,
$\varphi_{thermal}$, is the thermal neutron flux in n cm^{-2} s^{-1},
σ_1, is the thermal neutron capture cross section of the nuclear reaction $^{176}\mathrm{Lu}(n,\gamma)^{177m}\mathrm{Lu}$,
σ_2, is the burn-up cross section of ^{177m}Lu,
λ is the decay constant of ^{177m}Lu,
and *t* is the duration of exposure to the incident neutron flux.
The thermal and epithermal neutron flux contributions to the ^{177m}Lu production were accounted for separately, leading to the final Equation 3;

$$\frac{dN_{^{177m}\text{Lu}}}{dt} = N_{^{176}\text{Lu}} * \sigma\,(^{176}\text{Lu}(n,\gamma)^{177m}\text{Lu}) * \varphi_{thermal} + N_{^{176}\text{Lu}} * I_o(^{176}\text{Lu}(n,\gamma)^{177m}\text{Lu}) * \varphi_{epithermal} - N_{^{177m}\text{Lu}} * \lambda(^{177m}\text{Lu}) - N_{^{177m}\text{Lu}} * \sigma\,(^{177m}\text{Lu}(n,\gamma)^{178}\text{Lu}) * \varphi_{thermal} \quad \text{(Equation 3)}$$

where I_o represents the resonance integral for the epithermal flux $\varphi_{epithermal}$. $N_{^{176}\text{Lu}}$ are the number of target ^{176}Lu atoms undergoing the $^{176}\text{Lu}(n,\gamma)^{177m}\text{Lu}$ capture reaction.
$N_{^{176}\text{Lu}}$ changes with irradiation time because of the neutron capture reactions 1, 2 (see Figure 1). To take that into account, the ^{177m}Lu production defined by Equation 3 was re-defined as Equation 4 for small time steps *i* during the irradiation:

$$\frac{dN_{(^{177m}\text{Lu},\ i)}}{dt} = N_{(^{176}\text{Lu},\ i-1)} * \sigma\,(^{176}\text{Lu}(n,\gamma)^{177m}\text{Lu}) * \varphi_{thermal} + N_{(^{176}\text{Lu},\ i-1)} * I_o(^{176}\text{Lu}(n,\gamma)^{177m}\text{Lu}) * \varphi_{epithermal} - N_{(^{177m}\text{Lu},\ i-1)} * \lambda(^{177m}\text{Lu}) - N_{(^{177m}\text{Lu},\ i-1)} * \sigma\,(^{177m}\text{Lu}(n,\gamma)^{178}\text{Lu}) * \varphi_{thermal} \quad \text{(Equation 4)}$$

Similarly, the neutron capture reactions 1, 2 & 5 (see Figure 1) were used to calculate the change in the number of ^{176}Lu atoms ($\frac{dN_{(^{176}\text{Lu},\ i)}}{dt}$) with irradiation time. It was defined as Equation 5 below;

$$\begin{aligned}\frac{dN_{(^{176}\text{Lu},\ i)}}{dt} = & -N_{(^{176}\text{Lu},\ i-1)} * \sigma\,(^{176}\text{Lu}(\text{n},\gamma)^{177m}\text{Lu}) * \varphi_{thermal} \\ & - N_{(^{176}\text{Lu},\ i-1)} * I_o\,(^{176}\text{Lu}(\text{n},\gamma)^{177m}\text{Lu}) * \varphi_{epithermal} \\ & - N_{(^{176}\text{Lu},\ i-1)} * \sigma\,(^{176}\text{Lu}(\text{n},\gamma)^{177}\text{Lu}) * \varphi_{thermal} \\ & - N_{(^{176}\text{Lu},\ i-1)} * I_o\,(^{176}\text{Lu}(\text{n},\gamma)^{177}\text{Lu}) * \varphi_{epithermal} \\ & + N_{(^{175}\text{Lu},\ i-1)} * \sigma\,(^{175}\text{Lu}(\text{n},\gamma)^{176}\text{Lu}) * \varphi_{thermal} \\ & + N_{(^{175}\text{Lu},\ i-1)} * I_o\,(^{175}\text{Lu}(\text{n},\gamma)^{176}\text{Lu}) * \varphi_{epithermal}\end{aligned} \quad \text{(Equation 5)}$$

At the beginning of the irradiation at i = 0, the initial number of ^{175}Lu ($N_{(^{175}\text{Lu},0)}$)and ^{176}Lu ($N_{(^{176}\text{Lu},0)}$) atoms were dependent on the initial target mass used for irradiation. They were defined as:

$$mass_{Lu} = (mass_{Lu_2O_3} * 2 * molar\ mass_{Lu}) / (molar\ mass_{Lu_2O_3}) \quad \text{(Equation 6)}$$

$$N_{(^{175}\text{Lu},0)} = \left(mass_{Lu} * \left(1 - (enrichment\ factor)\right) * N_A\right) / 175 \quad \text{(Equation 7)}$$

$$N_{(^{176}\text{Lu},0)} = \left(mass_{Lu} * \left(1 - (enrichment\ factor)\right) * N_A\right) / 176 \quad \text{(Equation 8)}$$

where $mass_{Lu_2O_3}$ is the initial target mass, N_A is the Avogadro number. All other Lu isotopes were assumed to be absent at the beginning of the irradiation. During the irradiation, the ^{176}Lu, ^{177}Lu, ^{178}Lu, ^{177m}Lu, ^{176m}Lu, ^{177m}Lu are formed due to the capture reactions 1, 2, 3, 4, 5 and 6 respectively (Figure 1). Therefore equations similar to equation 4 and 5 were defined for all other Lu isotopes, ^{175}Lu, ^{176}Lu, ^{176m}Lu, ^{177}Lu, ^{178}Lu (see supplementary info S1). They were solved simultaneously for small time steps *i* using MATLAB to determine the change in the amounts of Lu isotopes with the increasing irradiation time. Finally, the activity (A= N λ) and specific activity (S.A = $A_{177m_{Lu}}$ / mass of $^{175+176+177+178+177m}$Lu) of the ^{177m}Lu was calculated by using the total number of isotopes present at any given time, t. The details on the neutron capture cross sections and neutron flux parameters used in the calculations is provided in the following subsections.

5.3.2. Neutron capture cross section

The thermal neutron capture cross sections, resonance integral for the neutron capture reactions co-occurring during the ^{177m}Lu production are shown in Table 2. The tabulated cross sections data have been adapted from the IAEA database.

Table 2: The neutron capture reactions co-occurring during the ^{177m}Lu production and the corresponding neutron capture cross sections (b).

Reaction number	Neutron capture reaction	Thermal Capture cross section, σ (b)	Resonance Integral, I_0 (b)
1	^{175}Lu(n,γ)^{176}Lu	6.6*	620*
2	^{176}Lu(n,γ)^{177}Lu	2020*	1087*
3	^{177}Lu(n,γ)^{178}Lu	1000*	-
4	^{175}Lu(n,γ)^{176m}Lu	16.7*	550*
5	^{176}Lu(n,γ)^{177m}Lu	2.8*	4.7*
6	^{177m}Lu(n,γ) ^{178}Lu	-	-

* International Atomic Energy Agency [12]

Apart from the cross sections, mentioned in Table 2, different values for the ^{177m}Lu production (^{176}Lu(n,γ)^{177m}Lu), and the ^{177m}Lu burn-up (^{177m}Lu(n,γ)^{178}Lu) have been reported in literature. These values are summarised in Table 3.

Table 3: The ^{177m}Lu related thermal neutron capture cross sections reported in literature

	Reported thermal neutron capture cross section [232323]
^{176}Lu(n,γ)^{177m}Lu	7 ± 0.3 b [8] 2.85 b [24] 2.8 ± 0.7 b [12] (IAEA, 2015) 2.1 ± 0.7 b [25] 3.18 ± 0.3 b [26]
^{177m}Lu(n,γ)^{178}Lu	4.8 b (EAF-2010) 2.97 b (TENDL-2010) 3.18 b [15] 590 b [14] 626 ± 45 b# [19]

represents the total burn up cross section (capture cross section + inelastic scattering)

The reported ^{177m}Lu production cross section ($^{176}Lu(n,\gamma)^{177m}Lu$) varies from 2.8 b to 7 b, while the ^{177m}Lu burn-up cross section ($^{177m}Lu(n,\gamma)^{178}Lu$) shows very large variation range from 4.8 b to 626 b. It should be pointed that, 417±26 b represents the ^{177m}Lu burn-up via $^{177m}Lu(n,\gamma)^{178}Lu$) reaction while 626 ± 45 b represents the total ^{177m}Lu burn-up (capture, $\sigma_{(n,\gamma)}$ + inelastic scattering, $\sigma_{(n,n')}$) cross section and accounts the total depopulation of the ^{177m}Lu by all possible reactions. Thus, it has been used while theoretically predicting the ^{177m}Lu production yield.

5.3.3. Neutron flux

The ^{177m}Lu production was evaluated for four different neutron flux values, mentioned in Table 4. The neutron flux available at the HFIR (Oak Ridge, USA) and ILL (Grenoble, France) reactors was based on the literature, while the thermal neutron flux at the BR2 reactor (Mol, Belgium) was experimentally estimated using Zinc flux monitors.

Table 4: Neutron flux values used in optimizing ^{177m}Lu production

Nuclear reactor	Neutron flux (n cm^{-2}. s^{-1})
High-Flux reactor (HFIR), ORNL, Oak Ridge, U.S.A [3]	Thermal flux: $2.5 \cdot 10^{15}$
High-Flux reactor (ILL), Laue Langevin Institute, Grenoble, France [19].	Thermal flux: $1.5 \cdot 10^{15}$
High-Flux reactor (BR2), SCK•CEN, , MoL, Belgium (present work)	Thermal flux: $2.1 \cdot 10^{14}$ & Epithermal flux $0.1 \cdot 10^{14}$ Thermal flux: $8.4 \cdot 10^{14}$ & Epithermal flux $0.4 \cdot 10^{14}$

5.4. Results and Discussion

5.4.1 Experimental validation of ^{177m}Lu related neutron capture cross sections

The discrepancy in the ^{177m}Lu related neutron capture cross sections was resolved by comparing the experimentally produced ^{177m}Lu activity with the theoretically predicted activity based on the existing literature. Figure 2 shows the theoretically predicted ^{177m}Lu activity as a function of time for different ^{177m}Lu production and burn-up neutron capture cross sections reported in literature. Additionally, it also shows the ^{177m}Lu activity obtained experimentally at the end of 26 days of irradiation of a natural Lu_2O_3 target (as the solid point).

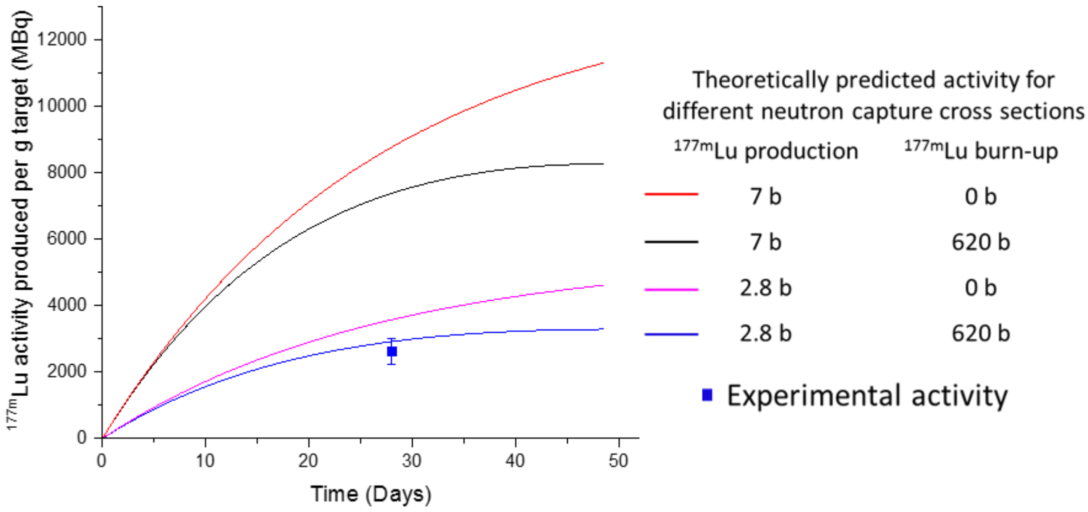

Figure 2: The lines represents the theoretically expected ^{177m}Lu activity as a function of time for different ^{177m}Lu production and burn-up neutron capture cross sections reported in literature. The symbol (■) represents the experimentally obtained ^{177m}Lu activity after 26 days irradiation of 0.1157 mg of natural Lu_2O_3 sample using a thermal neutron flux of $2 \cdot 10^{14}$ n cm^{-2} s^{-1} & an epithermal flux of $0.1 \cdot 10^{14}$ n cm^{-2} s^{-1}

It can be seen from Figure 2 that the experimentally obtained ^{177m}Lu activity supports well the theoretically predicted ^{177m}Lu activity based on the ^{177m}Lu production cross section of 2.8 b and a ^{177m}Lu burn-up cross section of 626 b. The inclusion of the ^{177m}Lu burn-up cross section significantly changes the time needed to reach the maximum ^{177m}Lu production. The ^{177m}Lu production reaches a maximum on increasing the irradiation time and then starts decreasing due to the burn-up of the product (^{177m}Lu). The experimental results from the irradiation of the two natural Lu_2O_3 targets have been tabulated in Table 5, which further support the previously reported cross-sections (i.e 2.8 b and 626 b).

Table 5: Comparison of the experimentally produced ^{177m}Lu activity with the theoretically expected ^{177m}Lu activities at EOI

	Theoretically expected activity at EOI (MBq)*	Experimentally obtained activity at EOI (MBq)
Irradiation 1	0.34 ± 0.09	0.30 ± 0.04
Irradiation 2	0.39 ± 0.10	0.29 ± 0.07

*expected activities are based on the reported ^{177m}Lu production cross section of 2.8 ± 0.7 b and burn-up cross section of 626 ± 45 b.

The error in the theoretically calculated values is based on the reported uncertainty of 25% for the neutron capture cross-section of the $^{176}Lu(n,\gamma)^{177m}Lu$ reaction (i.e. 2.8 ± 0.7 b). The errors in the experimentally obtained activity are a cumulative result of the uncertainties in the different stages of the experiments, starting from the sample preparation, neutron flux measurement, target processing and the gamma ray spectra measurements. The use of a single neutron flux monitor placed horizontally at 1 cm distance from the Lu containing quartz vial led to up to 10% error in the measured thermal neutron flux. In future research, a precise neutron capture cross section measurement should be performed by using multiple neutron flux monitors and the additional neutron flux parameters such as the epithermal flux contribution.

5.4.2 Theoretical investigation of large-scale ^{177m}Lu production

The following sections presents the theoretical results on the effect of neutron flux, irradiation time and ^{176}Lu enrichment on ^{177m}Lu production.

5.4.2.1 Effect of neutron flux on irradiation time and maximum ^{177m}Lu activity production

The effect of neutron flux and irradiation time on the maximum ^{177m}Lu activity production has been theoretically investigated for four different thermal neutron fluxes. The results are shown in Figure 3.

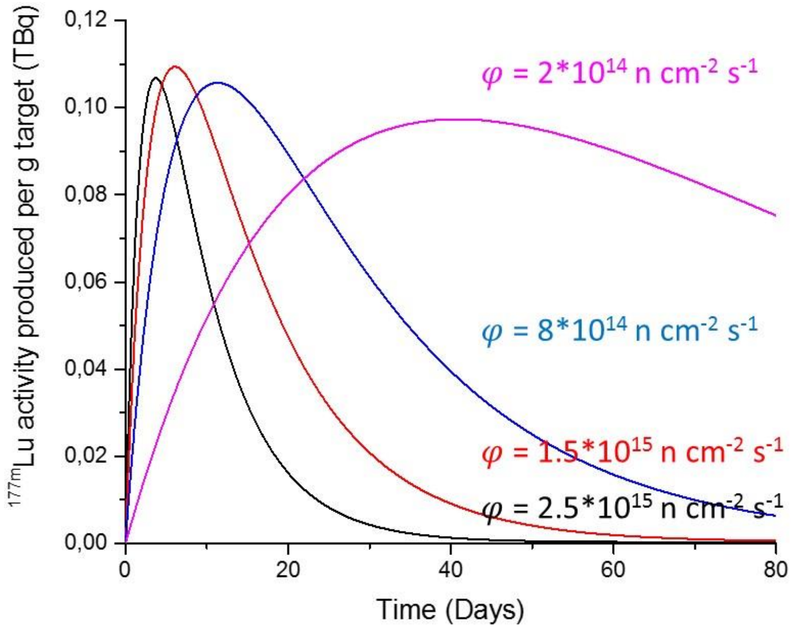

Figure 3: The production of ^{177m}Lu as function of irradiation time at different thermal flux values, $2*10^{14}$ n cm^{-2} s^{-1}, BR2, Mol, Belgium (in magenta), $8*10^{14}$ n cm^{-2} s^{-1} BR2, Mol, Belgium (in blue), $1.5*10^{15}$ n cm^{-2} s^{-1} , ILL, Grenoble, France (in red) and $2.5*10^{15}$ n cm^{-2} s^{-1}, HFIR, Oak Ridge, U.S.A (in black). The target consists of commercially available 84.44% ^{176}Lu enriched Lu_2O_3.

Figure 3 shows that the maximum ^{177m}Lu activity that can be produced using 1 g of 84.44% ^{176}Lu enriched Lu_2O_3 remains in the order of 0.1 TBq by increasing the thermal neutron flux about 10 times from $2.1*10^{14}$ n cm^{-2}. s^{-1} to $2.5*10^{15}$ n cm^{-2}. s^{-1}. However, the change in the thermal neutron flux has a significant impact on the irradiation time needed to reach the maximum ^{177m}Lu activity production. The irradiation time (t_{max}) decreases from 42, 12, 6 to 4 days with the increase in the thermal neutron flux from $2.1*10^{14}$ n cm^{-2} s^{-1}, $8*10^{14}$ n cm^{-2} s^{-1}, $1.5*10^{15}$ n cm^{-2} s^{-1} to $2.5*10^{15}$ n cm^{-2} s^{-1} respectively. During the ^{177m}Lu production in high-flux reactors the ^{177m}Lu activity starts growing quickly, reaches a maximum and then starts decreasing with a further increase in time. The observed decrease can be accounted to the high burn-up cross section of ^{177m}Lu 620 b, and should be considered carefully while designing the large scale ^{177m}Lu production. Overall, it can be concluded that the biggest advantage of using the high-flux reactors lies in the short irradiation times need to reach the maximum ^{177m}Lu activity production (4 days in comparison to 42 days). These short irradiation times could decrease the cost of ^{177m}Lu production subject to the availability of suitable irradiation devices allowing to load/unload the target material into/from the high-flux positions during operation of the reactor.

Additionally, it should be pointed that apart from ^{177m}Lu production, large amounts of ^{177}Lu will be co-produced along with ^{177m}Lu. The ^{177}Lu production ($^{176}Lu(n, \gamma)^{177}Lu$) has about 650 times higher neutron capture cross section than the ^{177m}Lu production ($^{176}Lu(n, \gamma)^{177m}Lu$) neutron capture cross section of 2.8 b. The excess ^{177}Lu will contribute to large radiation dose after the end of irradiation making the product handling difficult. In order to decrease the dose contribution coming from ^{177}Lu, and increase the ^{177m}Lu specific activity, long cooling times of around 60 days would be required (approximately 10 half-lives of ^{177}Lu). The specific activity of the ^{177m}Lu produced at the end of irradiation and after the end of cooling (EOC) are discussed in detail in the next subsection.

5.4.2.2 Evaluation of the specific activity of the produced ^{177m}Lu

The specific activity of the starting ^{177m}Lu will be a crucial parameter in determining the specific activity of the ^{177}Lu produced via a $^{177m}Lu/^{177}Lu$ radionuclide generator. The specific activity of the ^{177m}Lu produced at end of irradiation and at the end of cooling (EOC) for different neutron fluxes is presented in Figure 4 below. The plotted data (in red) represents the specific activity of ^{177m}Lu produced at the EOI, at the time of maximum ^{177m}Lu production (4, 6, 12, and 42 days for the thermal neutron flux of $2.5*10^{15}$, $1.5*10^{15}$, $8*10^{14}$, and $2*10^{14}$ n cm^{-2}. s^{-1} respectively). The plotted data in blue represents the specific activity of the ^{177m}Lu at the end of 60 days of cooling period starting right after the end of irradiation.

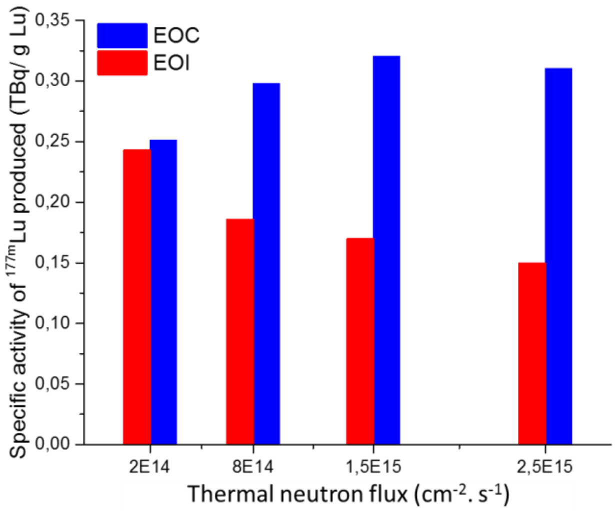

Figure 4: The specific activity of ^{177m}Lu produced at the End of Irradiation (in red), and at the end of cooling period of 60 days (EOC) (in blue) for the studied thermal neutron flux values. The target consists of commercially available 84.44% ^{176}Lu enriched Lu_2O_3.

Figure 4 shows that i) the specific activity of the ^{177m}Lu obtained at the EOI decreases with an increase in the used neutron flux and ii) the 60 days cooling period at the EOI has a significant effect on the specific activity of the ^{177m}Lu produced using high thermal neutron flux. The highest specific activity obtained at the EOI was found to be 0.25 TBq ^{177m}Lu. g^{-1} Lu on using a neutron flux of $2*10^{14}$ n cm^{-2} s^{-1} and irradiation period of 42 days. The 42 days irradiation will be accompanied with about 78% target ^{176}Lu target burn-up due to the $^{176}Lu(n,\gamma)^{177}Lu$ neutron capture reaction. Additionally, the ^{177}Lu co-produced will be burned up via the $^{177}Lu(n,\gamma)^{178}Lu$ neutron capture reaction having a neutron capture cross section of 1000 b. However, the ^{177m}Lu production at high flux reactors involves a short irradiation time ranging from 4 to 12 days. This will be accompanied by about 85% target burn-up, but a large amount of ^{177}Lu will be co-produced, (about 200 TBq per 0.1 TBq ^{177m}Lu) lowering the overall specific activity of ^{177m}Lu. The influence of ^{177}Lu activity on the specific activity of ^{177m}Lu also explains the observed increase in the specific activity after the EOC. For the ^{177m}Lu produced at high-flux reactors, the specific activity of about 0.15 to 0.2 TBq. g^{-1} Lu will be obtained at the EOI for the thermal neutron flux of $2.5*10^{15}$, $1.5*10^{15}$, $8*10^{14}$ n cm^{-2}. s^{-1}. The 60 days cooling period following the EOI will lead to decay of ^{177}Lu produced and increases the ^{177m}Lu specific activity to up to 0.32TBq. g^{-1} Lu. Any further increase in the cooling period will lead to loss of ^{177m}Lu activity due to its radioactive decay.

5.4.2.3 Effect of ^{176}Lu enrichment on irradiation time and ^{177m}Lu activity production

The ^{176}Lu target enrichment will play a crucial role in determining the cost of the ^{177m}Lu production. The effect of the ^{176}Lu enrichment (ranging from 2.56% ^{176}Lu natural abundancy Lu_2O_3 to 99.99% ^{176}Lu enriched Lu_2O_3) on ^{177m}Lu production has been evaluated for the available thermal neutron flux of $8*10^{14}$ n cm^{-2} s^{-1}. The results are shown in Figure 5 below:

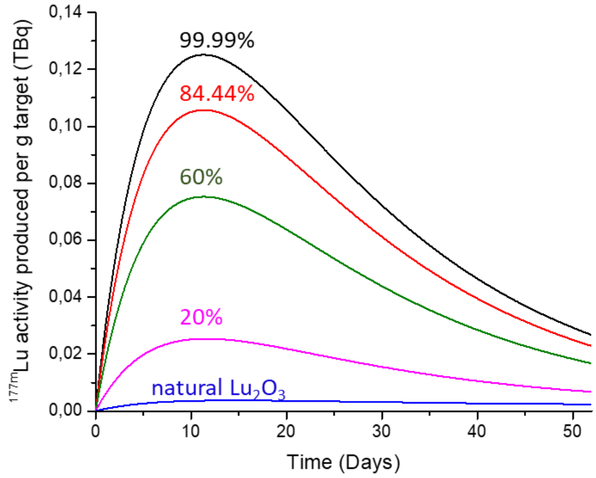

Figure 5: The ^{177m}Lu activity produced as a function of irradiation time for 1 g of targets having different ^{176}Lu enrichment. The irradiation of 1g of Lu_2O_3 target with 99.99% ^{176}Lu (in red), 84.44% ^{176}Lu (in red), 60% ^{176}Lu (in green), 20% ^{176}Lu (in pink) and 2.56% ^{176}Lu (natural Lu_2O_3) (in blue) using a thermal neutron flux of $8*10^{14}$ cm^{-2} s^{-1}.

Figure 5 shows that the irradiation time (t_{max}) needed to reach the maximum ^{177m}Lu activity will remain at about 12 days irrespective of the starting ^{176}Lu enrichment on using a thermal neutron flux of $8*10^{14}$ n cm^{-2} s^{-1} . However, an increase in the ^{176}Lu enrichment leads to a proportional increase in the maximum ^{177m}Lu activity production. At the EOI, the maximum ^{177m}Lu activity produced increases from 0.02, 0.07, 0.11, 0.12 TBq with the increase in the starting ^{176}Lu enrichment from 20%, 60%, 84.44% to 99.99% respectively. At the same time, the specific activities obtained also increases from 0.031, 0.11, 0.18 to 0.24 TBq g^{-1} Lu. This can be expected as the ^{176}Lu has high neutron capture cross section ($^{176}Lu(n,\gamma)^{177}Lu$ = 2000 b & $^{176}Lu(n,\gamma)^{177m}Lu$ = 2.8 b) compared to the neutron capture cross section of ^{175}Lu ($^{175}Lu(n,\gamma)^{176}Lu$ = 6.6 b) (also see Table 1). Thus, ^{176}Lu will get burned up readily during the neutron irradiation increasing the specific activity of the obtained ^{177m}Lu. Lastly, it has been observed that the 60 days cooling period followed by the EOI will result in a change in the specific activity only for the starting targets containing greater than 60% ^{176}Lu enrichment. For 60 days cooling period, the ^{177m}Lu specific activity will increase from 0.24, 0.18, 0.11 TBq g^{-1} Lu to 0.58, 0.30, 0.13 TBq g^{-1} Lu for the starting ^{176}Lu enrichments of 99.99%, 84%, 60%, respectively. For lower ^{176}Lu enrichment containing targets, the presence of unburned ^{175}Lu coming from the initial target mass will remain unchanged during the cooling period, thus the ^{177m}Lu specific activity also remains almost unaffected.

5.5. Conclusions

The present work investigates the large-scale ^{177m}Lu production in the current nuclear research reactors. All the relevant parameters and equations needed to estimate the ^{177m}Lu activity production are summarized, and a detailed literature overview on the possible ^{177m}Lu production and burn-up cross sections has been presented. The experimental results of ^{177m}Lu production clearly validate the 2.8 b as the ^{177m}Lu production and and 620 b as the ^{177m}Lu burn-up cross section, respectively. The presence of burn-up cross section for ^{177m}Lu should be taken into account while evaluating the ^{177m}Lu production as it will significantly reduce the irradiation time needed to reach the maximum specific activity. The calculations shown in the present work reveals that about 0.11 TBq ^{177m}Lu with a specific activity of 0.3 TBq g^{-1} Lu can be produced in short irradiation time of 4 days using 1g of 84.44% ^{176}Lu enriched Lu_2O_3 and a thermal neutron flux of $2.5*10^{15}$ n cm^{-2} s^{-1}. The present work confirms the possibility of large-scale ^{177m}Lu production, however the question of what activity and specific activity of ^{177m}Lu is needed for a ^{177m}Lu/^{177}Lu radionuclide generator is not yet answered. Our future efforts will be focused on defining the effect of the activity and specific activity of the starting ^{177m}Lu on the ^{177}Lu produced via the ^{177m}Lu/^{177}Lu radionuclide generator.

Finally, this work is aimed at bringing the attention of the nuclear scientist community towards the large-scale ^{177m}Lu production as it is crucial in developing a ^{177m}Lu/^{177}Lu radionuclide generator, thereby opening the doors for an onsite, on demand ^{177}Lu production.

Acknowledgements:

The authors would like to thanks Prof. dr. Marcel de Bruin and Dr. Menno Blaauw for their time in discussing the data and designing of experiments.

5.5. References

1 Banerjee, S., Pillai, M. R. & Knapp, F. F. Lutetium-177 therapeutic radiopharmaceuticals: linking chemistry, radiochemistry, and practical applications. *Chem Rev* 115, 2934-2974, (2015).

2 Kam, B. L. R. *et al.* Lutetium-labelled peptides for therapy of neuroendocrine tumours. *European Journal of Nuclear Medicine and Molecular Imaging* 39, 103-112, (2012).

3 Pillai, A. M. & Knapp, F. F., Jr. Evolving Important Role of Lutetium-177 for Therapeutic Nuclear Medicine. *Curr Radiopharm* 8, 78-85 (2015).

4 Vries*, D. J. D. & Wolterbeek, H. T. Tijdschrift voor nucleaire geneeskunde. 899-904 (2012).

5 Bhardwaj, R. *et al.* Separation of nuclear isomers for cancer therapeutic radionuclides based on nuclear decay after-effects. *Scientific Reports* 7, 44242, (2017).

6 Bhardwaj, R., Wolterbeek, H. T., Denkova, A. G. & Serra-Crespo, P. Radionuclide generator based production of therapeutic 177Lu from its long-lived isomer 177mLu. *EJNMMI Radiopharmacy and Chemistry* submitted (2019).

7 Knapp, F. F. & Mirzadeh, S. The continuing important role of radionuclide generator systems for nuclear medicine. *Eur J Nucl Med* 21, 1151-1165, (1994).

8 Nethaway, D. R. & Mendoza, B. The half-life and formation cross-section of 177mLu. *Journal of Inorganic and Nuclear Chemistry* 29, 865-867, (1967).

9 Deepa, S., Vijay Sai, K., Gowrishankar, R. & Venkataramaniah, K. The 160.44 day 177mLu as a new gamma calibration standard. *Radiation Physics and Chemistry* 81, 226-231, (2012).

10 Hnatowicz, V. Precise measurement of gamma-ray intensities in the decay of 160·9 day isomeric state in177Lu. *Czech J Phys* 31, 260-268, doi:10.1007/BF01604508 (1981).

11 Choppin, G. R., Liljenzin, J.-O. & Rydberg, J. in *Radiochemistry and Nuclear Chemistry (Third Edition)* (ed Gregory R. ChoppinJan-Olov LiljenzinJan Rydberg) 388-414 (Butterworth-Heinemann, 2002).

12 International Atomic Energy Agency. *IAEA Nuclear Data Section*, <https://www-nds.iaea.org/relnsd/NdsEnsdf/neutroncs.html> (2015).

13 Dash, A., Pillai, M. R. & Knapp, F. F., Jr. Production of (177)Lu for Targeted Radionuclide Therapy: Available Options. *Nucl Med Mol Imaging* 49, 85-107, (2015).

14 Roig, O. *et al.* High spin K isomeric target of 177mLu. *Nuclear Instruments and Methods in Physics Research Section A: Accelerators, Spectrometers, Detectors and Associated Equipment* 521, 5-11, (2004).

15 NGATLAS, I. A. E. A. *Atlas for neutron capture cross sections*, <https://www-nds.iaea.org/exfor/servlet/X4sZvd?file=https://www-nds.iaea.org/ngatlas2/zvd/Lu176-402.zvd> (

16 Erdtmann, G. *Neutron Activation Tables*. Vol. 6, Kernchemie in Einzeldarsrtellungen 109 (Weinheim, 1976).

17 G. Pffenig, H. K.-N., W. SEELMANN, Karlsruher Nuklidkarte,. KFK GmbH, Germany (1998).

18 Pritychenko, B. & Mughabghab, S. Neutron thermal cross sections, Westcott factors, resonance integrals, Maxwellian averaged cross sections and astrophysical reaction rates calculated from the ENDF/B-VII. 1, JEFF-3.1. 2, JENDL-4.0, ROSFOND-2010, CENDL-3.1 and EAF-2010 evaluated data libraries. *Nuclear Data Sheets* 113, 3120-3144 (2012).

19 Roig, O. *et al.* Evidence for inelastic neutron acceleration by the ^{177m}Lu isomer. *Physical Review C* 74, 054604 (2006).

20 Roig, O. *et al.* Direct evidence for inelastic neutron ``acceleration'' by ^{177m}Lu. *Physical Review C* 83, 064617 (2011).

21 Bélier, G. *et al.* Thermal neutron capture cross section for the K isomer ^{177}Lu^{m}. *Physical Review C* 73, 014603 (2006).

22 Ponsard, B. Production of radioisotopes in the BR2 high-flux reactor for applications in nuclear medicine and industry. *Journal of Labelled Compounds and Radiopharmaceuticals* 50, 333-337, (2007).

23 Barnett, G. C. *et al.* Normal tissue reactions to radiotherapy: towards tailoring treatment dose by genotype. *Nat Rev Cancer* 9, 134-142, (2009).

24 Knapp, F. F., Jr. *et al.* Nuclear medicine program progress report for quarter ending September 30, 1995. (United States, 1995).

25 Gryntakis, E. M. & Kim, J. I. Activation cross-sections for some (n, 2n), (n, p) and (n, γ)-reactions. *Journal of Radioanalytical Chemistry* 46, 159-163, doi:10.1007/BF02519739 (1978).

26 Gritaj, E. A. in *Neutron physics Vol 2.* 209-213.

Chapter 6

Modelling of the $^{177m}Lu/^{177}Lu$ radionuclide generator

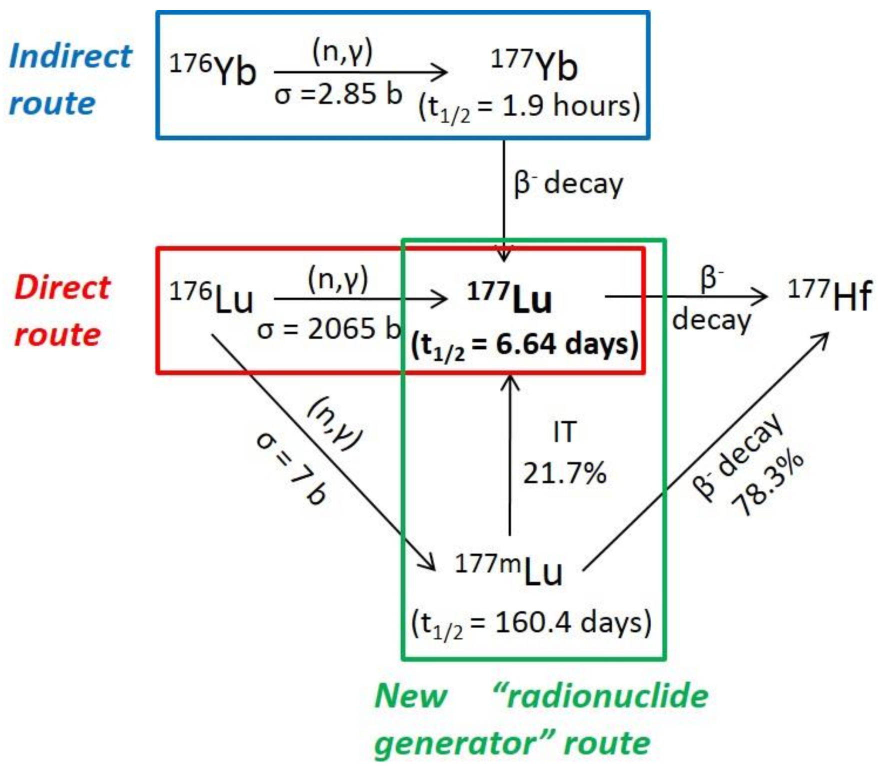

This Chapter has been adapted from:

Bhardwaj, R, Wolterbeek, H. T., Denkova, A.G., & Serra-Crespo, P. (2019). Modelling of the $^{177m}Lu/^{177}Lu$ radionuclide generator. Applied Radiation and Isotopes, submitted

Abstract

In order to determine the potential of $^{177m}Lu/^{177}Lu$ radionuclide generator in ^{177}Lu production it is important to establish the technical needs that can lead to a clinically acceptable ^{177}Lu product quality. In this work, a model that includes all the processes and the parameters affecting the performance of the $^{177m}Lu/^{177}Lu$ radionuclide generator has been developed. The model has been based on the use of a ligand to complex ^{177m}Lu ions, followed by the separation of the freed ^{177}Lu ions. The dissociation kinetics of the Lu-ligand complex has been found to be the most crucial aspect governing the specific activity, ^{177m}Lu content of the produced ^{177}Lu. The dissociation rate constants lower than $1*10^{-11}$ s^{-1} would be required to lead to onsite ^{177}Lu production with specific activity close to theoretical maximum of 4.1 TBq ^{177}Lu/ mg Lu and with ^{177m}Lu content of less than 0.01%. Lastly, the calculations suggests that more than one patient dose per week can be supplied for a period of up to 7 months on starting with the ^{177m}Lu produced using 3g Lu_2O_3 target with 60% ^{176}Lu enrichment. The requirements of the starting ^{177m}Lu activity production needs to be adapted depending on the required patient doses, and the technical specifications of the involved ^{177m}Lu-^{177}Lu separation process.

6.1 Introduction

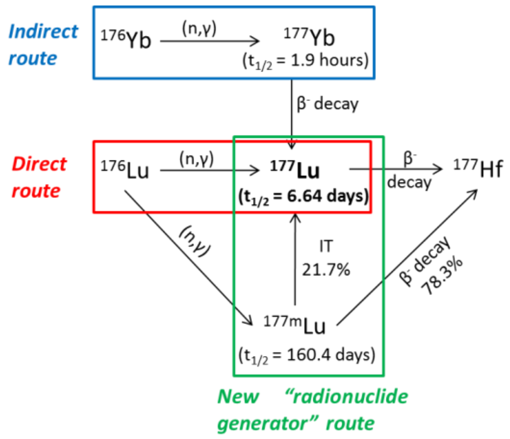

Figure 1: Different possible ^{177}Lu production routes: The currently employed "indirect" and "direct" production route in blue & red. The proposed radionuclide generator route in green.

Lutetium-177 is a β⁻ and γ ray emitting radionuclide with a half-life ($t_{1/2}$) of 6.64 days and with proven potential in the field of nuclear medicine [1,2]. The ^{177}Lu labelled [^{177}Lu]Lu-DOTATATE has been FDA approved for neuroendocrine tumour treatment. Other ^{177}Lu labelled compounds have shown promising application in the treatment of a wide range of tumours, such as prostate cancer, breast cancer, etc. [3-7]. It is believed that the tremendous potential of ^{177}Lu is not fully exploited yet and the application of ^{177}Lu in the treatment of tumours is expected to grow significantly in the coming years [1,8,9]. The present worldwide ^{177}Lu supply is fulfilled by the direct and the indirect production routes (shown in Figure 1 in red and blue respectively). The direct route involves the production of ^{177}Lu by the neutron capture of ^{176}Lu enriched Lu_2O_3 targets, while the indirect approach is based on the neutron irradiation of ^{176}Yb enriched Yb_2O_3 targets. Recently, an alternative ^{177}Lu production route via a $^{177m}Lu/^{177}Lu$ radionuclide generator has been proposed (shown in Figure 1 in green) [10]. The $^{177m}Lu/^{177}Lu$ radionuclide generator is based on the ^{177}Lu production from the decay of its long-lived nuclear isomer, ^{177m}Lu ($t_{1/2}$ = 160.44 days), and concerns the separation of two isomers in the form of complexed ^{177m}Lu and freed ^{177}Lu ions [11,12]. Like other radionuclide generators [13-19], the $^{177m}Lu/^{177}Lu$ radionuclide generator also offers unique advantages like an onsite and on demand ^{177}Lu supply. However, the development of $^{177m}Lu/^{177}Lu$ radionuclide generator is still at an early stage.

There are several uncertainties regarding the technical needs of a $^{177m}Lu/^{177}Lu$ radionuclide generator and what ^{177}Lu quality (specific activity and ^{177m}Lu content) & quantity (number of patient doses) can be delivered by the generator. It is unclear how much starting ^{177m}Lu activity would be needed to produce sufficient amounts of ^{177}Lu via a $^{177m}Lu/^{177}Lu$ radionuclide generator route. The existing literature shows that the dissociation kinetics of the complex used to hold ^{177m}Lu ions is of paramount importance in determining the quality of produced ^{177}Lu [11,12]. However, what dissociation rate constants are required to lead to clinically acceptable ^{177}Lu production is not known. In the present work, the existing knowledge regarding the ^{177m}Lu production and the ^{177m}Lu-^{177}Lu separation have been evaluated together in order to define the technical needs of a $^{177m}Lu/^{177}Lu$ radionuclide generator.

Here, the processes and the parameters affecting the development of a $^{177m}Lu/^{177}Lu$ radionuclide generator have been simulated. The effect of starting ^{176}Lu enrichment, the starting ^{177m}Lu activity (and specific activity) and the ^{177m}Lu-^{177}Lu separation on the quality, quantity of produced ^{177}Lu have been defined. Finally, the expected ^{177}Lu quality (its specific activity & ^{177m}Lu content) achievable via a $^{177m}Lu/^{177}Lu$ radionuclide generator has been compared with the ^{177}Lu produced by the commercially employed direct and indirect production routes.

6.2 Model description

The existing literature shows that the $^{177m}Lu/^{177}Lu$ radionuclide generator based ^{177}Lu production consists of three processes (i) the production of ^{177m}Lu (ii) the complexation of the produced ^{177m}Lu ions with a ligand and [20] the ^{177}Lu production by the separation of complexed ^{177m}Lu and freed ^{177}Lu ions [20]. The parameters affecting these individual processes are shown in Figure 2. The effect of these parameters have been simulated to determine the ^{177}Lu activity (number of patient doses) and the quality (its specific activity and ^{177m}Lu content) that can be produced from a $^{177m}Lu/^{177}Lu$ radionuclide generator.

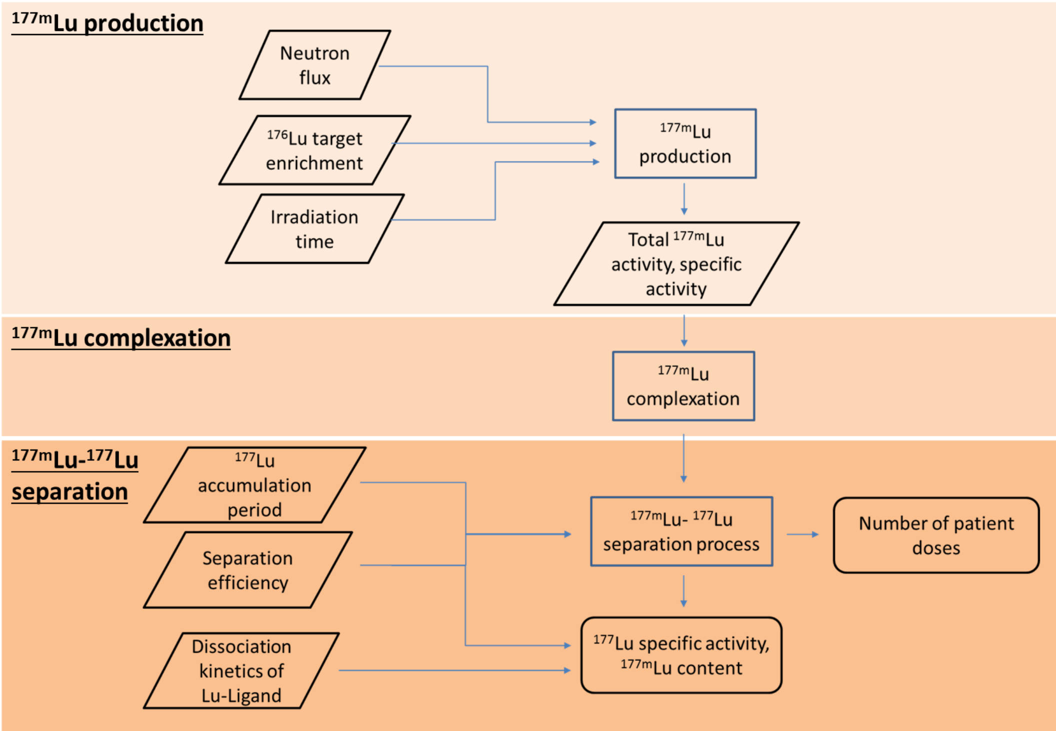

Figure 2: A schematic representation of the steps involved in ^{177}Lu production via a $^{177m}Lu/ ^{177}Lu$ radionuclide generator, the (▱) represents the input/ output parameters, while the (□), (▢) represents a process and end process, respectively.

The $^{177m}Lu/^{177}Lu$ radionuclide generator based ^{177}Lu production starts with the ^{177m}Lu production. The ^{177m}Lu production by the neutron irradiation of ^{176}Lu enriched Lu_2O_3 target has been shown to be affected by neutron flux, the starting ^{176}Lu enrichment and the irradiation time [21]. At the end of the ^{177m}Lu production, the ^{177m}Lu containing target needs to be dissolved and complexed with a ligand. The internal conversion decay of ^{177m}Lu would lead to ^{177}Lu production according to Equation 1,

$$A^t_{^{177}Lu} = A^0_{^{177m}Lu} \cdot \left(\frac{\lambda_{^{177}Lu}}{\lambda_{^{177}Lu} - \lambda_{^{177m}Lu}}\right) \cdot \left[exp^{-\lambda_{^{177m}Lu}.t} - exp^{-\lambda_{^{177}Lu}.t}\right] \cdot B.R \cdot P.I.C \quad \text{Equation 1}$$

where A_m^0 is the initial activity of ^{177m}Lu at time, t= 0, before ^{177}Lu separation, λ_g, λ_m are decay constants of ^{177}Lu, ^{177m}Lu respectively, A_g^t is the activity of ^{177}Lu at time t, B.R is the branching ratio for ^{177m}Lu to ^{177}Lu decay (21.4%) [22] and P.I.C is the probability of internal conversion (96.8%) [12].

The accumulation period (the period between two successive ^{177}Lu separations) and the starting ^{177m}Lu activity determines the maximum ^{177}Lu activity that can be produced from a $^{177m}Lu/^{177}Lu$ radionuclide generator. After the accumulation period, a separation process is needed to separate the freed ^{177}Lu from complexed ^{177m}Lu ions. The efficiency of this separation process determines the number of patient doses that can be provided from the $^{177m}Lu/^{177}Lu$ radionuclide generator. Further, the specific activity of the starting ^{177m}Lu is one of the crucial parameters in determining the amount of other Lu ions that gets complexed during the ^{177m}Lu complexation. The dissociation of the complex can release the complexed ions free, thereby making them inseparable from the ^{177}Lu ions freed by the internal conversion decay. This increases the ^{177m}Lu content and decrease the specific activity of the produced ^{177}Lu, in accordance with the Equation 2 below:

$$S.A._{^{177}Lu} = \frac{A_{^{177}Lu}}{\sum mass\ (^{176}Lu + {}^{175}Lu + {}^{177}Lu + {}^{177m}Lu + {}^{178}Lu)} \qquad \text{Equation 2}$$

In this work, the dissociation of the complex has been assumed to follow a first order dissociation kinetics according to the Equation 3, 4 below:

$$LuLig \rightleftharpoons Lu + Ligand \qquad \text{Equation 3}$$

$$\ln\left(\frac{[LuLig]_t}{[LuLig]_0}\right) = -k_d t \qquad \text{Equation 4}$$

where, $[LuLig]_0$ is the initial concentration of the complexed Lu ions and $[LuLig]_t$ represents the concentration of complexed Lu ions at time t. k_d is the dissociation rate constant in s^{-1} and t is the separation time taken to separate the complexed and free ions. The dissociation is majorly governed by the dissociation rate constant (k_d) which is dependent on the temperature (T), as per the Arrhenius equation, ($k_d = A.\exp(-E_a/RT)$, where T is the temperature) and time t. A decrease in temperature (T) or reducing the time (t) taken to achieve the separation can decrease the dissociation of starting complex. The effect of dissociation kinetics has been minimized by considering the temperature during the ^{177}Lu accumulation period to be 77K. It has been assumed that the dissociation of the complex can only take place during the time taken to separate the freed ^{177}Lu and the complexed ^{177m}Lu. This assumption is based on an experimental design proposed previously by Bhardwaj et al [10].

6.3 Methods

The ^{177m}Lu production was simulated using the previously proposed model (see chapter 5) and MATLAB program [21]. The ^{177m}Lu activity produced was used as an input and the Equations 1-4 were used to simulate the ^{177}Lu production. Amongst all the parameters shown in Figure 2, some were kept constant during the simulations with their values listed in Table 1, while the other parameters are discussed below:

6.3.1 Effect of ^{176}Lu enrichment on ^{177m}Lu production

The effect of the target ^{176}Lu enrichment (ranging from 2.56%, 40%, 60%, 80%, 99.99%) on the produced ^{177m}Lu activity and specific activity was studied. The four different neutron flux values and the irradiation conditions used in the calculations are listed in Table 1.

6.3.2 Effect of starting ^{177m}Lu activity on number of patient doses

The number of patient doses were determined as a function of time for different starting ^{177m}Lu activity produced from different ^{176}Lu enrichment (ranging from 40%, 60%, 99.99% ^{176}Lu) containing Lu_2O_3 target. It was assumed that ^{177}Lu would be separated after accumulation period of 7 days and the ^{177}Lu produced can be collected with a 100% separation efficiency, as mentioned in Table 1.

6.3.3 Effect of dissociation kinetics of the Lu-Ligand on ^{177m}Lu-^{177}Lu separation

A starting ^{177m}Lu activity of 0.08 TBq with a specific activity of 0.33 TBq g^{-1} Lu produced from 1g with an 84.44% ^{176}Lu enriched Lu_2O_3 target was used as an input for ^{177m}Lu complexation with a ligand. The effect of dissociation kinetics on the ^{177m}Lu content and the specific activity of the produced ^{177}Lu was considered only during the separation of complexed ^{177m}Lu and freed ^{177}Lu ions. The dissociation rate constants (ranging from $6.25*10^{-12}$ s^{-1} – $1.0*10^{-10}$ s^{-1}) for different ^{177m}Lu-^{177}Lu separation times (1 min, 5 min & 10 min) were used in the calculation, while keeping the ^{177}Lu accumulation period fixed to 7 days. The effect of dissociation rate constants was also studied at different ^{177}Lu accumulation period of 7, 14, and 21 days for a fixed ^{177m}Lu-^{177}Lu separation time of 10 minutes.

6.3.4 Effect of starting ^{177m}Lu specific activity on the ^{177}Lu production

The specific activity of ^{177}Lu produced in the studied dissociation rate constant range, $6.25*10^{-12}$ s^{-1} – $1.0*10^{-10}$ s^{-1} was evaluated as a function of the starting ^{177m}Lu specific activity (or starting ^{176}Lu enrichment used in ^{177m}Lu production) for fixed ^{177m}Lu- ^{177}Lu separation time of 10 minutes, 1 minute and ^{177}Lu accumulation period of 7 days.

Table 1: List of the values ascribed to different parameters used during the modelling of processes involved in $^{177m}Lu/^{177}Lu$ radionuclide generator.

Parameter	**Value**	**Reference**
Neutron flux and irradiation time	$2.5*10^{15}$ cm^{-2}. s^{-1}, t_{irr} = 4 days, $t_{cooling}$ = 60 days	Bhardwaj et al [21]
	$1.5*10^{15}$ cm^{-2} s^{-1}, t_{irr} = 6 days, $t_{cooling}$ = 60 days	
	$8*10^{14}$ cm^{-2} s^{-1}, t_{irr} = 11 days, $t_{cooling}$ = 60 days	
	$2*10^{14}$ cm^{-2} s^{-1}, t_{irr} = 40 days, $t_{cooling}$ = 60 days	
One patient dose	7.4 GBq	Bakker et al [23]

^{177m}Lu-^{177}Lu separation efficiency	100%	Assumption [10]
^{177}Lu accumulation temperature	77K	Bhardwaj et al
Starting ^{177m}Lu activity, specific activity	0.08 TBq, specific activity of 0.33 TBq g^{-1} Lu	

6.4 Results and Discussion

The section begins with evaluating the influence of ^{176}Lu enrichment on the ^{177m}Lu production. Subsequently, the effect of starting ^{177m}Lu activity, specific activity (or starting ^{176}Lu enrichment) on the produced ^{177}Lu activity, specific activity have been defined for different dissociation rate constants and the ^{177m}Lu-^{177}Lu separation time.

6.4.1 Effect of ^{176}Lu enrichment on ^{177m}Lu production

The availability of sufficient ^{177m}Lu activity is an important requirement for the $^{177m}Lu/^{177}Lu$ radionuclide generator. The ^{177m}Lu production has been based on the irradiation of ^{176}Lu enriched Lu_2O_3 targets in nuclear reactor. Figure 3 shows the effect of different ^{176}Lu target enrichment on the maximum ^{177m}Lu activity, specific activity produced under the irradiation conditions listed in Table 1.

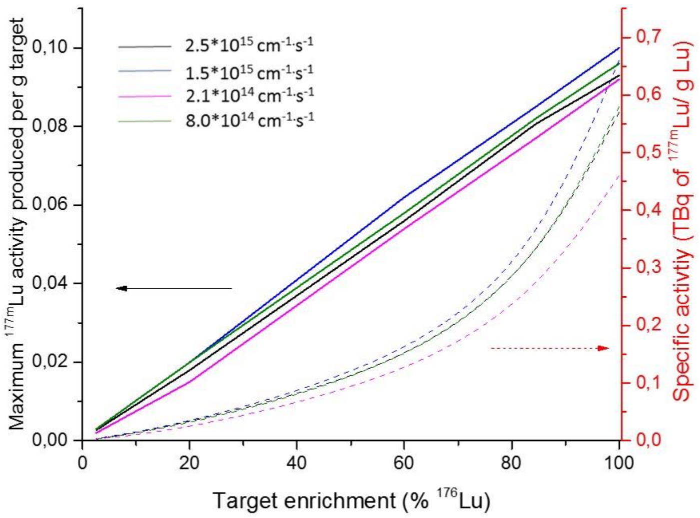

Figure 3: The maximum ^{177m}Lu activity produced (solid line and y axis, on the left) and its specific activity (dashed lines and y axis, on the right) as a function of ^{176}Lu enrichment in the starting Lu_2O_3 target. The time needed to reach the maximum irradiation ($\mathbf{t_{irradiation}}$) is 4, 6, 11, 40 days for the thermal neutron flux of $2.5*10^{15}$, $1.5*10^{15}$, $2*10^{14}$, $8*10^{14}$ $cm^{-2}.s^{-1}$ respectively and the cooling time is $\mathbf{t_{cooling}}$ = 60 days.

It can be seen from Figure 3 that the increase in the ^{176}Lu target enrichment leads to an increase in both the activity and specific activity of ^{177m}Lu produced. The ^{177m}Lu activity increases proportionally with the increase in the starting ^{176}Lu enrichment [21]. However, the increase in the ^{177m}Lu specific activity do not follow a proportional behaviour and increases rapidly with an increase in the ^{176}Lu enrichment. A maximum ^{177m}Lu activity of 0.09 TBq, with a specific activity of 0.65 TBq ^{177m}Lu/ g Lu can be produced using 1 g of 99.99% ^{176}Lu enriched

Lu_2O_3 target. The decrease in the ^{176}Lu enrichment from to 99.99% to 84.44% leads to about a half of the specific activity of the produced ^{177m}Lu. The initial ^{176}Lu enrichment used in the ^{177m}Lu production is crucial in evaluating the overall cost and the feasibility of the radionuclide generator based ^{177}Lu production. In addition, the starting ^{177m}Lu activity and specific activity are important in determining the activity, ^{177m}Lu content and the specific activity of produced ^{177}Lu.

6.4.2 Effect of starting ^{177m}Lu activity (or ^{176}Lu enrichment) on the number of patient doses

The number of patient doses that can be delivered from a $^{177m}Lu/^{177}Lu$ radionuclide generator is an important practical aspect that should be considered before evaluating the possibility of its commercialization. Figure 4 displays the number of patient doses that can be obtained from the ^{177m}Lu produced using 1g of different ^{176}Lu enriched targets.

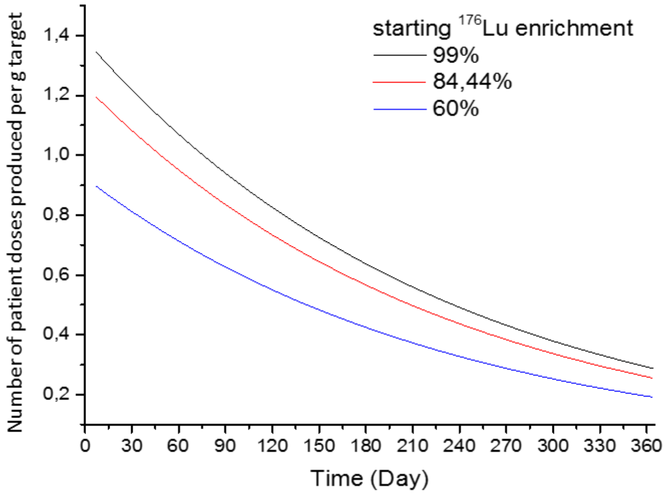

Figure 4: The total number of patient doses that can be produced weekly from the ^{177m}Lu produced using 1g of different ^{176}Lu enrichment containing targets

It can be seen from Figure 4 that the number of patient doses that can be produced from a $^{177m}Lu/^{177}Lu$ radionuclide generator decreases on decreasing the ^{176}Lu enrichment used in ^{177m}Lu production. This is expected as the amount of patient doses will be determined by the ^{177}Lu activity produced which is directly proportional to the starting ^{177m}Lu activity (or the starting ^{176}Lu enrichment), in accordance with Equation 1. The use of 99.99% ^{176}Lu enriched target can provide up to 1 patient dose weekly in the first 90 days and decreases to less than one patient dose weekly with the further increase in time. The use of 60% ^{176}Lu enriched Lu_2O_3 target would provide less than 1 patient dose weekly during the life of generator. Thus, the irradiation of larger masses of starting Lu_2O_3 target would be needed in order to reach more than one patient dose. For instance, the use of 3g 60% Lu_2O_3 target will result in more than one patient dose per week for a period of up to 7 months. A further decrease in the starting ^{176}Lu enrichment would increase the target mass needed to produce one patient dose per week for a long period of time. To the best of our knowledge, the ^{176}Lu enriched Lu_2O_3 (60%-84.44%) is commercially available in the order of few milligrams and its availability in the order of grams should be investigated in future research.

Further it should be noted that the current direct route ^{177}Lu production uses 1-5 mg of enriched target to provide about 100 patient doses while the indirect route can lead to about 50 patient doses using 100 mg of the target (depending on the target enrichment and the neutron flux) [10,24,25]. The irradiation has to be performed every week and the produced patient doses (^{177}Lu) should be used preferably within one week owing to its half-life of 6.64 days. In the case of $^{177m}Lu/^{177}Lu$ radionuclide generator, the irradiation would be needed once in 6-7 months and the ^{177}Lu could be produced when needed.

Lastly, it should also be mentioned that the number of patient doses (or produced ^{177}Lu activity) will also get effected by the efficiency of the separation process responsible for obtaining the freed ^{177}Lu ions. The separation efficiency will depend on the chemical design of a radionuclide generator system and it can be expected to vary from 60%-99% on the basis of the available literature [11,12]. Moreover, with an increasing number of separations and storage, the elution efficiency may drop further for chemical, physicochemical or radiolytic reasons and should be evaluated in future research.

6.4.3 Effect of the dissociation kinetics on the ^{177m}Lu content and specific activity of the produced ^{177}Lu

The specific activity of the ^{177}Lu produced and its $^{177}Lu/^{177m}Lu$ activity ratio is largely dependent on the dissociation of the complexed Lu. The effect of dissociation rate constant on the specific activity of the produced ^{177}Lu and the accompanying $^{177}Lu/^{177m}Lu$ activity ratio for different ^{177m}Lu-^{177}Lu separation time is shown in Figure 5(a) and for different ^{177}Lu accumulation period is shown in Figure 5(b).

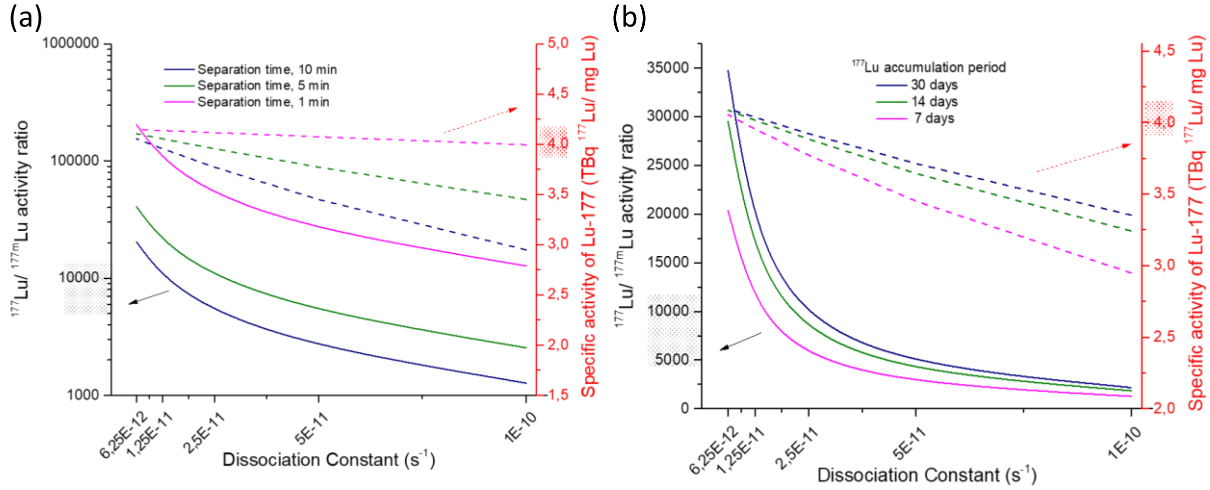

Figure 5: The change in $^{177}Lu/^{177m}Lu$ activity ratio (solid line and y axis on the left) and the specific activity of ^{177}Lu (dashed lines and y axis on the right) (a) as a function of dissociation for different ^{177m}Lu-^{177}Lu isomer separation time and fixed ^{177}Lu accumulation period of 7 days (b) for different ^{177}Lu accumulation period and fixed ^{177m}Lu- ^{177}Lu isomer separation time of 10 minutes. (Input: ^{177m}Lu produced using 1 g 84.44% ^{176}Lu enriched Lu_2O_3 and thermal flux $8*10^{14}$ $cm^{-2}.s^{-1}$, A_{max} = 0.08 TBq, S.A= 0.33 TBq/ g Lu, t_{irr} = 11 days, $t_{cooling}$ = 60 days). The shaded regions on the y-axis (left) represents the $^{177}Lu/$ ^{177m}Lu activity ratios that can be achieved commercially and the y-axis is the theoretical maximum specific activity of 4.1 TBq/ mg Lu [26].

Figure 5(a) shows that the decrease in the ^{177m}Lu-^{177}Lu separation time leads to a proportional increase in the $^{177}Lu/^{177m}Lu$ activity ratio while the specific activity remains close to the theoretical maximum of 4.1 TBq ^{177}Lu/ mg Lu. A ^{177m}Lu-^{177}Lu separation time of 1 minute would provide with an ideal separation leading to ^{177m}Lu content of less than 0.01% for the studied dissociation rate constants (i.e. ranging from $6.25*10^{-12}$ - $1*10^{-10}$ s^{-1}). A ^{177m}Lu-^{177}Lu separation time of 10 minutes will result in a 10 times decrease in the $^{177}Lu/^{177m}Lu$ activity ratio making the use of dissociation rate constants higher than $2.5*10^{-11}$ s^{-1} clinically unacceptable. It should be noted that the ^{177m}Lu- ^{177}Lu separation time of 10 minutes has already been experimentally achieved in the existing literature [11]. Further, the existing technologies such as microfluidics[27], capillary electrophoresis [28] are few attractive options that can allow reaching ^{177m}Lu- ^{177}Lu separation time up to 1 minute. However, their potential in ^{177}Lu-^{177m}Lu separation have not been experimentally proved yet and should be evaluated in future investigations.

Figure 5(b) shows that an increase in the ^{177}Lu accumulation period increases the $^{177}Lu/^{177m}Lu$ activity ratio while keeping the ^{177}Lu specific activity in the range of 2.9- 4.1 TBq ^{177}Lu/ mg Lu. The use of a ligand with a dissociation rate constant ranging from $1.25*10^{-11}$ - $5*10^{-11}$ s^{-1} would result in the $^{177}Lu/^{177m}Lu$ activity ratios ranging from 3000- 10000, depending on the ^{177}Lu accumulation period. Accumulation period of about 15-30 days would be needed to get the $^{177}Lu/^{177m}Lu$ activity ratio higher than 3000. This is expected as the ^{177}Lu activity increases with the increase in ^{177}Lu accumulation period (in accordance with Equation 1). The 64% of the maximum ^{177}Lu activity grows after about 7 days of accumulation period, increasing from 90% to 98% after 14 days and 21 days of accumulation, respectively. The use of complexes with dissociation rate constants lower than $1.25*10^{-11}$ s^{-1}, will keep the ^{177m}Lu content less than 0.01% and ^{177}Lu specific activity close to theoretical maximum of 4.1TBq ^{177}Lu/ mg Lu irrespective of used ^{177}Lu accumulation period.

Overall, the achievable ^{177}Lu quality is better than the one produced by the current direct and indirect production route. The indirect ^{177}Lu production has been reported to result in ^{177}Lu specific activity ranging from 2.9 TBq/ mg Lu to theoretical maximum of 4.1 TBq/ mg Lu with ^{177m}Lu content less than 0.01% ^{177m}Lu (the $^{177}Lu/^{177m}Lu$ activity ratio ≥ 10,000) [29-32,27,33]. The reported specific activity values produced via the direct route production ranges from 500 GBq/ mg Lu – 2.8 TBq/ mg Lu depending on the starting target enrichment and the neutron flux [29,34,35,31,32,36]. Further, the direct production has been reported to lead to the $^{177}Lu/^{177m}Lu$ activity ratios ranging from 4,000 - 10,000 (at the EOI) depending on the used irradiation time, neutron flux and the target enrichment [37-41]. It should be pointed out that the reported values have been based at the end of irradiation. However, the hospitals use ^{177}Lu up to one week after the end of irradiation and during this time the $^{177}Lu/^{177m}Lu$ activity ratio is likely to be halved [1].

6.4.4 Effect of starting ^{177m}Lu specific activity on the specific activity of produced ^{177}Lu

Apart from the dissociation rate constant, the specific activity of the produced ^{177}Lu also gets affected by the specific activity of the starting ^{177m}Lu which is related to the initial ^{176}Lu enrichment (as shown previously in Figure 3). Figure 6 presents the ^{177}Lu specific activity that can be produced when starting with 1g of different ^{176}Lu enrichment containing targets and dissociation rate constants ranging from 6.25*10^{-12} s^{-1} –1*10^{-10} s^{-1}. Figure 6(a), (b) has been based on a ^{177m}Lu- ^{177}Lu separation time of 10 minute and 1 minute respectively.

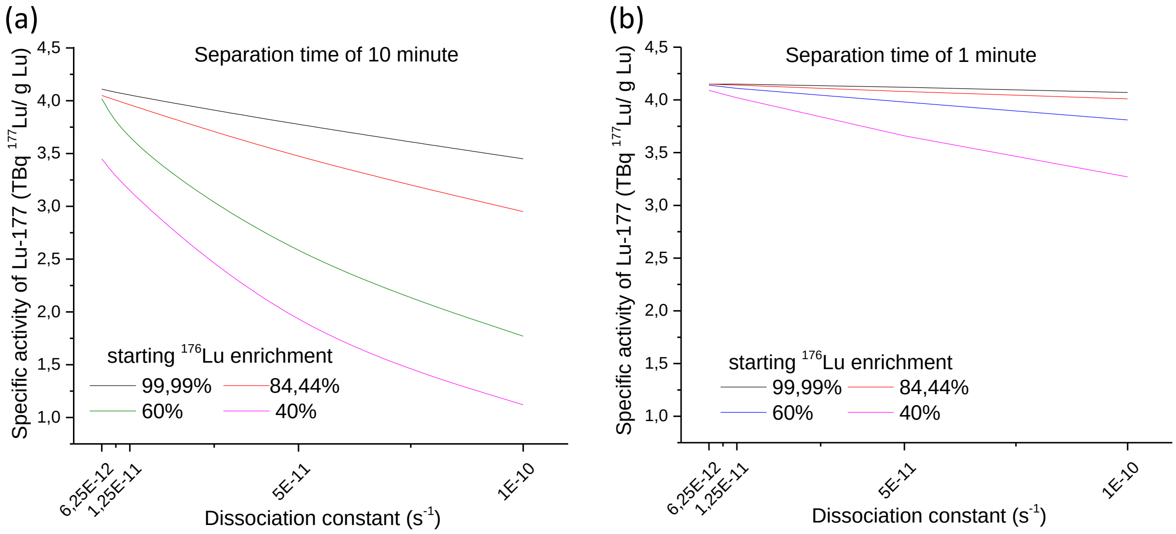

Figure 6: The specific activity of the produced ^{177}Lu as a function of dissociation rate constant for different ^{176}Lu enrichment containing targets and (a) a ^{177m}Lu- ^{177}Lu separation time of 10 minutes, (b) ^{177m}Lu- ^{177}Lu separation time of 1 minute.

Figure 6(a) and (b) clearly highlights the important role of the ^{177m}Lu-^{177}Lu separation time in determining the specific activity of ^{177}Lu produced. The use of a ^{177m}Lu-^{177}Lu separation time of 1 minute will keep the ^{177}Lu specific activity close to the theoretically maximum of 4.1 TBq/ mg Lu irrespective of the starting ^{176}Lu enrichment (Figure 6(b)) while it gets affected on using a ^{177m}Lu-^{177}Lu separation time of 10 minutes.

The decrease in the starting ^{176}Lu enrichment would decrease the specific activity of the produced ^{177m}Lu (see Figure 3). The use of low starting specific activity ^{177m}Lu results in high Lu (^{177m}Lu, ^{176}Lu, ^{175}Lu) ion contribution due to dissociation, thereby lowering the specific activity of produced ^{177}Lu ions. The use of complex with a dissociation rate constant of an order of 1.25*10^{-11} s^{-1} can lead to specific activity close to 4.1 TBq/ mg Lu irrespective of the initial ^{176}Lu enrichment and ^{177m}Lu-^{177}Lu separation time. However, the use of a complex with dissociation rate constants higher than 5*10^{-11} s^{-1} results in a considerable difference in the specific activity of the produced ^{177}Lu, ranging from 3.9 TBq/ mg Lu to 1.12 TBq/ mg Lu, depending on the starting ^{176}Lu enrichment and ^{177m}Lu-^{177}Lu separation time. It should be noted that the lowest specific activity of 1.12 TBq/ mg Lu produced on starting with 1g 40% ^{176}Lu enrichment containing target is very well comparable to the ^{177}Lu produced during the direct route.

Overall, the results from Figure 5 & 6 indicate that the dissociation rate constants higher than 1*10^{-10} s^{-1} are unacceptable irrespectively of the employed ^{177}Lu accumulation period or ^{177m}Lu- ^{177}Lu separation time (1 minute – 10 minutes) as they lead to high ^{177m}Lu content in the produced ^{177}Lu. The dissociation rate constant of the order of 10^{-7} s^{-1} (at pH-5, 20°C) has been reported in the literature for the chemically similar Y-DOTA complex [42] and dissociation rate constants of the order of 10^{-8} s^{-1} has been reported for Lu-DOTATATE complex (at pH-4.3, and 20°C) [43]. The dissociation rate constant (k_d) can be further decreased by lowering the temperature or the time taken to achieve the separation, as per the Arrhenius equation, ($k_d = A.exp(-E_a/RT)$, where T is the temperature). It has been experimentally demonstrated in Chapter 4, where the dissociation rate constant of $5*10^{-8}\pm1.3*10^{-8}$ s^{-1} has been achieved using Lu-DOTA complex, ^{177}Lu accumulation temperature of 77K and a ^{177m}Lu-^{177}Lu separation time of 10 minutes[11].

6.5 Conclusions

The presented work establishes the technical needs and potential of the $^{177m}Lu/^{177}Lu$ radionuclide generator in the ^{177}Lu production. The effect of ^{176}Lu enrichment and the ^{177m}Lu-^{177}Lu separation conditions on ^{177}Lu production have been studied. Depending on the starting ^{176}Lu enrichment, large target masses might be required to produce sufficient ^{177}Lu. For instance, the irradiation of 3g, 60% ^{176}Lu enriched Lu_2O_3 target would be needed to produce more than one patient dose per week for a period of up to 7 months. Further, the use of initial ^{176}Lu enrichment varying from 40%- 99.99% could lead to ^{177}Lu specific activity ranging from 1.2- 3.9 TBq ^{177}Lu/ mg Lu, depending on the used ^{177m}Lu-^{177}Lu separation conditions. The dissociation rate constants involved during the ^{177m}Lu-^{177}Lu separation would be crucial in governing the specific activity and ^{177m}Lu content of produced ^{177}Lu. The dissociation rate constants ≤ $1*10^{-11}$ s^{-1} would be needed to produce ^{177}Lu with less than 0.01% of the ^{177m}Lu content and with specific activity close to a theoretical maximum of 4.1 TBq ^{177}Lu/ mg Lu.

Finally, it should be noted that this work has been based on the use of a ligand for complexing Lu ions post ^{177m}Lu production and provides a reflection on the order of kinetic stability needed for the immobilization of Lu ions. The method for Lu ion immobilization can very well be varied while keeping in mind the needed kinetic stability.

Acknowledgements

The authors would like to thanks Prof. dr. Marcel de Bruin for his time in discussing the data and designing of experiments.

6.6 References

1 Banerjee, S., Pillai, M. R. & Knapp, F. F. Lutetium-177 therapeutic radiopharmaceuticals: linking chemistry, radiochemistry, and practical applications. Chem Rev 115, 2934-2974, doi:10.1021/cr500171e (2015).

2 Volkert, W. A., Goeckeler, W. F., Ehrhardt, G. J. & Ketring, A. R. Therapeutic radionuclides: production and decay property considerations. Journal of nuclear medicine : official publication, Society of Nuclear Medicine 32, 174-185 (1991).

3 <transition metals into azamacrocycle±gallophosphate.pdf>.

4 Hofman, M. S. et al. [(177)Lu]-PSMA-617 radionuclide treatment in patients with metastatic castration-resistant prostate cancer (LuPSMA trial): a single-centre, single-arm, phase 2 study. Lancet Oncol 19, 825-833, doi:10.1016/s1470-2045(18)30198-0 (2018).

5 Rasaneh, S., Rajabi, H., Babaei, M. H. & Daha, F. J. 177Lu labeling of Herceptin and preclinical validation as a new radiopharmaceutical for radioimmunotherapy of breast cancer. Nuclear medicine and biology 37, 949-955 (2010).

6 Repetto-Llamazares, A. H. V. et al. Combination of (177) Lu-lilotomab with rituximab significantly improves the therapeutic outcome in preclinical models of non-Hodgkin's lymphoma. European journal of haematology, doi:10.1111/ejh.13139 (2018).

7 Blakkisrud, J. et al. Tumor-Absorbed Dose for Non-Hodgkin Lymphoma Patients Treated with the Anti-CD37 Antibody Radionuclide Conjugate 177Lu-Lilotomab Satetraxetan. Journal of nuclear medicine : official publication, Society of Nuclear Medicine 58, 48-54, doi:10.2967/jnumed.116.173922 (2017).

8 Das, T. & Banerjee, S. Theranostic Applications of Lutetium-177 in Radionuclide Therapy. Current Radiopharmaceuticals 9, 94-101 (2016).

9 Vallabhajosula, S. et al. Lutetium-177 may be a better choice for radionuclide therapy than iodine-131 and yttrium-90. Eur J Nucl Med 28, 967-967 (2001).

10 De Vries, D. J. & Wolterbeek, H. The production of medicinal 177Lu and the story of 177mLu: detrimental by-product or future friend? Tijdschr. Nucl. Geneeskd 34, 899-904 (2012).

11 Bhardwaj, R., Wolterbeek, H. T., Denkova, A. G. & Serra-Crespo, P. Radionuclide generator based production of therapeutic 177Lu from its long-lived isomer 177mLu. EJNMMI Radiopharmacy and Chemistry submitted (2019).

12 Bhardwaj, R. et al. Separation of nuclear isomers for cancer therapeutic radionuclides based on nuclear decay after-effects. Scientific Reports 7, 44242, doi:10.1038/srep44242

13 Roesch, F. & J. Riss, P. The Renaissance of the 68Ge/68Ga Radionuclide Generator Initiates New Developments in 68Ga Radiopharmaceutical Chemistry. Current Topics in Medicinal Chemistry 10, 1633-1668, doi:10.2174/156802610793176738 (2010).

14 Pillai, M. R. A., Ashutosh, D. & Knapp, F. F. Rhenium-188: Availability from the 188W/188Re Generator and Status of Current Applications. Current

Radiopharmaceuticals 5, 228-243, doi:http://dx.doi.org/10.2174/1874471011205030228 (2012).

15 Roesch, F. Maturation of a Key Resource- The Germanium-68/Gallium-68 Generator: Development and New Insights. Current Radiopharmaceuticals 5, 202-211 (2012).

16 Knapp, F. F. & Dash, A. in Radiopharmaceuticals for Therapy (eds F. F. Knapp & Ashutosh Dash) Ch. 7, 131-157 (Springer India, 2016).

17 Boyd, R. E. Technetium-99m generators—The available options. The International Journal of Applied Radiation and Isotopes 33, 801-809, doi:https://doi.org/10.1016/0020-708X(82)90121-1 (1982).

18 Knapp, F. F. & Mirzadeh, S. The continuing important role of radionuclide generator systems for nuclear medicine. Eur J Nucl Med 21, 1151-1165, doi:10.1007/bf00181073 (1994).

19 Dash, A. & Chakravarty, R. Pivotal role of separation chemistry in the development of radionuclide generators to meet clinical demands. RSC Advances 4, 42779-42803, doi:10.1039/C4RA07218A (2014).

20 Piscitelli, F., Ballatore, C. & Smith Iii, A. B. Solid phase synthesis of 2-aminobenzothiazoles. Bioorg. Med. Chem. Lett. 20, 644-648, doi:http://dx.doi.org/10.1016/j.bmcl.2009.11.055 (2010).

21 Bhardwaj, R. et al. Large-scale production of lutetium-177m for the 177mLu/177Lu radionuclide generator. Applied radiation and isotopes : including data, instrumentation and methods for use in agriculture, industry and medicine (2019).

22 Kondev, F. G. Nuclear data sheets for A = 177. Nuclear Data Sheets 98, 801- 1095 (2003).

23 Bakker, W. H., Breeman, W. a P., Kwekkeboom, D. J., De Jong, L. C. & Krenning, E. P. . Practical aspects of peptide receptor radionuclide therapy with [177Lu][DOTA0, Tyr3]octreotate. Nucl. Med. Mol. Imaging 50, 265-271 (2006).

24 Lebedev, N. A., Novgorodov, A. F., Misiak, R., Brockmann, J. & Rösch, F. Radiochemical separation of no-carrier-added 177Lu as produced via the 176Ybn,γ177Yb→177Lu process. Applied Radiation and Isotopes 53, 421-425, doi:https://doi.org/10.1016/S0969-8043(99)00284-5 (2000).

25 Dash, A., Pillai, M. R. & Knapp, F. F., Jr. Production of (177)Lu for Targeted Radionuclide Therapy: Available Options. Nucl Med Mol Imaging 49, 85-107, doi:10.1007/s13139-014-0315-z (2015).

26 Wright, G. L., Grob, B. M. & Haley, C. Upregulation of prostate-specific membrane antigen after androgen-deprivation therapy. Urology 48, 326 (1996).

27 Ciceri, D., Perera, J. M. & Stevens, G. W. The use of microfluidic devices in solvent extraction. Journal of Chemical Technology & Biotechnology 89, 771-786, doi:10.1002/jctb.4318 (2014).

28 Zhu, X. & Lever, S. Z. Formation kinetics and stability studies on the lanthanide complexes of 1,4,7,10-tetraazacyclododecane-N,N',N",N"'-tetraacetic acid by capillary

electrophoresis. Electrophoresis 23, 1348-1356, doi:10.1002/1522-2683(200205)23:9<1348::aid-elps1348>3.0.co;2-v (2002).

29 Valery, A. T. et al. Production of No-Carrier Added Lutetium-177 by Irradiation of Enriched Ytterbium-176. Current Radiopharmaceuticals 8, 95-106, doi:http://dx.doi.org/10.2174/1874471008666150312160855 (2015).

30 Knapp, F. F., Mirzadeh, S., Beets, A. L., Du, M. & Garland, M. Reactor production of high specific activity lutetium-177 (Lu-177). European Journal of Nuclear Medicine and Molecular Imaging 31, S387-S387 (2004).

31 Ponsard, B. Production of radioisotopes in the BR2 high-flux reactor for applications in nuclear medicine and industry. Journal of Labelled Compounds and Radiopharmaceuticals 50, 333-337, doi:doi:10.1002/jlcr.1377 (2007).

32 Ketring, A. R. et al. Production and supply of high specific activity radioisotopes for radiotherapy applications. ALASBIMN Journal 5, 7 (2003).

33 <Production and chemical processing of 177Lu.pdf>.

34 Knapp, F. F., Mirzadeh, S. & Beets, A. L. Reactor production and processing of therapeutic radioisotopes for applications in nuclear medicine. J Radioanal Nucl Chem 205, 93-100, doi:10.1007/BF02040554 (1996).

35 Knapp Jr, F. F., Mirzadeh, S., Beets, A. L. & Du, M. Production of therapeutic radioisotopes in the ORNL High Flux Isotope Reactor (HFIR) for applications in nuclear medicine, oncologyand interventional cardiology. J Radioanal Nucl Chem 263, 503-509, doi:10.1007/s10967-005-0615-y (2005).

36 Mikolajczak, R. et al. Reactor produced 177 Lu of specific activity and purity suitable for medical applications. Vol. 257 (2003).

37 Dvorakova, Z., Henkelmann, R., Lin, X., Türler, A. & Gerstenberg, H. Production of 177Lu at the new research reactor FRM-II: Irradiation yield of 176Lu(n,γ)177Lu. Applied Radiation and Isotopes 66, 147-151, doi:https://doi.org/10.1016/j.apradiso.2007.08.013 (2008).

38 Pawlak, D., Parus, J. L., Sasinowska, I. & Mikolajczak, R. Determination of elemental and radionuclidic impurities in 177Lu used for labeling of radiopharmaceuticals. J Radioanal Nucl Chem 261, 469-472, doi:10.1023/B:JRNC.0000034887.23530.f6 (2004).

39 Knapp, F. F. J. A., K.R.; Beets, A.L.; Luo, H.; McPherson, D.W. & Mirzadeh, S. Nuclear medicine program progress report for quarter ending September 30, 1995, report,.

40 Das, T., Chakraborty, S., Banerjee, S. & Venkatesh, M. On the preparation of a therapeutic dose of 177Lu-labeled DOTA–TATE using indigenously produced 177Lu in medium flux reactor. Applied Radiation and Isotopes 65, 301-308, doi:https://doi.org/10.1016/j.apradiso.2006.09.011 (2007).

41 Chakraborty, S., Vimalnath, K. V., Lohar, S., Shetty, P. & Dash, A. On the practical aspects of large-scale production of 177Lu for peptide receptor radionuclide therapy using direct neutron activation of 176Lu in a medium flux research reactor: the Indian

experience. J Radioanal Nucl Chem 302, 233-243, doi:10.1007/s10967-014-3169-z (2014).

42 Jurkin, D., Gildehaus, F. J. & Wierczinski, B. Kinetic Stability Studies on Yttrium(III)−1,4,7,10- Tetraazacyclododecane-1,4,7,10-tetraacetic Acid by Free-Ion Selective Radiotracer Extraction. Analytical Chemistry 79, 9420-9426, doi:10.1021/ac701786w (2007).

43 van der Meer, A., Breeman, W. A. P. & Wolterbeek, B. Reversed phase free ion selective radiotracer extraction (RP-FISRE): A new tool to assess the dynamic stabilities of metal (-organic) complexes, for complex half-lives spanning six orders of magnitude. Applied Radiation and Isotopes 82, 28-35, (2013).

Chapter 7

Conclusions and outlook

Radionuclide generators are radionuclide production devices that allows onsite availability of a radionuclide without the need for local access to a nuclear reactor or accelerator [1]. They offer no-carrier added, high specific activity radionuclide production, and also allow repeated extraction of the daughter radionuclide from its parent radionuclide for a long period of time. A large number of ^{99}Mo, ^{68}Ga, ^{188}Re, ^{90}Y based nuclear medicine studies would not have been possible without the availability of corresponding radionuclide generators [2,3].

A radionuclide generator for lutetium-177 (^{177}Lu) production does not exist yet. ^{177}Lu is a β^- and gamma emitting radionuclide which is very well known for its potential in targeted radionuclide therapy and others [4]. Currently, its worldwide supply is completely dependent on the availability of nuclear reactors. Like other radionuclide generators, a ^{177m}Lu/^{177}Lu radionuclide generator can reduce the nuclear reactor dependency for its availability. The objective of this thesis was to evaluate the possibility of developing a ^{177m}Lu/^{177}Lu radionuclide generator based lutetium-177 (^{177}Lu) production. However, it is unique and different from the existing generators as it involves the separation of physically and chemically identical nuclear isomers, ^{177m}Lu & ^{177}Lu. Further, there are many requirements that needs to be established before its commercialization such as chemical, radiochemical and radionuclidic purity of the produced ^{177}Lu and shelf life of the generator. This thesis was specifically aimed at providing the proof of concept of ^{177m}Lu-^{177}Lu separation and identify the basis for the future work towards a clinically acceptable ^{177m}Lu/^{177}Lu radionuclide generator. The main aspects covered in this thesis are as follows, 1) the separation of physically and chemically alike nuclear isomers, ^{177}Lu & ^{177m}Lu 2) the production ^{177m}Lu and lastly 3) a ^{177m}Lu/^{177}Lu radionuclide generator was simulated to evaluate the quality, quantity of ^{177}Lu that can be produced. In the following paragraphs, the main conclusions and a future outlook on these aspects is presented:

Based on the work in this thesis, it is concluded that the nuclear isomers ^{177m}Lu and ^{177}Lu can be chemically separated. The ^{177m}Lu-^{177}Lu separation requires firstly, a very stable complexing agent to coordinate the ^{177m}Lu ions. Secondly, the complexed ^{177m}Lu results in free ^{177}Lu ion production via the decay by internal conversion and provides an opportunity to separate the two nuclear isomers in the form of complexed ^{177m}Lu and freed ^{177}Lu ions. Lastly, separation conditions where the freed ^{177}Lu ions could not re-associate back with the complexing agent and the complexed ^{177m}Lu ions could not dissociate are required. Thus, the kinetic stability of the complexing agent and the low association- dissociation kinetics appeared as the major parameters determining the degree of ^{177m}Lu-^{177}Lu separation. In this thesis, 1,4,7,10-Tetraazacyclododecane-1,4,7,10-tetraacetic acid (DOTA) and DOTA based peptide, DOTA-(Tyr^3)-octreotate (DOTATATE) were used as ^{177m}Lu complexing agent. The separation of freed ^{177}Lu ions was achieved using reversed phase column chromatography (Chapter 2), liquid-liquid extraction (Chapter 3) and solid phase extraction (Chapter 4).

In Chapter 2, a ^{177}Lu/^{177m}Lu activity ratio of 250 was achieved after separation in comparison to the equilibrium ^{177}Lu/^{177m}Lu activity ratio of 0.25. It was realized using reversed phase column chromatography where the ^{177m}Lu-DOTATATE complex was retained on a tC-18 silica filled column and the free ^{177}Lu ions produced after bond rupture were collected using a mobile phase flow. This method offered advantages such as ease of use, operational simplicity, and collection of ^{177}Lu in suitable aqueous phase. However, it required that the usually hydrophilic Lu complex had to be made hydrophobic by conjugating them with a radiolytically unstable peptide chains. The peptide chains can degrade over the period of time due to the radiation damage and can release the ^{177m}Lu ions free out of the column. This makes the adaptation of this technique into a commercial ^{177m}Lu/^{177}Lu radionuclide generator uncertain for possible future investigations.

In Chapter 3, the ^{177}Lu/^{177m}Lu activity ratio close to 3500 was achieved after the ^{177m}Lu-^{177}Lu separation which is close to the ^{177}Lu/^{177m}Lu activity ratio obtained during the direct route ^{177}Lu production. It employed liquid-liquid extraction where the ^{177m}Lu ions were complexed in the aqueous phase and the freed ^{177}Lu ions were extracted into organic phase using a cation extracting agent. The use of 77K during ^{177}Lu accumulation prevented the dissociation of complexed ^{177m}Lu and the re-association of freed ^{177}Lu ions with the complexing agent. The extraction of free ^{177}Lu ions were performed at room temperature in about 10 minutes. The 10 minutes time allowed to reach the ^{177}Lu extraction efficiencies of 58±2% while keeping the ^{177m}Lu contribution due to the dissociation low to 0.0020±0.0010% of the initial ^{177m}Lu activity. Overall, it is a very easy and convenient way to evaluate the potential of any complexing agent in ^{177m}Lu-^{177}Lu separation.

However, the presented method is not automatized yet, it was performed at lab-scale with very low activity levels and is far from commercialization. The additional effects due to the radiation damage and the back extraction of ^{177}Lu from organic phase to aqueous phase were not considered here and should be accounted carefully in the future research. Further, the recent innovations in the automated LLE based systems should be applied in taking this technology forward to lead to a commercial ^{177m}Lu/^{177}Lu radionuclide generator [5]. Some of these examples includes an on-column solvent extraction, shown in Figure 1(a) [6] and a continuous flow extraction, membrane-based phase separation, shown in Figure 1(b) [7].

(a) (b)

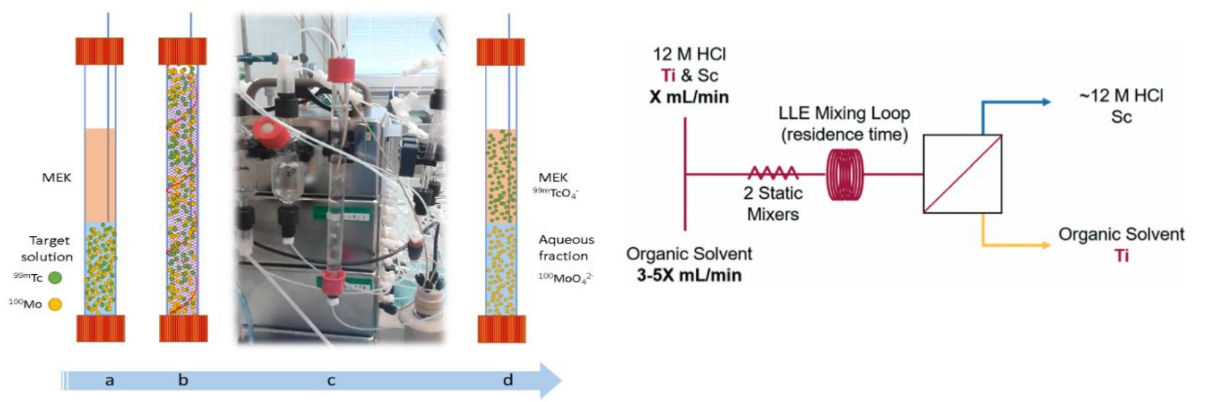

Figure 1: Schematic description of automated liquid-liquid extraction modules used in radionuclide purification adapted from Martini et al [6] Figure 1(a) and Pedersen et al [7] Figure 1(b)

These previously published automated modules were designed for the extraction of ^{99m}Tc and ^{45}Ti in organic phase respectively. Notably, for the set up shown in Figure 1(b), a residence time of 13.2 s was used to achieve extraction efficiencies up to 90%. Such automated modules can be applied in ^{177m}Lu-^{177}Lu separation during future research. Furthermore, apart from these automated systems, microfluidics based on-chip LLE should also be considered as an attractive option that can allow to reach fast ^{177m}Lu-^{177}Lu separation time of few seconds [8,9]. Once the ^{177m}Lu-^{177}Lu separation is automatized, it can certainly lead to a ^{177m}Lu/^{177}Lu radionuclide generator to provide ^{177}Lu with the specific activities close to 4.1 TBq/ mg Lu and with negligible ^{177m}Lu content.

Chapter 4 dealt with a solid phase extraction (SPE) based ^{177m}Lu-^{177}Lu separation. The SPE involves the complexation of ^{177m}Lu on a solid support and the elution of the freed ^{177}Lu using a mobile phase flow. The SPE based radionuclide generators are traditionally the most common ones, owing to their favorable characteristics such as ease of operation, easy automatization and free of organic solvents. In this work, DOTA has been grafted on a silica support and use for ^{177m}Lu complexation while the released ^{177}Lu ions have been collected in a mobile phase flow. A ^{177}Lu/^{177m}Lu activity ratio of 25 has been achieved after separation, in comparison to ^{177}Lu/^{177m}Lu activity ratio of 3500 on using ^{177m}Lu-DOTA complex in LLE. It was postulated that after the grafting on DOTA on silica support, it can no longer form the stable cage coordinated complex with Lu ions thus leading to high ^{177m}Lu contribution from dissociation. Overall, for the use of SPE in a ^{177m}Lu/^{177}Lu radionuclide generator development, it is essential that the support should retain ^{177m}Lu ions with a very high degree of kinetic stability and it should not have any reactive sites that can interact with the released ^{177}Lu ions.

Lastly, the large scale production of ^{177m}Lu has been addressed in Chapter 5 and the question on what amounts of ^{177m}Lu would be needed to produce sufficient ^{177}Lu via a ^{177m}Lu/^{177}Lu radionuclide generator has been addressed in Chapter 6. It was found that the neutron capture cross section for ^{177m}Lu production is close to 2.8 b and it has an additional burn up neutron capture cross section close to 620 b. Based on this cross sections, it was theoretically estimated that the ^{177m}Lu production will require a short irradiation time of 5- 11 days at high flux reactors ($8*10^{14}$ n.cm^{-2}.s^{-1} – $2.5*10^{15}$ n.cm^{-2}.s^{-1}). A starting ^{177m}Lu activity of the order of 0.1 TBq would be needed to produce about 7.4 GBq of ^{177}Lu (one patient dose) per week for a period of up to 7 months. This in turn would require irradiation of 2-4 g of ^{176}Lu enriched Lu_2O_3 targets (depending on the starting ^{176}Lu enrichment). Presently, the ^{176}Lu enriched Lu_2O_3 targets are available in the order of few milligrams. The big question remains, whether the current infrastructure support the production of few grams of ^{176}Lu enriched target? If so, what would be the costs involved. This is an important question that needs to be addressed to assess the possibility of commercialization of ^{177m}Lu/^{177}Lu radionuclide generator.

The specific activity and the ^{177}Lu/^{177m}Lu activity ratio that can be achieved via the ^{177m}Lu/^{177}Lu radionuclide generator have been theoretically addressed in Chapter 6. It has been found that the ^{177}Lu with specific activity close to theoretical maximum of 4.1 TBq ^{177}Lu/ mg Lu having less than 0.01% ^{177m}Lu can be produced. However, it requires that the complexing agent with the dissociation rate constant of the order of 10^{-11} s^{-1} has to be employed possibly in combination with short ^{177m}Lu-^{177}Lu separation time. The favorable coordination chemistry of Lu ions provides with numerous possibilities of complexing agents, and the advances in the separation chemistry can potentially lead to a ^{177m}Lu-^{177}Lu separation process needed to achieve the clinically acceptable ^{177}Lu quality [10-12]. The question that needs to be answered in the future research is the feasibility of large scale ^{177m}Lu production needed as the starting material for $^{177m}Lu/^{177}Lu$ radionuclide generator.

7.1. References

1 Knapp, F. F. & Dash, A. in *Radiopharmaceuticals for Therapy* (eds F. F. Knapp & Ashutosh Dash) Ch. 7, 131-157 (Springer India, 2016).

2 F. Knapp, F. & P. Baum, R. Radionuclide Generators; A New Renaissance in the Development of Technologies to Provide Diagnostic and Therapeutic Radioisotopes for Clinical Applications). *Current Radiopharmaceuticals* 5, 175-177 (2012).

3 <The continuing important role of radionuclide generator systems for nuclear medicine..pdf>.

4 Banerjee, S., Pillai, M. R. & Knapp, F. F. Lutetium-177 therapeutic radiopharmaceuticals: linking chemistry, radiochemistry, and practical applications. *Chem Rev* 115, 2934-2974, doi:10.1021/cr500171e (2015).

5 Martini, P. *et al.* Perspectives on the Use of Liquid Extraction for Radioisotope Purification. *Molecules (Basel, Switzerland)* 24, 334 (2019).

6 Martini, P. *et al.* In-house cyclotron production of high-purity Tc-99m and Tc-99m radiopharmaceuticals. *Applied Radiation and Isotopes* 139, 325-331, doi:https://doi.org/10.1016/j.apradiso.2018.05.033 (2018).

7 Pedersen, K. S. *et al.* Liquid–liquid extraction in flow of the radioisotope titanium-45 for positron emission tomography applications. *Reaction Chemistry & Engineering* 3, 898-904, doi:10.1039/C8RE00175H (2018).

8 Ciceri, D., Perera, J. M. & Stevens, G. W. The use of microfluidic devices in solvent extraction. *Journal of Chemical Technology & Biotechnology* 89, 771-786, doi:10.1002/jctb.4318 (2014).

9 Sepini, L. C., Jarvis, N. V., Jansen, D. R. & Zeevaart, J. R. Thermodynamic evaluation of the stability of the bone-seeking radiopharmaceutical [177Lu]Lu(III)–DOTP under simulated blood plasma conditions. *Analytica Chimica Acta* 730, 66-70, doi:https://doi.org/10.1016/j.aca.2011.10.068 (2012).

10 Dash, A. & Chakravarty, R. Pivotal role of separation chemistry in the development of radionuclide generators to meet clinical demands. *RSC Advances* 4, 42779-42803, doi:10.1039/C4RA07218A (2014).

11 Parus, J. L., Pawlak, D., Mikolajczak, R. & Duatti, A. Chemistry and bifunctional chelating agents for binding (177)Lu. *Curr Radiopharm* 8, 86-94 (2015).

12 Liu, S. & Edwards, D. S. Bifunctional Chelators for Therapeutic Lanthanide Radiopharmaceuticals. *Bioconjugate Chemistry* 12, 7-34, doi:10.1021/bc000070v (2001).

List of Publications

Patent

Patent - NL2017628B1- Isomeric Transition Radionuclide Generator, such as a ^{177m}Lu/^{177}Lu Generator.

Research articles

Bhardwaj, R., van der Meer, A. J. G. M., Das, S. K., De Bruin, M., Gascon, J., Wolterbeek, H. T., & Serra-Crespo, P. (2017). Separation of nuclear isomers for cancer therapeutic radionuclides based on nuclear decay after-effects. *Scientific reports*, *7*, 44242.

Bhardwaj, R., Wolterbeek, H. T., Denkova, A. G., & Serra-Crespo, P. (2019). Radionuclide generator-based production of therapeutic ^{177}Lu from its long-lived isomer ^{177m}Lu. *EJNMMI Radiopharmacy and Chemistry*, *4*(1), 13.

Bhardwaj, R., Bernard, P., Sarilar, M., Wolterbeek, H. T., Denkova, A.G., & Serra-Crespo, P. (2019). Large scale production of Lutetium-177m for use in ^{177m}Lu/^{177}Lu radionuclide generator. *Applied Radiation and Isotopes*, submitted.

Bhardwaj, R., Wolterbeek, H. T., Denkova, A. G., & Serra-Crespo, P. Solid phase extraction based separation of nuclear isomers ^{177}Lu and ^{177m}Lu. *Applied Radiation and Isotopes*, submitted.

Bhardwaj, R., Wolterbeek, H. T., Denkova, A. G., & Serra-Crespo, P. Modelling of a ^{177m}Lu/ ^{177}Lu radionuclide generator. *Applied Radiation and Isotopes*, submitted.

Oral presentations

Bhardwaj, R., Wolterbeek, H. T., Denkova, A. G., & Serra-Crespo, P, Lutetium-177 production via solvent extraction based ^{177m}Lu/^{177}Lu radionuclide generator, RadChem2018, Marianske Lazne, 14 May 2018.

Bhardwaj, R., Wolterbeek, H. T., Denkova, A. G., & Serra-Crespo, P, Lutetium-177 production via solvent extraction based ^{177m}Lu/^{177}Lu radionuclide generator, NKRV, June 2018.

Serra-Crespo, P, **Bhardwaj, R**., M. de Bruin, J. Gascon, H. T. Wolterbeek, and A. G. Denkova, A radionuclide generator for the production of lutetium-177 based on the decay of its nuclear isomer lutetium-177m. 6th Asia-Pacific Symposium on Radiochemistry - September 17 ~ 22, 2017, ICC Jeju, Jeju Island, Korea.

Serra-Crespo, P, **Bhardwaj, R**., M. de Bruin, J. Gascon, H. T. Wolterbeek, and A. G. Denkova, A radionuclide generator for the production of lutetium- 177 based on the decay of its nuclear isomer lutetium-177m. INCC2017, Gothenburg 30 August 2017.

Poster presentations

Bhardwaj, R., J. Gascon, Wolterbeek, H. T., Denkova, A. G., & Serra-Crespo, P, Exploring Metal-Organic frameworks for applications in nuclear medicine and diagnostics, presented at the conference Molecular and Supramolecular Carrier for Imaging and Therapy, Lisboa, 13-15 July 2015.

Bhardwaj, R., J. Gascon, Wolterbeek, H. T., Denkova, A. G., & Serra-Crespo, P, Study of the Dissociation Kinetics of DOTA Derivatives by Immobilization on Solid Supports at NKRV.

Bhardwaj, R., J. Gascon, Wolterbeek, H. T., Denkova, A. G., & Serra-Crespo, P, Development of a $^{177m}Lu/^{177}Lu$ radionuclide generator for the production of Lutetium-177at NKRV on June 30, 2017.

Bhardwaj, R., Wolterbeek, H. T., Denkova, A. G., & Serra-Crespo, P, Lutetium-177 production via solvent extraction based $^{177m}Lu/^{177}Lu$ radionuclide generator, RadChem2018, Marianske Lazne, 14 May 2018.

Acknowledgements

Finally, I can see an end to the quest of getting a doctoral degree and thus now is the perfect moment to thanks everybody who had made an invaluable contribution in this thesis. For me it was not just a PhD journey but a PhD plus baby, i embraced the motherhood in 3rd year of my PhD. It was not easy but luckily I was surrounded by people who helped me not just professionally but also personally☺.

The thesis is an outcome of discussions/ contributions from many people. I would like to begin with my daily supervisor Dr. Pablo Serra Crespo, Pablo, I can't thank you enough for supporting me in the last four years. Your availability and enthusiastic welcome for the discussions was always a big advantage for me. I will never forget the first time, I saw the gamma ray spectra proving the possibility of Lu isomer separation. Astonished, excited and happy me ran to your office and we came back together to see, discuss it further ☺. I must say that you have a great eye for looking into small details, your feedback has allowed me to grow significantly in the last four years. Whenever I panicked or gave up, you calmly said "its ok, its normal" rupali, lets talk it out, let's find a solution to the problem. Next in my list is Dr. Antonia Denkova, Dear Antonia, I always felt a very friendly and warm relation with you. I really appreciate your down to earth, empathetic attitude towards everybody, I hope i can learn it from you. You praised me when I did well but also you provided me with subtle and gentle pushes when needed. It was very comforting that I could always walk to you, and talk about any professional/ personal problem. More than a professor, you were always a mentor, a friend for me. I would also like to thank my promoter Prof. Bert Wolterbeek for the insightful discussions and always providing with a perspective on the bigger picture. Further, I would like to thank Prof. Marcel De Bruin, for his precious contributions in this thesis, starting from the idea of Lu isomer separation to all the technical discussions we had. It was a great learning experience, you always left me with a solution to my previous problem and a hint on the next direction. Next, I would like to thank Dr. Menno de Blauw for his vital contribution in the thesis. The availability of INAA software, the presence of calibrated germanium detectors, your experience and expertise were an invaluable aid to me. You humbly refused to be a co-author in the papers, but in my perspective you have always contributed substantially, especially in the Chapter 5 on Lu-177m production. I will also like to thank Prof. Jorge Gascon for his time during the first two years of this PhD project, you helped me in getting a good start and always guided the discussions towards a conclusion.

I would also like to thank STW to provide funding for the project, and IDB Holland for their in kind contributions. The regular availability of Lu-177m, provided by IDB was a very important aid in facilitating this research. I would also like to thank all the user committee members, Dr. Wout Breeman, Prof. Phillip Elsinga, Dr. Jeroen Hendrikx, Dr. Yann Seimible for your very valuable inputs during different stages of this thesis. Their perspectives allowed to direct the research while taking into account the user requirements. I would also like to thank, Dr. Karthick Sai Sankar Gupta from Leiden University for all his help in the NMR measurements and your endless energy, enthusiasm. A big thanks to Dr. Volkert Van Steijn and Kartik Totlani for collaborating on application of microfluidics in radionuclide generator development. Kartik, it was great working with you, wish you all the best with your career ahead.

I would also like to thank all the technical staff for their invaluable contributions in the thesis. The technical staff of ARI, Astrid van der Meer, Baukje Terpstra, Adrie Laan, Folkert Geruink, many thanks to all of you. Astrid, I always enjoyed working with you in the lab and further discussing the results. You are always so full of energy, enthusiasm and open to discuss new ideas, it is so inspiring. Baukje, thankyou for your help in ICP measurements and for being a good friend. More than professionally, you always helped me personally when needed. I always enjoyed a coffee, dinner, yoga lessons with you. Thank you for being an oma to my daughter and for all your love and support. Adrie, thanks for bearing with me in the lab and thanks for all the times when you helped me in cleaning the mess especially for all the support in the last phase of my PhD. I always enjoyed our philosophical, technical discussions, hope to keep having them in the future. Folkert, I can’t thank you enough for providing me with a warm & comforting space in the RID. I could always go to you for any technical help. I respect you and if I am ever in the same office space with you, I would love to open the doors for you ☺. A big thanks also to Mehmet, for all your help in designing the experiments for Lu-177m production, and also during the data analysis. Delia, I would also like to thank you for giving me the training on INAA software and helping me to work with it. Other than technical help, you were a great colleague, with whom I can talk about the sleepless nights, eating tantrums, and all the motherly things. A big thank to Anouk for being always very welcoming and for all your help in last days in arranging everything. Also, many thanks to the technical staff from Catalysis Engineering, Harrie Jansma, Willy Rook, Bart van der Linden for their support during the thesis. Bart, thankyou for all the discussions on Infra Red, TGA spectra.

A big thank to all the students who have worked me with me on this project. Luis, Soraya, Pien, Maikel, Thom, Dennis, Guido, Huub, thanks to all of you for being a part of my PhD journey. Thom and Dennis you were a great technical help to me, when I could not myself go to the lab because of pregnancy. I wish you a great future ahead. A big thanks to the cdp project design team, Kirsten, Philippe, Jaen, Loes, Sneha, Joost for being a part of my PhD thesis, it was great working with you all. And thanks to all of you for your contribution in modelling a theoretical Lu radionuclide generator and Lu-177m production. Joppe, you started on a very challenging project without much experimental support from me. I wish you all the best in wrapping up your thesis, and in your future ahead.

To all the fellow PhDs and postdocs, thank you for making my time during PhD unforgettable experience. Robin, it was awesome sharing the office with you, thank you for always listening

to me. You were always a big support to me, both personally and professionally. You are an awesome person with infinite energy levels, I wish you always everything best. I really missed you last year in Netherlands, and hope to catch up with you more often in coming time. Alexandra, you didn't came to delft often but whenever you were there the coffee/ lunch breaks were more fun. I always enjoyed your company, you and Javier form a lovely couple together, I wish you loads of love and happiness always. Elisabeth, you were the first person I met when I joined ARI, you are a very kind and helping person. I will never forget my first baking experience under your supervision:-D, I loved it and wish you everything best in Aachen. Vallin, I really appreciate your helping attitude and hope we keep seeing each other in Petten. Josette, you were always very helpful and it was nice to work on the same project together and complaint about Lutetium :-D. Also, thanks to you Alexandra and Esra, for sharing the office with me in the last few days best wishes to you in your career ahead. All my colleagues from reactor institute, Jasper, Huanhuan, Guzman, Tiantian, Alessia, Eleco, Jeremy, Tayser, thank you all for the wonderful time at lunch and coffee table. All the colleagues from CE, Alla, Anastasiya, Ina, Irina, Maria, Eduardo, Agi, Ana, Dimitri, Sonia, Beatriz, Emmanuel, Lide, Meixia.., thank you all for being a wonderful companion to me.

Next I would like to thank all my colleagues NCSV group, Klazien, I can't thank you enough for all the comforting moments you have provided me. A hug when I am low in energy, your time to hear me during all the up-downs. For me, you are one of my go-to person without any hesitation. I could call you 7 o' clock in the morning when I was worried about Ushma's health, thanks a lot for being there and for all your love and kindness. The dressed you stiched for Ushma is one of the most precious cloth that I will keep with us for years to come. Jolanda, you are an awesome mother and an awesome colleague, I always enjoyed taking the tips and tricks from you about motherhood. Monique, you have a great heart and a lovely smile, thank you for your time and kindness. Marcel, to me you are the one of the kindest heart person I have ever seen. You are a wonderful teacher and an awesome human being, thank you for introducing me to pindakaas, and you made me like cherries when you used to bring along during summer holidays. Dosti, your name symbolizes friendship and you truly justifies it, you are a very helpful and an awesome friend. I must say that I passed the Level 3 because I did it together with you, it was great fun doing it together with you. I wish you all the best in your career ahead. Next, I would like to thank all my colleagues from SBD, Koos and Henk, from the day 1 of joining the RID you are the police guys to me :-D, thank you all very much for helping me out in all those contaminations, I created. Koos, wish you best in your career at NCSV. Marlies, thank you very much for helping me writing all the permits, and thinking about experiment design. Next I would like to thank my new colleagues from curiumpharma, my manager Dr. Luis Barbosa, thankyou for allowing me to take leave for finishing up the thesis and supporting me always. Anouk and Sven, thankyou for listening to all my frustrations and problems in the last days of finishing up thesis. You all are truly awesome colleagues.

Further, I would like to thank all my friends who made my time much more enjoyable. Aadi, lalit, Sumit, Purvil, Trinath, Ajith, Maulik and Bhaskar, Venkatesh, Krishna bhai thank you all for the wonderful trips, celebrations we had together. I wish you everything best with your better-half's, and a wonderful life ahead. Thankyou Ashwiti for our chai time. Also thanks to art of living group, Vandana, Olga, for welcoming me in meditation sessions with a great heart and helping me in relieving stress. A big thanks to, Anne-Niels, Zohre-Sohail, and Martijna-Jan for all the lovely time we had together. A big thank to you Ida, for all your love and warmth, you have provided with in all the past years. I love talking to you, sitting with you, sharing my anxieties for future, learning from your experiences.

Last but not the least, I would like to thank my family who are largely responsible for who I am today. First, thanks goes to my grandparents, my grandma used to say I will become a doctor one day (she meant literally the doctor). Amma, I am sure you will be proud seeing me atleast getting the title. Also thanks to my grandpa, for giving me a strong upbringing. A big thanks goes to my grandfather in law, dadaji you were a great person, I admire and adore so much. Your words, our weekend talk helped me sailing the tough times in life. You were my go-to person when I am lost, few minutes with you and I could see a direction. I miss you a lot, I am sure you will be proud seeing me holding this degree. Next, I would like to my parents, papa thankyou for all the unconditional you have given me. Mumma, thankyou for making me a strong and independent person, you have always been a great support to me. I can just call you anytime, any moment and you are there to listen me, to laugh with me and to cry with me. I love you loads..!! Next, I would like to thank my parents in law, I entered your family just 6 years back with a dream to pursue my education and get a PhD degree and you made my dream your dream. When, we announced the news of me being pregnant, you first worry was about my studies. I am blessed to have you in my life, thank you for all your love and support. Further, I would like to thank my brothers and sister in laws, Rahul bhai, you are like father to me, caring, protective and supporting always. Rohit bhai, you love and care for me more than anybody but at the same time you gently pushed to break barriers and go for something higher. Khushboo, and Megha Bhabhi, we are blessed to have you in our family, thank you for loving and caring for us. I don't have to worry about my parents, because you both are always there for them. Mayank bhai and Vasudha di, I share a special bond with you, you both have played a crucial role in my life, as our friends say, you are the catalyst behind bringing Rajat and Rupali close to each other. Thank you for all your love and support.

Lastly, thanks to the person who largely made this thesis possible. My better half, Rajat, this thesis is because of you, it is for you and with you. If you are with me, I don't need much more, together we can conquer anything. My daughter, Ushma, the best part of having you is that you make me feel special. Everytime, you run toward me saying mijn mumma, I feel important and needed (a good to have feeling on the day when nothing looks working).

About the author

Rupali Bhardwaj was born in Shamli, Uttar Pradesh, India on 23rd May, 1990. She finished her high school from Shmali in 2008. Her interest in chemistry motivated her to pursue B.Sc (Hons) in Chemistry from Hindu college, University of Delhi. After successfully completing her bachelor's degree in 2011, she followed her master's degree in Organic Chemistry from University of Delhi. After finishing the academic training in 2013, she worked for 6 months at Chemical Biology lab in University of Delhi on the synthesis of HIV-1 integrase inhibitors.

In 2014, she moved to Delft, Netherlands with her husband, Rajat Bhardwaj, and started her PhD at the Delft University of Technology. She started on a collaboration project between the Catalysis Engineering & Applied Radiation and Isotopes for Health group. Her PhD was aimed at the development of radionuclide generator for the production of therapeutic lutetium-177. During her PhD project she developed different chemical separation methods that can allow the separation of physically and chemically identical nuclear isomers, Lu-177 and Lu-177m. She investigated the potential and requirements for radionuclide generator based lutetium-177 production. The results of her thesis are described in this dissertation and other peer reviewed journal articles. She has presented her research orally and using poster presentation at several conference. In 2019, she started working as Research scientist at Curiumpharma.